

182
9

**A FEASIBILITY STUDY OF PVDF PIEZOELECTRIC
SENSORS TO DETECT DAMAGE IN ADHESIVE JOINTS.**

by

Joseph Mommaerts

Thesis submitted to the Faculty of the
Virginia Polytechnic Institute and State University
in partial fulfillment of the requirements for the degree of
Master of Science
in
Engineering Mechanics

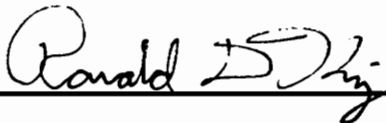
APPROVED:



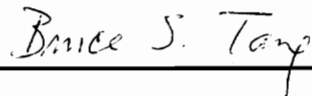
Dr. David A. Dillard
(co-advisor)



Dr. John C. Duke, Jr
(co-advisor)



Dr. Ronald D. Kriz



Dr. Shiu L. Tang

December 1990
Blacksburg, Virginia

LD
5655
V855
1990

M658
C.2

**A FEASIBILITY STUDY OF PVDF PIEZOELECTRIC
SENSORS TO DETECT DAMAGE IN ADHESIVE JOINTS.**

by

Joseph Mommaerts

Dr. David A. Dillard, co-chairman

Dr. John C. Duke, Jr, co-chairman

Engineering Mechanics

(ABSTRACT)

Poly(vinylidene fluoride) (PVDF) films can be easily etched into sensor devices. Since these sensors are relatively inexpensive, thin and light-weight, they can be attached to adhesively bonded joints permanently to measure bond integrity. The present study shows the different steps to design such sensors and proper techniques to attach them near the adhesive bondline. PVDF sensors have been successfully used as NDT transducers in pulse-echo, through-transmission, and acousto-ultrasonic techniques to monitor curing, to detect porosity and crack propagation in different model joint geometries. The potential of using these techniques for practical bonded structures has then been evaluated.

Acknowledgements

I wish to express here my gratitude to my family and to all those who assisted me during my stay in Blacksburg.

First to my co-advisors Dr. David A. Dillard and John C. Duke, Jr. for their qualification, pedagogical qualities and enthusiasm in work. Thanks to Dr. Ronald D. Kriz for his valuable remarks, and to Dr. Bruce Tang for his helpful suggestions. I would like also to thank Danny L. Reed for his technical advice.

I am very grateful to Dr. Bernard Laberge, Assistant Dean of the International office of the Graduate School and to Dr. Grynzpan, researcher at ENSAM and CNRS for providing me the opportunity to study at Virginia Polytechnic Institute.

Finally, thousands of thanks to all my friends who contributed to make these past 15 months an unforgettable experience: Anne "la tatarde", Thierry "podzob", Benoit "grongnon", Remi, Laurent, Dolly, Bruno, Jean-yves, Antonio, Pascale et Cathy, fred, GI Jeff, Marten, Joe and Dave, Guy, Christophe "le Duck looser", Sabrina and all the others who shared some time with me.

Table of Contents

1.0 INTRODUCTION	1
2.0 LITERATURE REVIEW	3
2.1 Ultrasonic technique	3
2.1.1 Types of waves	7
2.1.2 Generation of ultrasonic waves	10
2.1.3 Techniques	11
2.1.4 Damage monitoring	16
2.2 Piezopolymer	17
2.2.1 Structure	17
2.2.2 Properties	17
3.0 PVDF TRANSDUCER DESIGN	25
3.1 Electrode pattern	25
3.2 Electrical lead attachment	27
3.3 Sensor design	31
3.3.1 Size of the active area	31
3.3.2 Shape of the sensor	33

3.4 Embedment	33
4.0 CHARACTERIZATION OF ADHESIVE JOINTS BEFORE SERVICE	40
4.1 Porosity study	40
4.2 Setting of an adhesive	50
5.0 MONITORING DAMAGE IN SEVERAL JOINT GEOMETRIES	59
5.1 Single lap shear joint	60
5.1.1 Loading by prying	60
5.1.2 Tensile test	68
5.2 Mechanically loaded blister.	77
5.2.1 Monitoring of debonded area	77
5.2.2 Detection of crack propagation	81
5.3 Double cantilever beam	90
5.3.1 Crack propagation	90
5.3.1.1 Same thickness of adherends	91
5.3.1.2 Different adherend thicknesses	97
5.3.2 Delamination of composites	100
6.0 SUMMARY AND CONCLUSION	109
REFERENCES	115

APPENDIX A

Ingression of water 122

APPENDIX B

Fact sheet of PVDF transducer 129

APPENDIX C

Analytical method to calculate the acoustic impedance of
an adhesive during curing 130

VITA 139

List of Illustrations

Figure 1. Pulse echo technique for the determination of wall thickness	4
Figure 2. Pulse-echo technique to detect flaw	6
Figure 3. Particle motion and wave propagation	8
Figure 4. A schematic of the pulse-echo technique	12
Figure 5. A schematic of the through-transmission technique	13
Figure 6. A schematic of the acousto-ultrasonic technique	14
Figure 7. Net dipole within a unit volume of piezofilm	18
Figure 8. Axis designation	20
Figure 9. Different steps to obtain the desired sensor	28
Figure 10. Sensor design for the electrical connection	30
Figure 11. Influence of sensor's size on the amplitude of the signal	32
Figure 12. Shape of sensor to detect water ingress ion	34
Figure 13. Shape of the sensors for the characterization of a joint by the AU technique	35
Figure 14. Schematic diagram of the adhesively bonded joint with PVDF sensors inside to detect moisture absorption	36

Figure 15. Typical PVDF transducer used in our experiments	39
Figure 16. Schematic diagram of the specimen	42
Figure 17. Schematic diagram of the experiment	44
Figure 18. Schematic diagram of the ultrasonic signals for urethane bonded joints with little air bubbles in the adhesive bond	45
Figure 19. Schematic diagram of the ultrasonic signals for urethane bonded joints with many air bubbles in the adhesive bond	46
Figure 20. Micrograph of the urethane adhesive bond with few air bubbles	47
Figure 21. Micrograph of the urethane adhesive bond with many air bubbles	48
Figure 22. Specimen used for the setting of a 5 minute epoxy . . .	51
Figure 23. Schematic diagram of the experiment	52
Figure 24. Pulse-echo signal for the setting of a 5 minute epoxy .	54
Figure 25. Pulse-echo signal for the setting of a 5 minute epoxy .	55
Figure 26. Amplitude of the first signal versus time for the setting of a 5 minute epoxy	56
Figure 27. Amplitude of the second signal versus time for the setting of a 5 minute epoxy	57
Figure 28. Schematic diagram of the specimen	61
Figure 29. Micrograph of the finger-like micro-cracks in the silicone rubber adhesive bond	62

Figure 30. Amplitude and FFT spectra of signal received by sensor #1 and sensor #2	64
Figure 31. Amplitude and FFT spectra of signal received by sensor #2 during crack propagation	66
Figure 32. Adhesively bonded lap shear joint with PVDF sensors	70
Figure 33. Results for the shear lap joint with two crystals	71
Figure 34. Results for the shear lap joint with one crystal and one PVDF	72
Figure 35. Results for the shear lap joint with two PVDF sensors .	73
Figure 36. Change of central frequency for the specimen with two crystals	74
Figure 37. Change of central frequency for the specimen with one crystal and one PVDF	75
Figure 38. Change of central frequency for the specimen with two PVDF sensors	76
Figure 39. Bonded specimen with a large PVDF sensor for monitoring of debonding	78
Figure 40. Results for the monitoring of debonding area	79
Figure 41. Specimen used for crack propagation	82
Figure 42. Pulse-echo signal for crack propagation	84
Figure 43. Amplitude of signals for each increment of the circular crack area	85
Figure 44. Amplitude of signals for each increment of the circular crack area	86
Figure 45. Specimen during non circular crack propagation	88

Figure 46. Amplitude of signals for each increment of crack area with arbitrary shape	89
Figure 47. Double cantilever beam used for crack propagation . . .	92
Figure 48. Pulse-echo signal for crack propagation	93
Figure 49. Amplitude of the signal versus the crack front	94
Figure 50. Amplitude of the signal when a failure occurs at the bottom of the bond	95
Figure 51. Amplitude of the signal when a failure occurs at the upper side of the bond	96
Figure 52. Pulse-echo signal for crack propagation	98
Figure 53. Amplitude of the signal versus the crack front	99
Figure 54. Specimen used to detect the delamination of a composite	101
Figure 55. Pulse-echo signal for sensor #1, #2, and #3	102
Figure 56. Location of sensor #4 and #5	103
Figure 57. Pulse-echo signal for sensor #4 and #5	104
Figure 58. Pulse-echo signal in plexiglas for PVDF and ceramics	107
Figure 59. Pulse-echo signal in plexiglas for PVDF and ceramics	108
Figure 60. Specimen used to detect the ingress of water	123
Figure 61. Pulse-echo signal for monitoring of water ingress	125
Figure 62. Amplitude of signal versus time	126
Figure 63. Comparison of the signal before and after time	127
Figure 64. Schematic diagram showing the penetration of water at the interface	128
Figure 65. Pulse-echo signals used for the calculations	131

Figure 66. Pulse-echo signals when the adhesive is thin 134
Figure 67. Acoustic impedance of the epoxy during curing 136
Figure 68. Amplitude of the second pulse-echo versus time 137

List of Tables

Table 1. Comparison of typical piezoelectric material properties . 22
Table 2. Acoustic properties of common materials 24

1.0 INTRODUCTION

Following World War II, the use of structural adhesives has become widespread in industry as a result of chemical research and technical development. Adhesive bonding offers many advantages compared with joints made using conventional techniques (welding, brazing, riveting, bolting) including weight reductions, manufacturing cost decreases and improved performances for a wide variety of applications. However, many of these benefits have not yet been realized because of the uncertainties concerning bond quality, durability and reliability. Appropriate non-destructive evaluation techniques and procedures are needed to evaluate structural integrity, to monitor damage development, and to assure the reliability of the bonded structure in the as-received condition and during service loading. Among various nondestructive methods, the ultrasonic technique is a simple and promising method to evaluate adhesively bonded joints¹⁻⁵. In general, ceramic crystals are used as transducers to send out and receive ultrasonic signals. The transducers may be used in either a pulse-echo or through-transmission mode⁶⁻⁹. An alternative method called the acousto-

ultrasonic (AU) method, developed by Vary^{10,11}, is in the developmental stage for the characterization of adhesively bonded joints¹²⁻¹⁴. With proper design, poly(vinylidene fluoride) films can be made into ultrasonic transducers¹⁵⁻²⁰. In monitoring and detecting damage in adhesive joints, the advantages of PVDF over ceramic crystals are many¹⁹⁻²². PVDF is relatively inexpensive and easy to etch into intricate sensor patterns. It is thin and light-weight, hence it is possible to attach PVDF films to the bonded joint permanently. Furthermore, the PVDF transducers respond to a wide-banded frequency and are heavily damped.

The objective of the study is to show the feasibility of developing PVDF sensors to detect the presence of damage and monitor their propagation in adhesive joints. A variety of PVDF sensors for measuring bond degradation has been considered and proper techniques to attach these sensors in or near the adhesive bondline have been identified. The most successful prototypes have been used on several joint geometries which have been damaged by mechanical and environmental exposure. The potential of using these techniques for practical bonded structures have then been evaluated.

2.0 LITERATURE REVIEW

2.1 *Ultrasonic techniques*

Ultrasonic techniques are widely used in the field of nondestructive testing. They can indeed measure wall thickness, detect flaws and determine differences in material properties²³⁻²⁵.

The thickness of a homogenous material with known velocity is determined by measuring the distance traveled by the ultrasonic pulse which is proportional to the time taken between the emission of the pulse from the transducer and its reflection from the back surface. Fig. 1 shows the path of the pulse through the material and the value of its amplitude versus time at the upper surface.

If V is the velocity in the medium (V depends on material properties),

t is the time between the initial pulse and its back reflection, and

L is the thickness of the material,

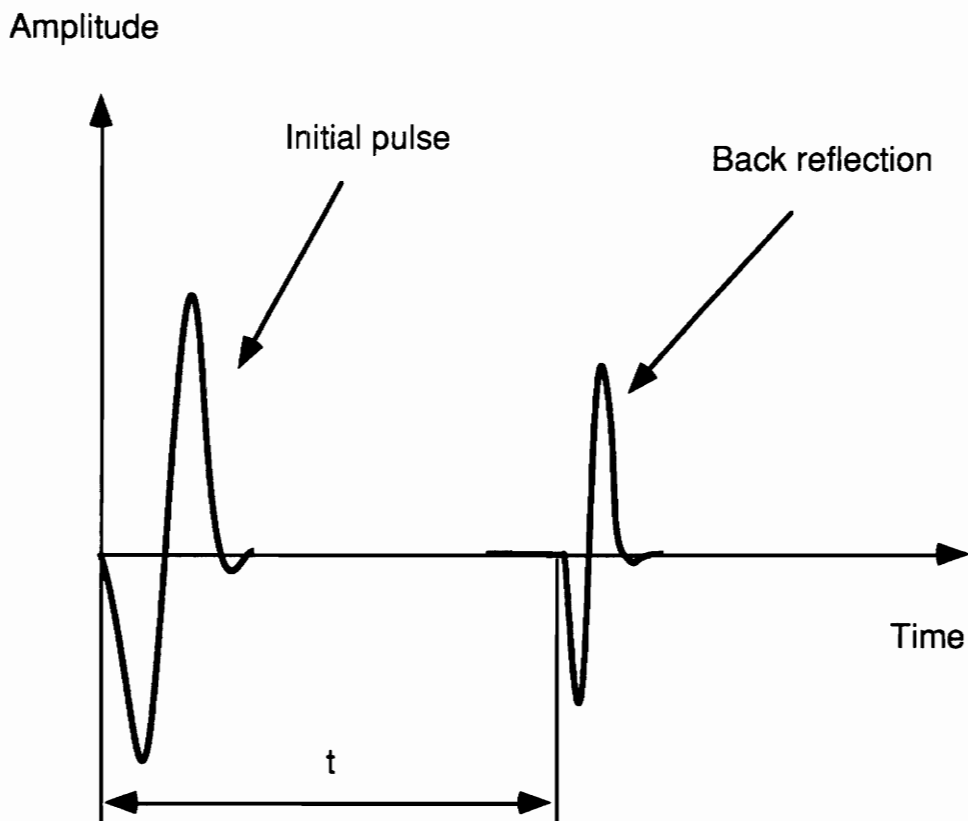
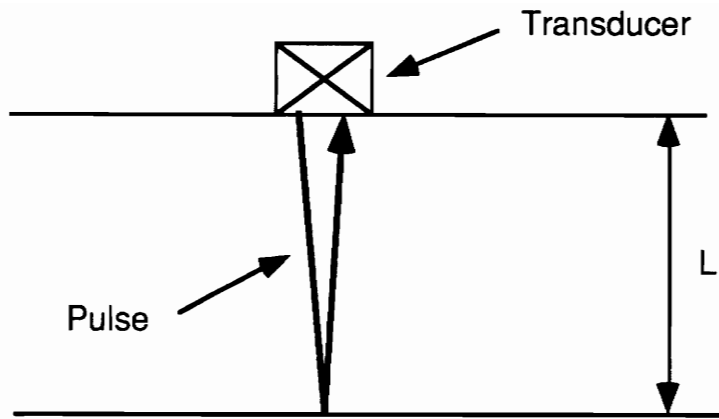


Figure 1. Pulse-echo technique for the determination of wall thickness.

then $V = \frac{2L}{t}$ hence $L = \frac{Vt}{2}$

The same technique is used to detect flaws in a material. If there is a discontinuity in the material, a part of the signal reflects back to the transducer at a different time (fig. 2). It is possible to determine the location of the flaw, its size and its shape, such as in a C-scan.

As the velocity in the medium of a material depends on the physical properties of this material, ultrasonic techniques can be used to determine changes in its properties. The attenuation of an ultrasonic signal can be due to changes in material grain size²⁵ and elastic properties²⁵.

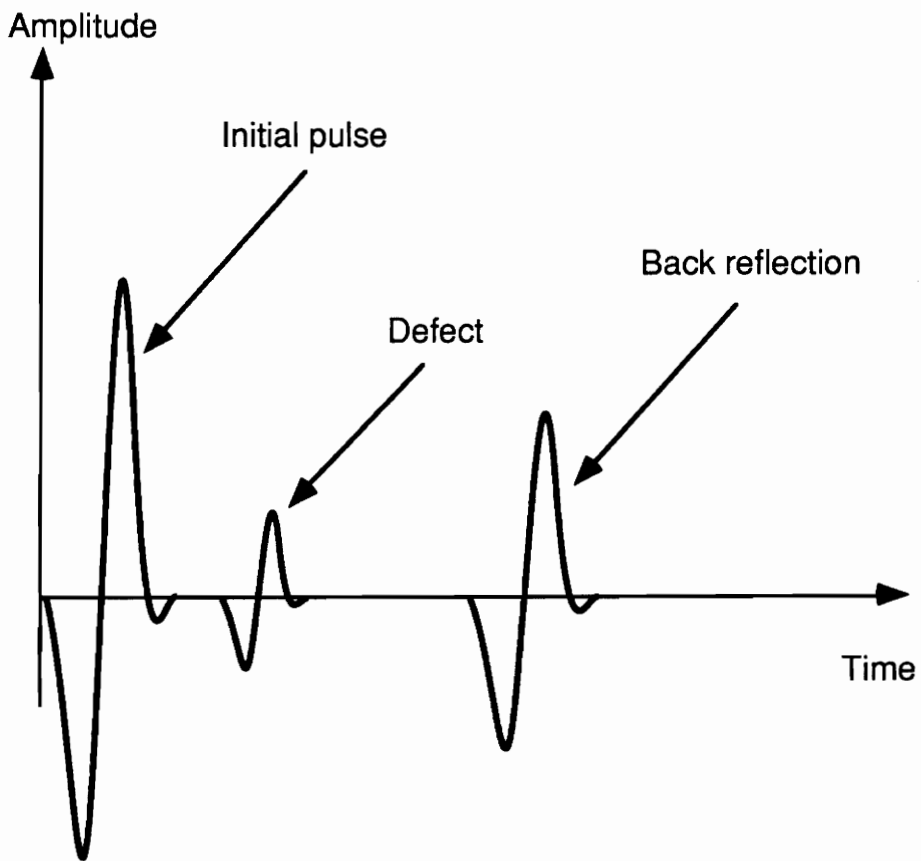
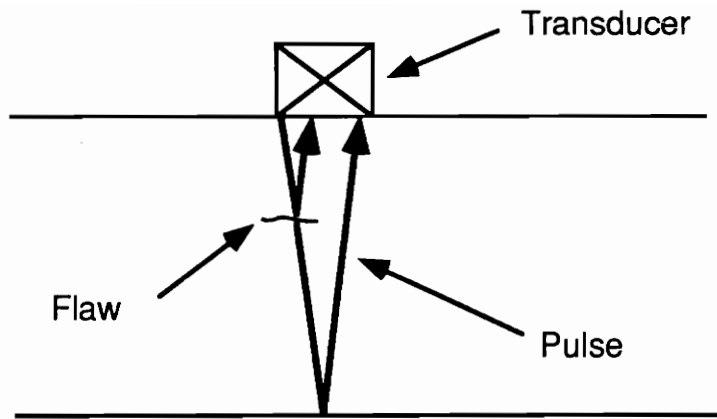


Figure 2. Pulse-echo technique to detect flaw.

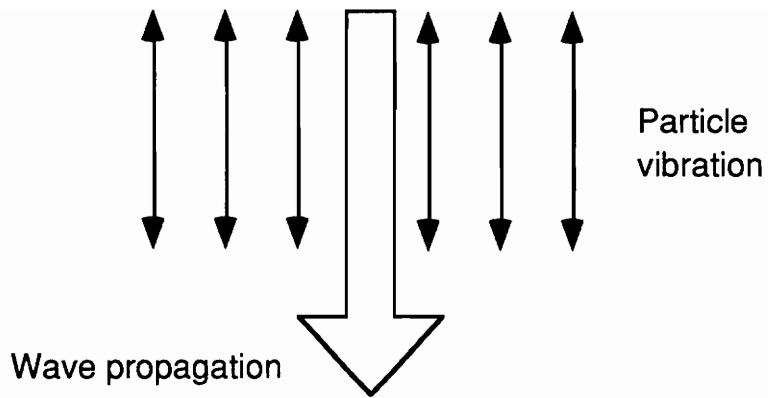
2.1.1 Types of waves

The four modes of ultrasonic waves most frequently used for NDT are:

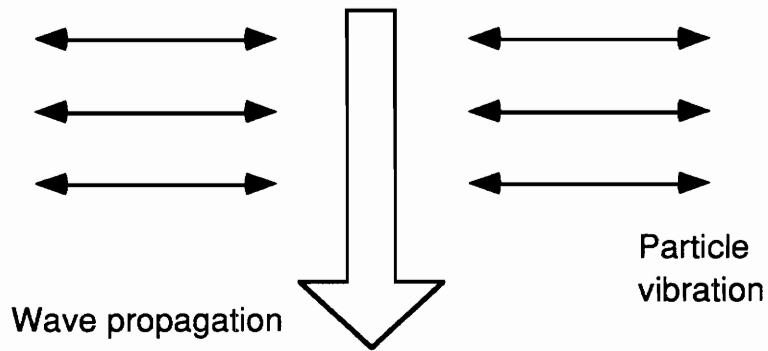
- longitudinal waves.
- transverse waves
- surface or Rayleigh waves
- Lamb waves

When a wave travels through a medium, its particles are displaced. The way these particles vibrate defines the mode of wave propagation.

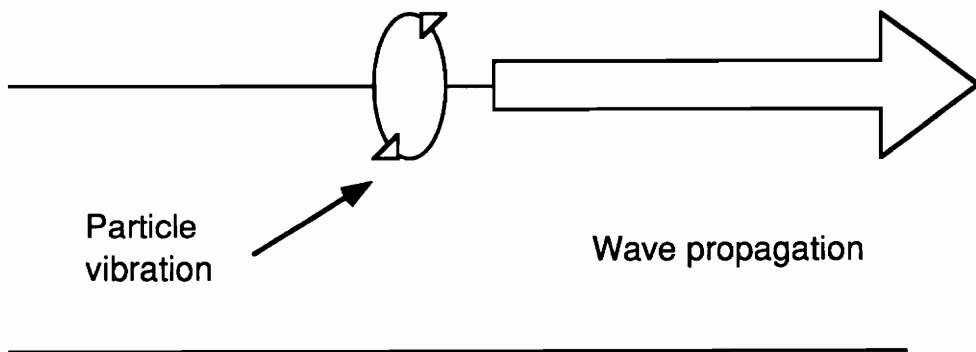
Longitudinal waves are waves in which the particles move in the same direction as the wave is being propagated (fig. 3-a). Transverse (or shear) waves are waves in which the particles move at a right angle to the direction of wave propagation (fig. 3-b). Surface waves are waves which propagate at the surface of the medium. The particle vibrations of the waves follow a retrograde elliptical motion and occur in the plane containing the direction of propagation and the normal to the surface of the medium (fig. 3-c). Lamb waves are waves which propagate in thin plates. Their velocity depends on the thickness of the material and frequency. The associated modes of particle vibrations are complicated.



a. with longitudinal waves.



b. with transverse waves.



c. with surface waves.

Figure 3. Particle motion and wave propagation

The velocities of longitudinal waves and transverse waves for isotropic materials are given by the following expressions:

Longitudinal wave velocity:

$$V_L = \sqrt{\frac{E(1-\nu)}{\rho(1+\nu)(1-2\nu)}}$$

Transverse wave velocity:

$$V_T = \sqrt{\frac{E}{2\rho(1+\nu)}}$$

where E : Young's modulus
 ρ : density
 ν : Poisson's ratio

2.1.2 Generation of ultrasonic waves

There are different ways to produce ultrasonic waves but the most common phenomenon used for nondestructive testing is the piezoelectric effect. W.G. Cady²⁶ defines the piezoelectric effect as follows: " Piezoelectricity is electric polarization produced by mechanical strain in certain crystals, the polarization being proportional to the amount of strain and changing sign with it. The reverse is also true; that is ... an electrical polarization will induce a mechanical strain in piezoelectric crystals. "

This effect has been observed in materials such as lithium niobate, barium titanate (BaTiO_3), lead metaniobate, lead zirconate titanate (PZT), lithium sulfate, tourmaline, quartz and polymer films such as poly(vinylidene fluoride) (PVDF) or poly(vinylidene trifluoroethylene) (P(VDF-TrFE)). Among these materials, the most common ones used in the field of nondestructive testing are quartz, lithium sulfate, polarized ceramics (BaTiO_3 , PZT), and, more recently, polymer films such as PVDF.

These materials are used as piezoelectric transducers by putting electrodes on opposite sides of a crystal which expands and contracts when subjected to an alternating electric field, thereby sending an ultrasonic wave. On the other hand electrical signals will be produced if crystals are subjected to mechanical pressure.

2.1.3 Techniques

There are several techniques used in ultrasonic testing: pulse-echo, through-transmission, resonance, frequency modulation, acoustic image, and the acousto-ultrasonic techniques.

- In the pulse-echo technique, a pulse is sent by the transducer through the specimen. It is reflected at the opposite surface and the echo is received by the same transducer (fig. 4).

- The through transmission technique requires two transducers: a sender and a receiver. A pulse is sent by the sender into the specimen; the receiver picks up the signal at the opposite surface (fig. 5).

- In the acousto-ultrasonic technique¹⁰⁻¹², at least two transducers are used. An ultrasonic pulse is sent by one of the transducers. The receiving transducers intercept the propagating stress waves resulting from the injected ultrasonic pulses (fig. 6). The stress waves undergo multiple reflections at the boundary surfaces of the specimen. Thus they can be affected by those microstructural and morphological properties that also determine structural performance. Stress-wave propagation can be related to several parameters that are measurable from an AU waveform. One of the

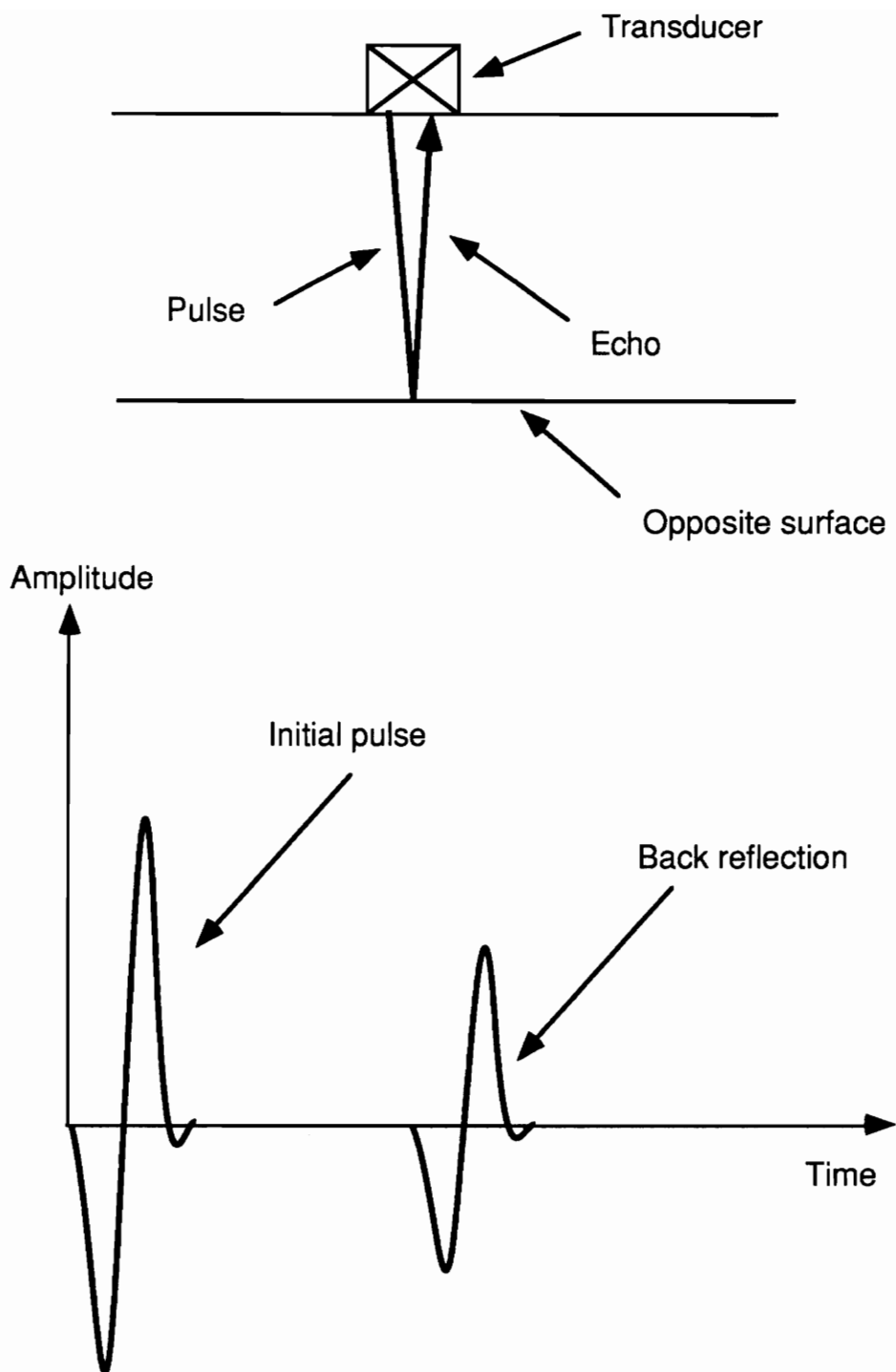


Figure 4. A schematic of the pulse-echo technique.

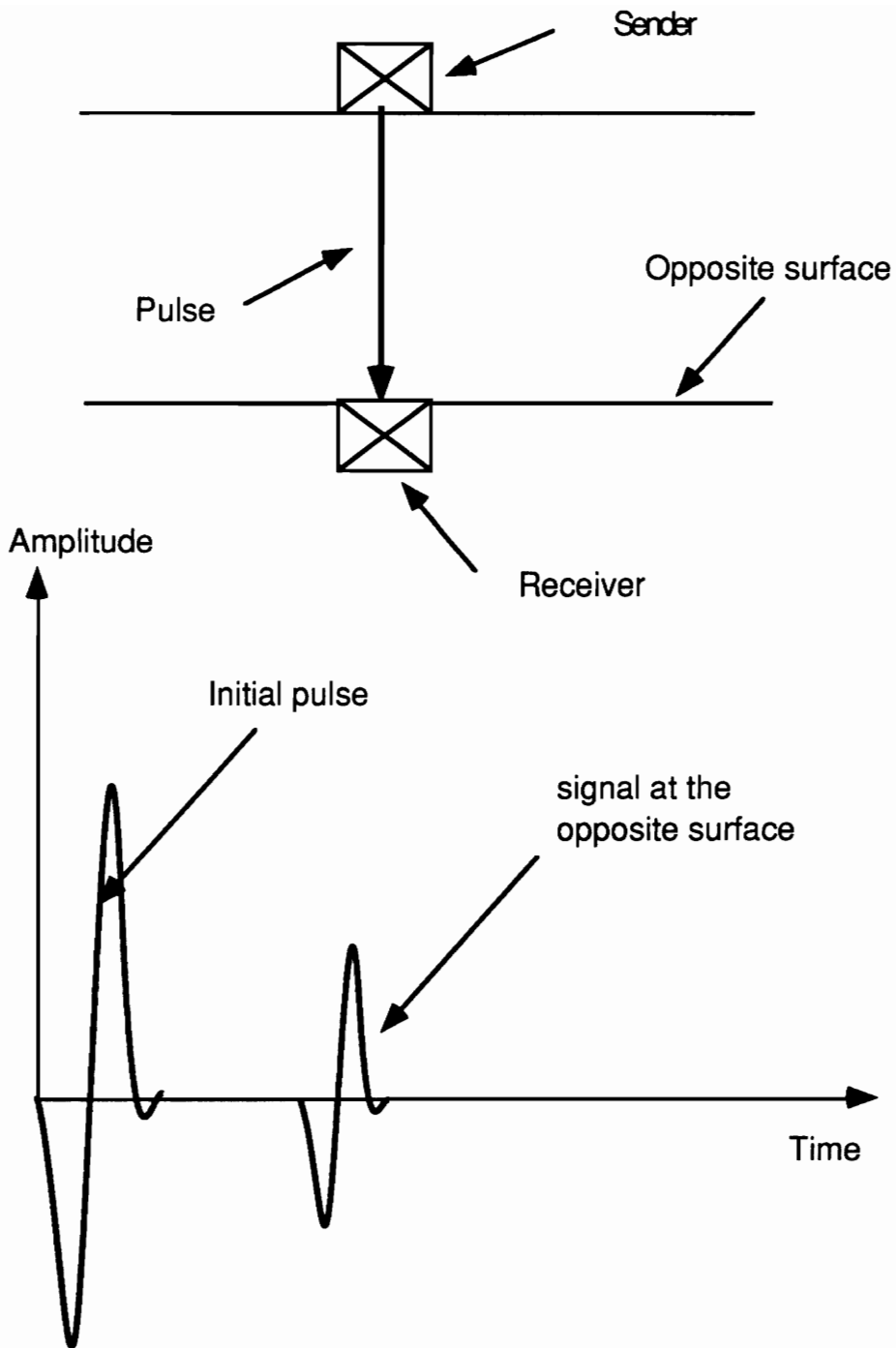


Figure 5. A schematic of the through transmission technique.

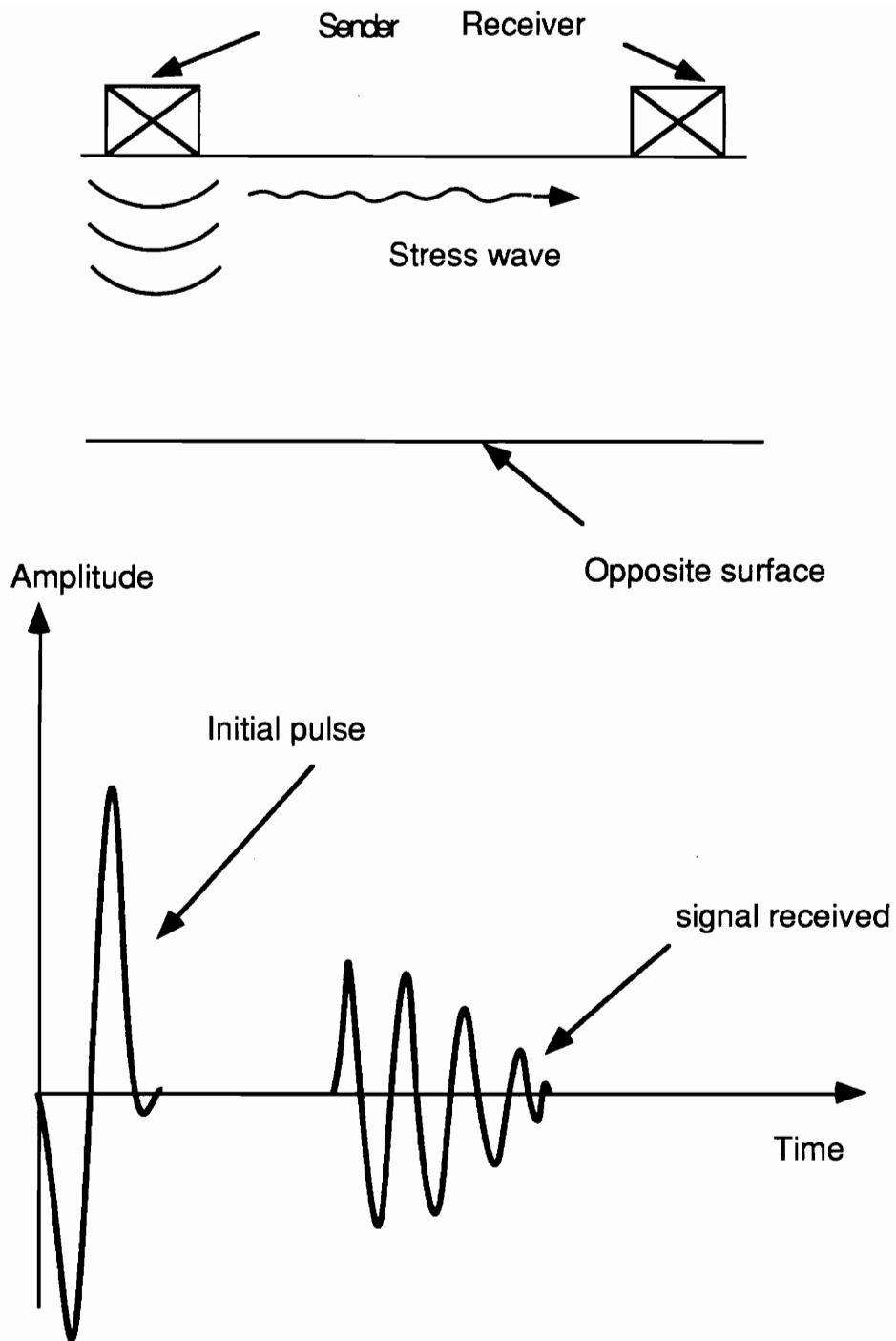


Figure 6. A schematic of the acousto-ultrasonic technique.

parameters defined by Vary¹⁰ is known as stress-wave factor (SWF) and is given by the expression:

$$SWF = RTC$$

where R = repetition rate of input waveforms

T = predetermined time interval

C = number of oscillations in the received waveforms that exceed a preselected voltage threshold.

Others AU parameters known as moment parameters^{11,27} are given by the expression:

$$M_n = \int_0^{f_{\max}} W(f) f^n df$$

where W(f) = power spectral density function

f = frequency

f_{max} is the maximum frequency, or Nyquist frequency

Theoretically, M₀ represents the area under the power spectral density curve and thus is a measure of the energy of the signal. M₁/M₀ correlates to the centroid of the power spectral density curve. Physically, it indicates the center frequency of the signal relative to the amount of energy. For example, a signal with a higher M₁/M₀ value would be a signal with proportionally more energy transferred at higher frequencies.

2.1.4 Damage monitoring

Monitoring of fatigue cracks in parts during laboratory tests and while in service in the field has been extensively performed using the ultrasonic technique. The pulse-echo technique has been used to monitor fatigue cracks in pressure vessels in laboratory tests⁴¹. These techniques use several overlapping angle-beam (shear wave) search units, which are glued in place to ensure reproducible results as fatigue testing proceeded. The in-service monitoring of fatigue cracking of machine components is often accomplished without removing the component from its assembly. For example, 150 mm dia., 8100 mm long shafts used in pressure rolls in papermaking machinery developed fatigue cracks in their 500 mm long threaded end sections after long and severe service²⁵. These cracks were detected and measured at 3-month intervals, using a contact-type straight-beam search unit placed at the end of each shaft, without removing the shaft from the machine. When the cracks were found to cover over 25% of the cross section of a shaft, the shaft was removed and replaced. In another case²⁵, fatigue cracking in a weld joining components of the shell of a ball mill 4.3 m in diameter by 9.1 m long was monitored using contact-type angle-beam search unit. The testing was done at 3-month intervals until a crack was detected; then it was monitored more frequently. When a crack reached a length of 150 mm, milling was halted and the crack repaired.

2.2 Piezopolymer

2.2.1 Structure

Poly(vinylidene fluoride) (PVDF) is a long chain semi-crystalline polymer^{21,22,28} with the repeat unit (CF₂-CH₂). It exhibits four crystalline forms: β (or I), α (or II), γ (or III) and α_p (or IIp) among which only α and β are common forms.

The α phase, which is non-polar, results when the polymer is cooled from its melt. The polar β phase may be produced by deforming the α crystallites. To obtain significant piezoelectricity, PVDF must be stretched to get the polar β phase and then poled in a high static electric field at high temperature (80 to 150°C). The level of piezoactivity depends on the amount of stretch, poling time, field strength and temperature.

2.2.2 Properties

The piezoelectric effect²⁰ can be explained by the model shown in fig. 7. In this figure two dipoles with their respective polarities represent the net dipole within a unit volume of piezofilm. When the unit volume is placed in tension, the net film volume increases, resulting in lower charge density at the positive and negative electrode surfaces. To achieve electrical neutrality, electrons flow out of the top electrode and into the bottom electrode. The reverse

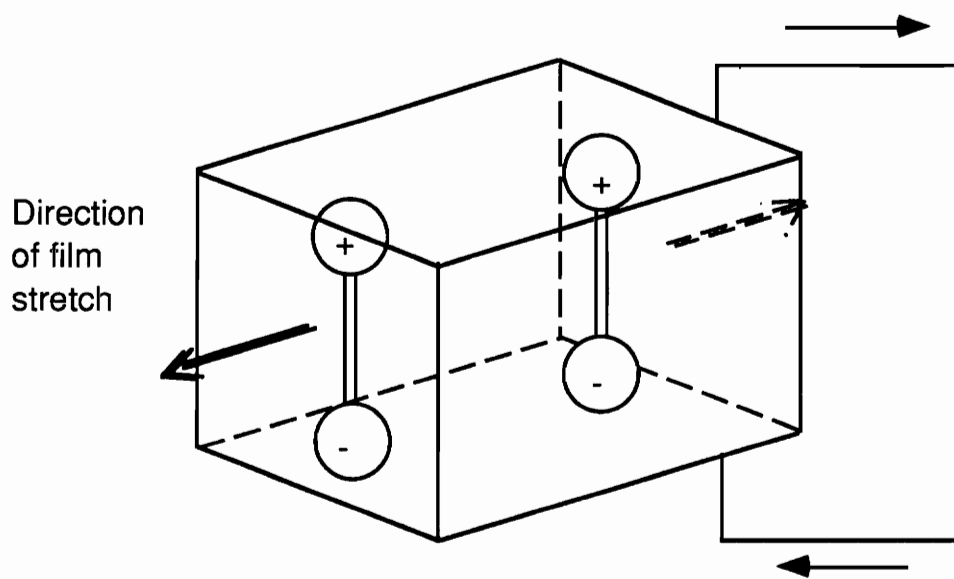
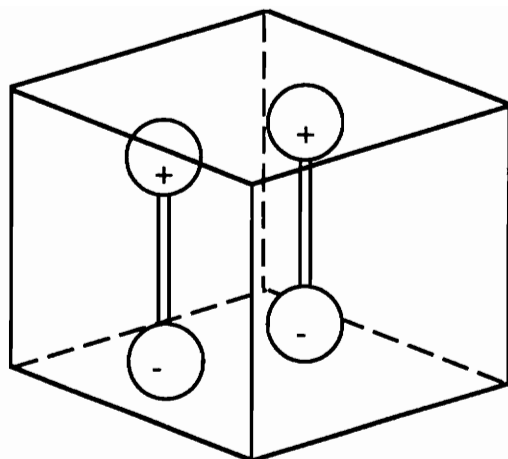


Figure 7. Net dipole within a unit volume of piezofilm.

occurs in compression.

Piezoelectric materials are anisotropic^{20,21,29} (fig. 8 shows the film's axes: 1 corresponds to length, 2 to width, and 3 to thickness) and are characterized by the following piezoelectric constants:

- Piezoelectric strain tensor d:

when a field is applied to piezofilm, the film dimensions change in all three axes under stress-free conditions. The degree to which these dimensions change relative to the applied field depends on the d tensor. So d is the stress-free ratio of developed strain to applied field. For example,

$$d_{31} = \frac{\text{Strain developed along 1 axis}}{\text{Field applied along 3 axis}} \left(\frac{\text{m/m}}{\text{V/m}} = \frac{\text{m}}{\text{V}} \right)$$

- Piezoelectric stress tensor g:

The g tensor expresses the negative of the electric field developed under open circuit conditions by the film relative to the stress applied along a specific axis. Thus g is the ratio of the negative of the induced field to applied stress.

$$g_{31} = - \frac{\text{Field developed along 3 axis}}{\text{Stress applied along 1 axis}} \left(\frac{\text{V/m}}{\text{N/m}^2} = \frac{\text{Vm}}{\text{N}} \right)$$

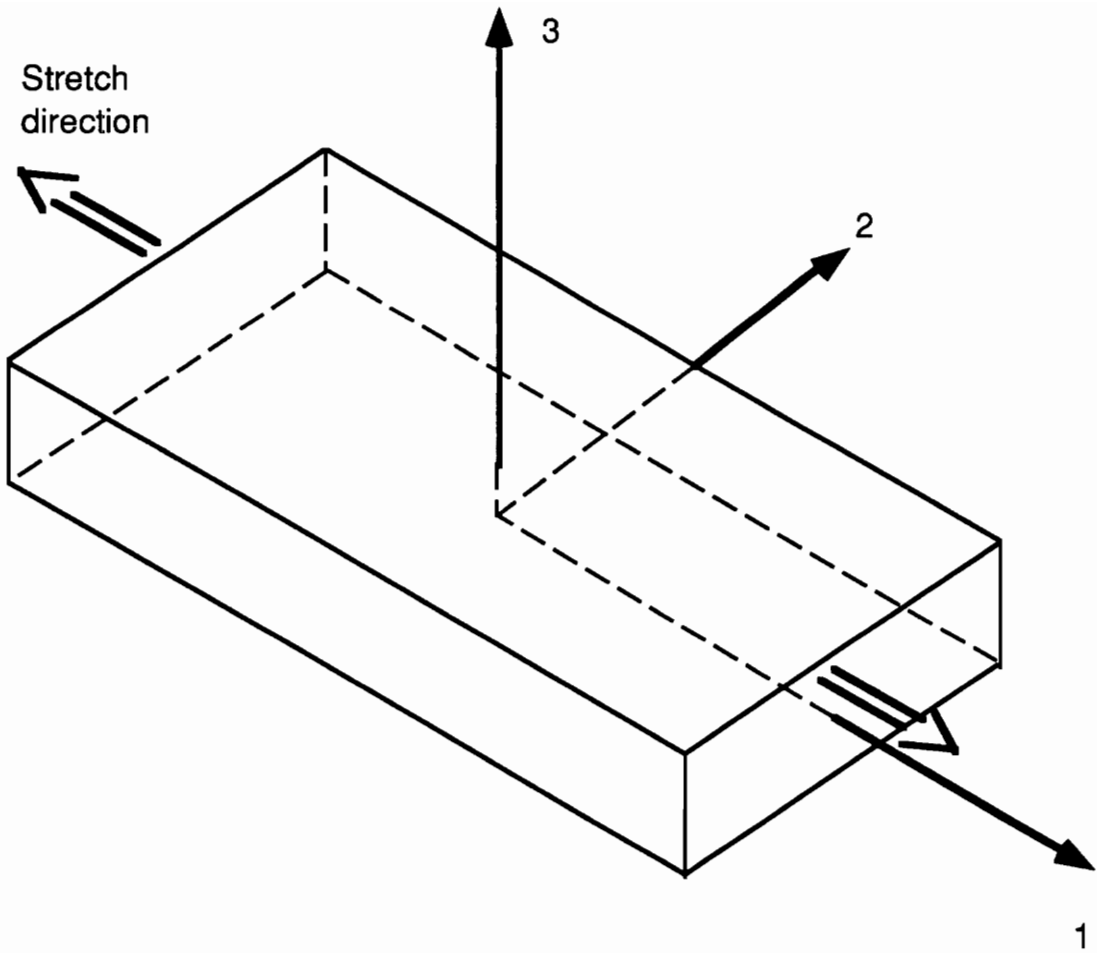


Figure 8. Axis designation.

- Electromechanical Coupling Factor k:

Coupling is an expression for the ability of a piezoelectric film to exchange electrical energy to mechanical energy and vice versa. For instance:

k^2_{31} is the transformed electrical energy causing mechanical strain in the 1 direction divided by electrical energy input in the 3 direction.

k^2_{31} is also the transformed mechanical energy causing electrical charge to flow between connected electrodes in the 3 direction divided by mechanical energy input through the application of stress in the 1 direction.

According to table 1, one might think that PVDF would be inadequate for NDE applications because of its low d-constants. Although PVDF has almost an order-of-magnitude lower d-constants than PZT, the maximum field strength that can be applied to the polymer is about 100 times greater. Therefore the maximum strain achievable with PVDF transducers is 10 times larger than for ceramics. Furthermore because of the small dielectric constant of PVDF, its g-constants are high and the electromechanical coupling factors k_{31} and k_{33} reach values of 12 and 20 %. Although k_{31} and k_{33} are low compared to ceramic transducers, piezo film can be used at much higher electric fields than ceramics.

Table 1. Comparison of typical piezoelectric material properties¹³⁻¹⁵.

Property	Unit	PVDF	PZT	BaTiO ₃
Density	g/cm ³	1.78	7.75	5.7
Dielectric Constant	ϵ/ϵ_0	12	1700	1700
Sound velocity	m/s	2200	3780	5000
d ₃₁	10 ⁻¹² C/N	23	120	78
d ₃₃	10 ⁻¹² C/N	30	375	190
g ₃₁	10 ⁻³ mV/N	216	10	5
g ₃₃	10 ⁻³ mV/N	300	25	13
k ₃₁	%	12	30	21
k ₃₃	%	20	50	21
Acoustic impedance	10 ⁶ kg/m ² s	2.7	30	30

The other advantages of piezoelectric PVDF are as follows:

- flexibility: it withstands mechanical shocks.
- small density and thickness makes PVDF sensors lightweight.
- ease of processing: it is available in a wide variety of thicknesses and has almost no limitation on size or curvature.
- wide frequency range: 0 to 10^9 Hz.
- low acoustic impedance: it offers good acoustic matching to water, body tissues, composites, and polymers (see table 2).
- high break-down strength: it withstands high input power.
- high stability: it resists moisture and most chemicals.
- moderately low raw material and fabrication costs.

Among the drawbacks of PVDF are its relatively poor electrical stability which is, in part, due to mechanical relaxation. This makes long-term measurements of weak signal somewhat problematic. Also the service temperature of PVDF is limited to about 80°C. Moreover exposed electrodes are sensitive to electromagnetic radiation (which could be overcome by shielding the sensors)³⁰ as well as moisture (which could be solved by using gold electrodes)³¹.

Table 2. Acoustical properties of common materials²⁰.

Material	Longitudinal velocity (m/s)	Acoustic impedance (MRayls)
METAL		
Aluminium	6300	17
Steel	5800	45
POLYMER		
Plexiglas	2700	3.2
Epoxy	2500	3
Silicone	940	1.4
Polyurethane	-	1.9
COMPOSITE MATERIALS		
Fiberglas	3100	6
Graphite/epoxy	3000	4.6
Boron/epoxy	3300	6.4
LIQUIDS		
Water	1500	1.5
GASES		
air	330	0.0004
PIEZO. MATERIALS		
PVDF	2200	2.7
Ceramic	3200	24

3.0 PVDF TRANSDUCER DESIGN

The Kynar[®] PVDF films can be obtained from the Pennwalt Corporation (currently Atochem North America) in stretched, poled and electroded form. They are available in different thicknesses and are coated on both sides with conductive metals to provide intimate electrical contact. The metallic layers are vacuum deposited and can include the following metals: copper, silver, nickel, aluminium, chromium, and gold

The PVDF film used in our experiments was 52 μm thick and coated with a 200-400 \AA thick copper-nickel alloy.

3.1 *Electrode pattern*

Patterns must be etched so that electrical leads can be attached to the active part of the sensors. As specified in Pennwalt's application note³², there are several ways to etch off the metallic layer to achieve the desired electrode pattern:

OPTION 1:

- hand paint desired pattern, with brush and enamel paint or indelible marker.
- allow to dry.
- do the same on the other side.
- dip marked film in dilute solution of FeCl_3 .
- rinse with water.
- to remove paint, use toluene or lacquer thinner.

OPTION 2:

- silk screen pattern on film - with ink designed for vinyls - such as is typically available for decals.
- continue as above and use lacquer thinner to remove ink.

OPTION 3: photo etching

- procure photo resist solution called photoposit.
- coat film with the emulsion.
- make positive artwork on transparent substrate such as with Rubylith or Photographic Reproduction Artwork.
- expose both sides of film through artwork to ultraviolet light.
- develop film, by dipping in developing agent, such as with PC board developer.
- etch in FeCl_3 .
- Rinse with lacquer thinner to remove photo resist.

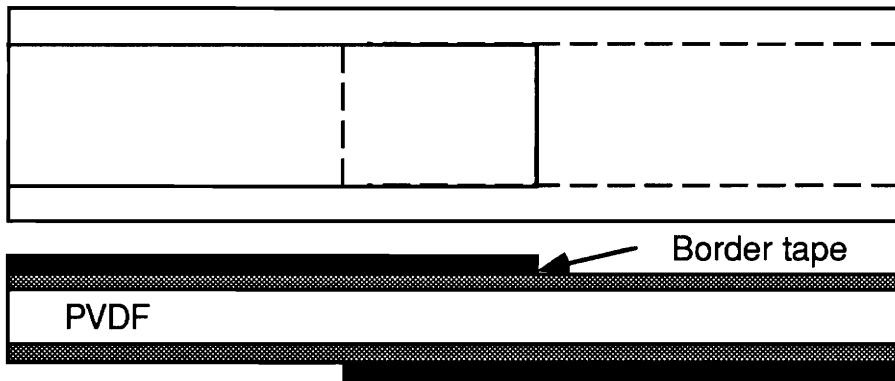
The electrode pattern of our sensors are prepared differently. The following method has the advantage of being simple and quick. Although this method cannot produce as intricate patterns as the photoetching method, it can produce 0.75 mm or wider sensors (see fig. 9).

- put border tape (Letraline) on the desired pattern on both metallic layers.
- dip marked film in dilute solution (95% of water) of FeCl_3 (etchant made by Archer) enough time to allow FeCl_3 to remove the metallic layer (approximately 2 seconds).
- rinse immediatly with water for 5 seconds.
- dry the film with paper napkin.
- remove slowly the border tape to avoid damaging the metallic layer.

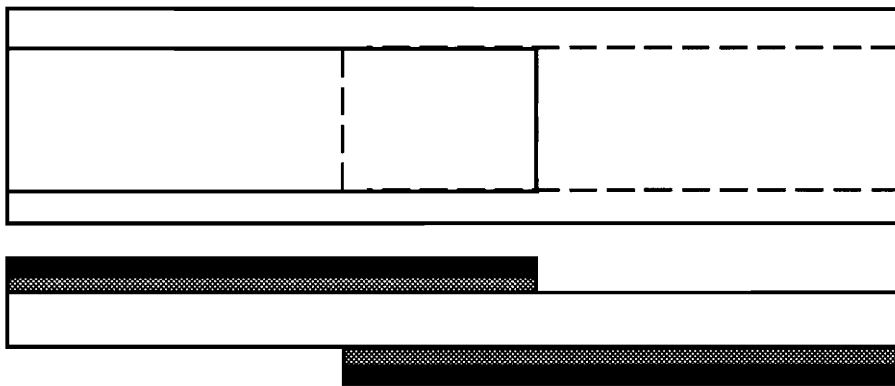
One important precaution is that PVDF film must never be touched by bare hands (use latex gloves). The sweat in the skin can affect the metallic layer.

3.2 Electrical lead attachment

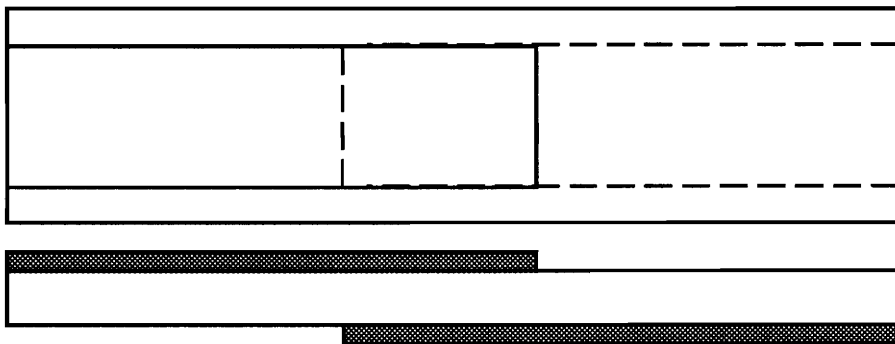
Pennwalt's application note number 20³³ shows several lead-attach methods which are summarized as follows:



i - Border tape is put where the metallic layer is to stay



ii - FeCl3 removed part of the metallic layer



iii - obtained sensor

Figure 9. Different steps to obtain the desired sensor.

A. Penetrative methods:

- "POP" or "blind" rivets.
- nuts and bolts.
- eyelets.
- crimp connectors.

B. Non-penetrative methods:

- conductive-adhesive coated copper foil tape (e.g. 3M #1181).
- conductive transfer tape (e.g. 3M #9702)
- conductive epoxy.
- low melting temperature alloy.
- "zebra" connectors: conductive rubber spliced with insulating rubber as used to form contacts to LCD displays.
- mechanical clamping (alligator clips...)

Our sensors were connected to electrical leads by using copper foil tape (3M #5012 AB) or copper foil tape with conductive epoxy (TRA-CON #BA-2916) for experiments dealing with detection of water inside the bond. When compared to the copper foil tape connection, the latter seems to be less sensitive to moisture.

As recommended by Pennwalt³³, a "reasonable" area (40 mm²) of tape was used in order to have a good electrical contact between the metallic layer and the tape (fig. 10). The obtained sensors were then connected to electrical devices by alligator clips.

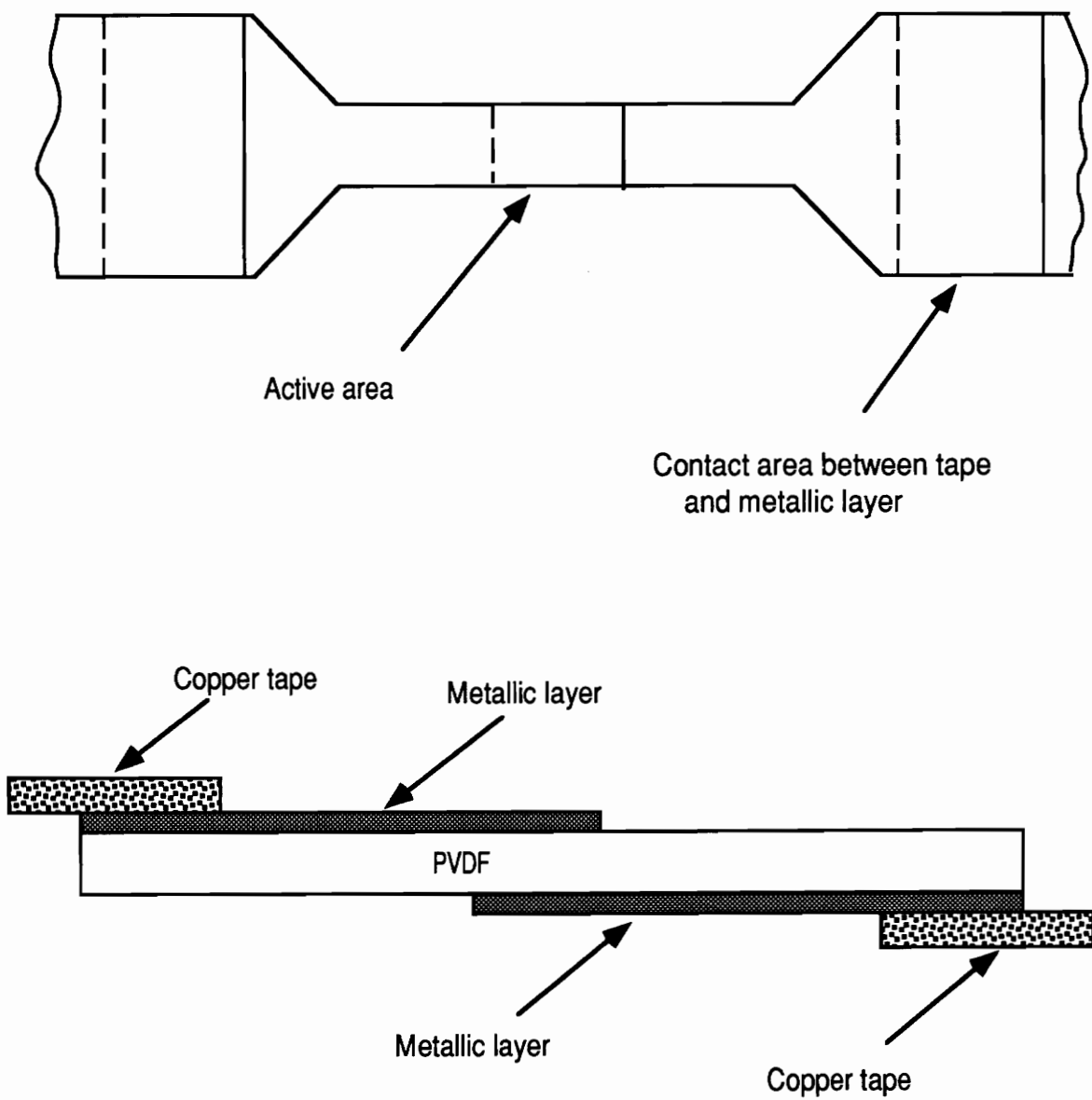


Figure 10. Sensor design for the electrical connection (not to scale).

3.3 Sensor design

3.3.1 Size of the active area

A 12.5 X 12.5 mm PVDF sensor has been bonded to a 8 mm thick piece of plexiglas. Its pulse-echo signal has been taken by a data acquisition system shown in fig. 23 after each decrease of its active area. This has been done by removing part of the metallic layer with a solution of FeCl₃. The results show that the amplitude of the pulse-echo signal is proportional to the size of the sensor (fig. 11). The size of a sensor is influenced by three factors:

- medium: The attenuation of a signal is different from one medium to another. For instance, plexiglas attenuates ultrasonic signals more severely than metal. Therefore, a larger size sensor will be needed for plexiglas.

- path of the signal: Signals will be more attenuated by a long path than a short one. Therefore, the size of the sensor will depend on the path of the signal being studied.

For instance, the minimum size of PVDF sensors traveling through a 14 mm thick piece of plexiglas has been found to be 1.6 X 1.6 mm. In the case of a 0.8 mm thick graphite epoxy (AS4/J2), the minimum size of PVDF sensors had the dimensions: 3mm X 3mm.

- purpose of the study: if the location of a crack is to be detected then one needs an array made with small sensors. If the operator wants just to detect cracks in the structure and does not

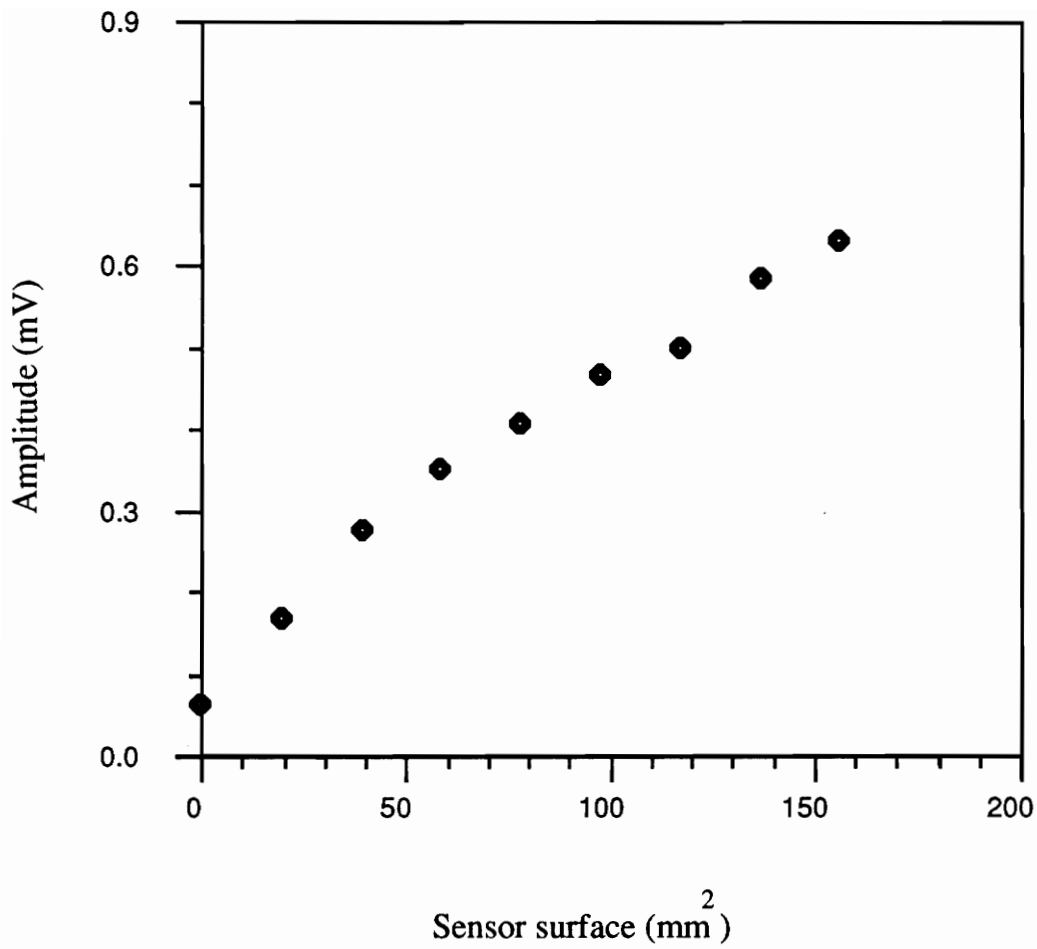


Figure 11. Influence of sensor's size on the amplitude of the signal.

care about their specific locations then one can use a big sensor covering the whole surface studied.

3.3.2 Shape of the sensor

The shape of the sensor depends on the purpose of the study. If the size of a sensor is restricted in only one direction then its surface can be extended in the other direction to get a better signal. For example, in the experiment to detect the ingress of water (appendix A), long PVDF sensors were used to interpret the effect of ingress of water in the direction perpendicular to the ingress as shown in fig. 12. In the characterization of an adhesive joint by the acousto-ultrasonic method, long PVDF sensors were also used to get a better signal as shown in fig. 13.

3.4 Embedment

One of the objectives of our study was to identify a proper technique to embed the sensors in or near the bondline. Adhesively bonded joints were fabricated with three 1.5mm X 10 mm PVDF sensors imbedded in the bondline between two plexiglas plates, as shown in fig. 14, to detect moisture absorption in the adhesive bond. To improve the wettability of PVDF metallic layers³⁴ for better bonding, a plasma treatment was applied (2 minutes of Argon).

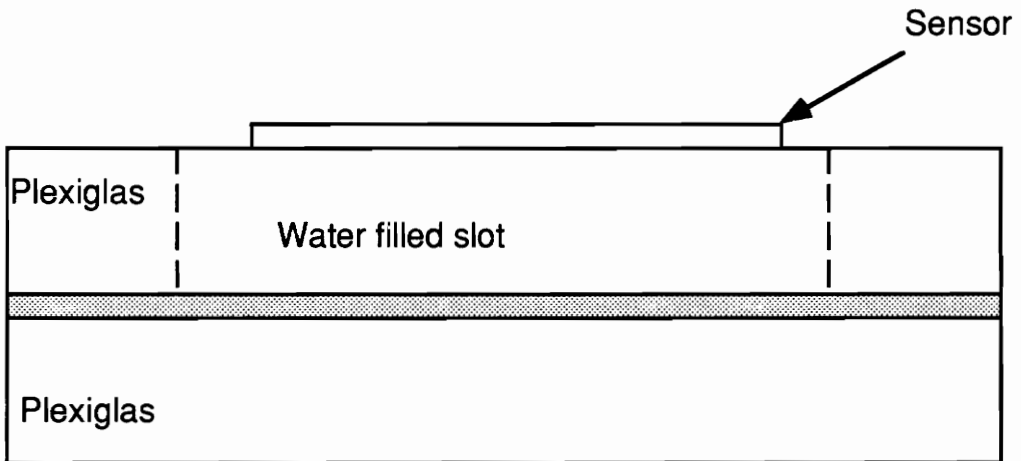
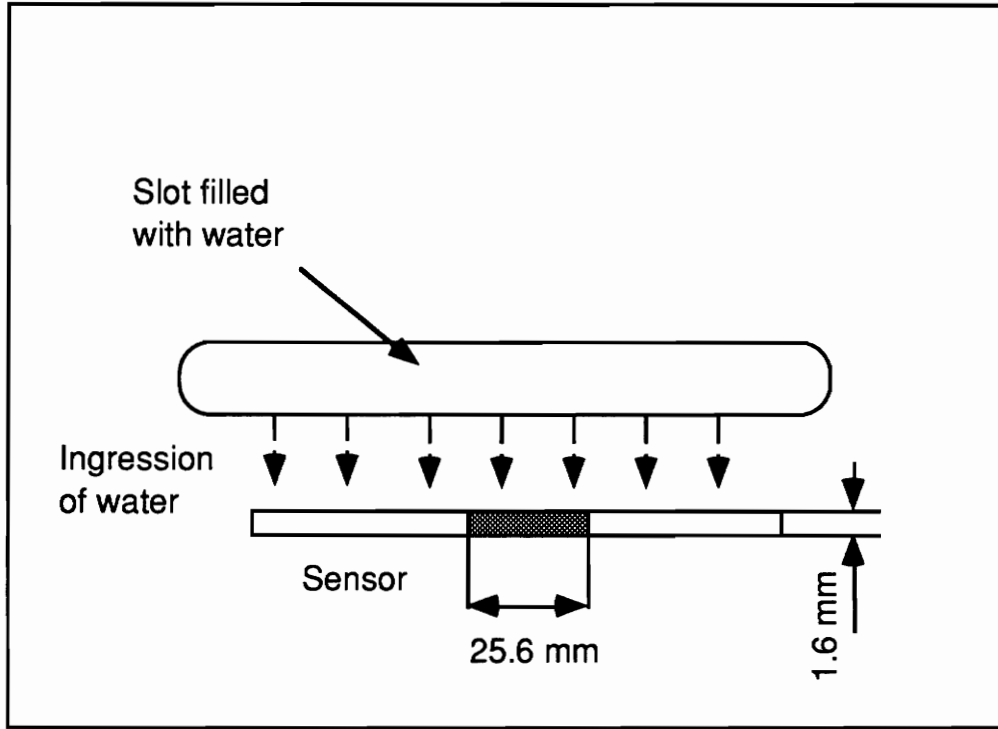


Figure 12. Shape of sensor to detect water ingress (not to scale)

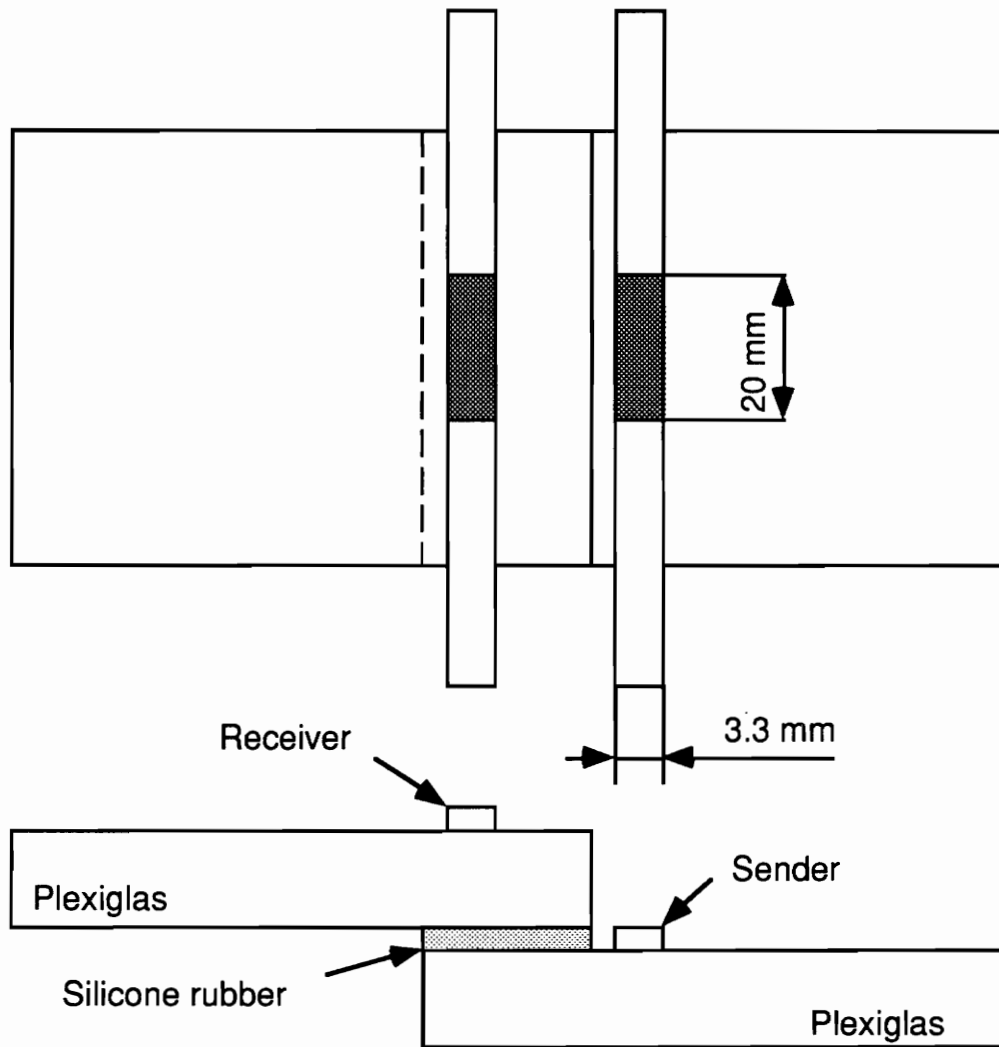


Figure 13. Shape of the sensors for the characterization of a joint by AU technique (not to scale).

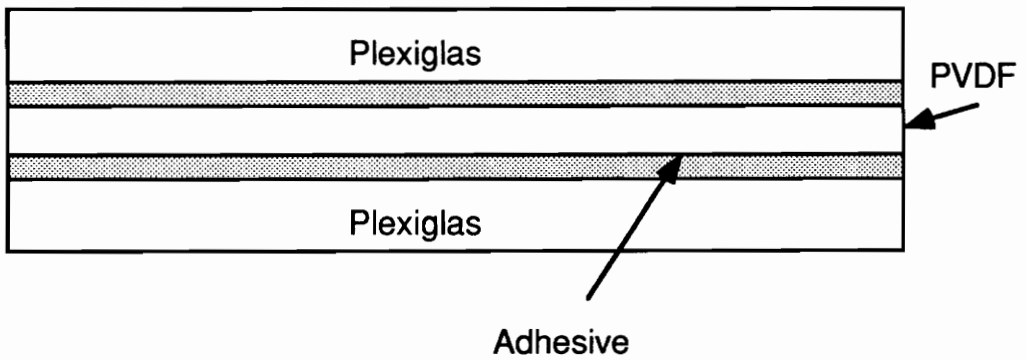
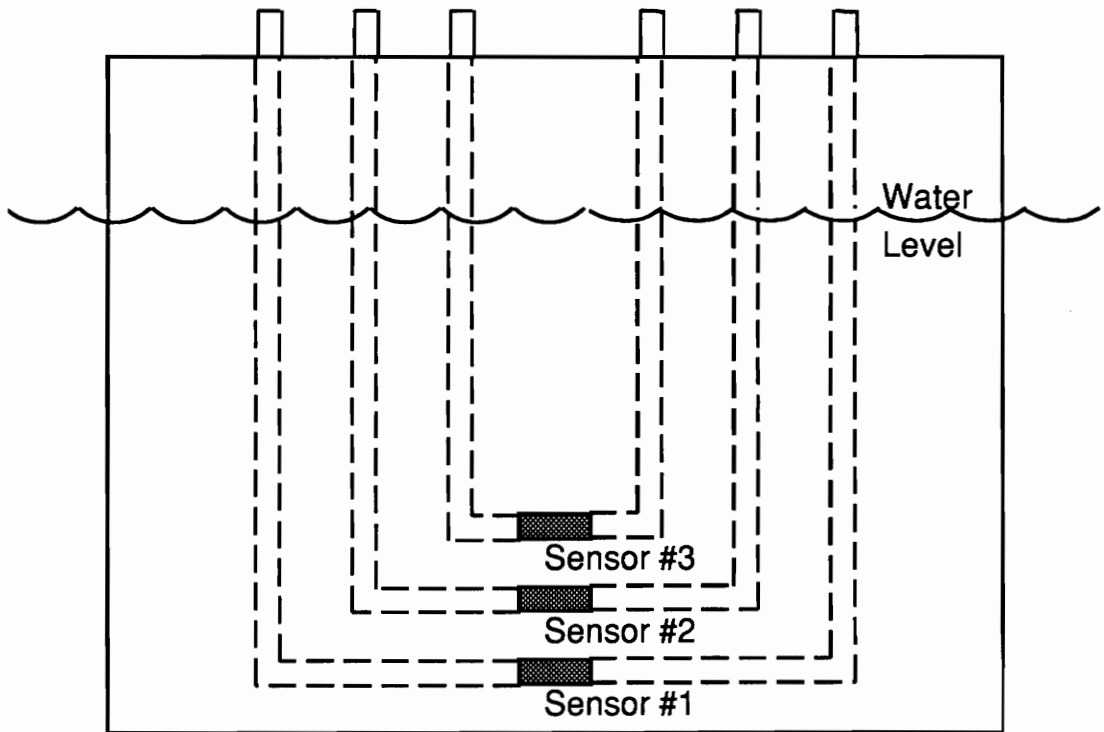


Figure 14. Schematic diagram of the adhesively bonded joint with PVDF sensors inside to detect moisture absorption in the adhesive bond.

The specimens were put in a moist environment for a few days and signals of the three different sensors were taken. The results were unsatisfactory: moisture corroded the metallic electrodes the adhesive bonds. Big chunks of the electrodes disappeared after the specimens were put into a moist environment for several days. On the other hand, the electrical contact between the copper foil tape and the PVDF electrodes was also affected by the moisture: the copper tape seemed to debond and pressure on the contact area was needed to get a signal.

It became necessary to monitor moisture absorption with PVDF sensors attached on the exterior of the structure. Another solution would have been to coat the electrodes with water-resistant coatings or to use inert electrodes (for instance gold like for PZT transducers). As far as mechanical damage monitoring is concerned, PVDF sensors were also attached to the exterior of the joint since inherent problems remain for bonding PVDF sensors within highly loaded structural bonds³⁵. Indeed experiments were carried out in our laboratories³⁴ which conclude that even if plasma treatment improved the adhesion of PVDF films inside the bondline, it still weakened the strength of the resulting bond.

Our sensors were bonded to the material using a cyano acrylate (M-bond 200, Measurements Group, Inc., Raleigh, N.C.) adhesive. This adhesive is easy to use and cures at room temperature in less than

Our sensors were bonded to the material using a cyano acrylate (M-bond 200, Measurements Group, Inc., Raleigh, N.C.) adhesive. This adhesive is easy to use and cures at room temperature in less than one minute. Since it is very sensitive to moisture, cyano acrylate is not recommended for long-term experiments. Information concerning adhesives is available from Pennwalt³⁶. The PVDF sensors may also be protected from finger prints by putting an adhesive tape on the top of the sensors (fig. 15).

Recommendations from literature and experiments done in our laboratories are gathered together in a fact sheet (appendix B)

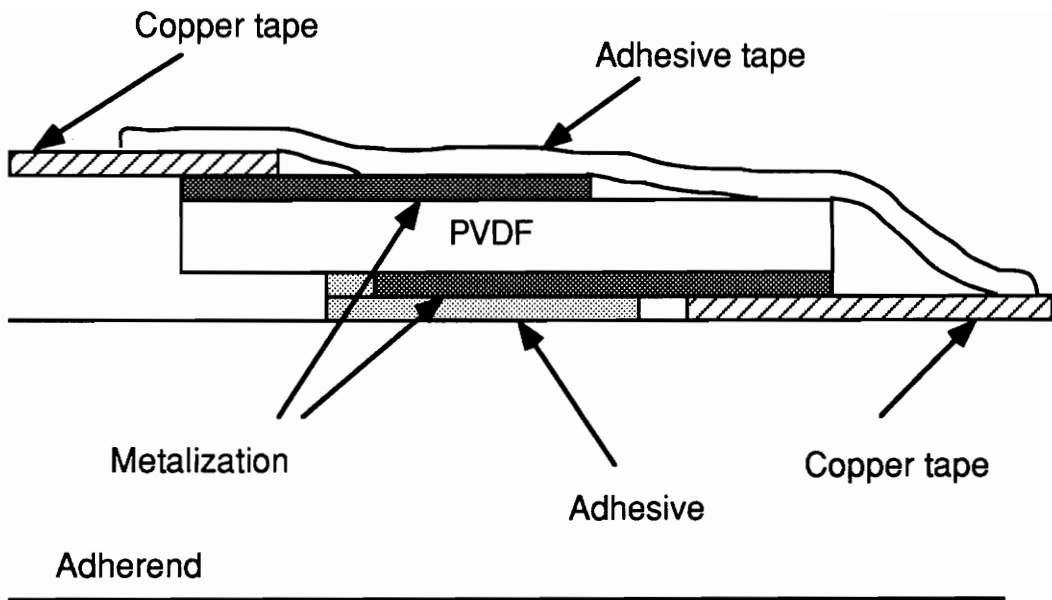


Figure 15. Typical PVDF transducer used in our experiments (not to scale).

4.0 CHARACTERIZATION OF ADHESIVE JOINTS BEFORE SERVICE

The two experiments described in this chapter do not deal with the detection of adhesive joint damage due to mechanical or environmental exposure but with the determination of the bond quality before service. During preliminary studies, it was found that PVDF sensors could be used in through-transmission mode to detect porosity in adhesive joints. Moreover, PVDF films were also successfully used in pulse-echo mode to detect the setting of an adhesive. These could be of great interest in determining the quality of a bond.

4.1 Porosity study

A urethane adhesive (3549 B/A, 3M, St. Paul, MN.) lap joint was fabricated with two 90 mm X 100 mm X 5 mm plexiglas adherends with two 3.5 mm X 3.5 mm PVDF sensors located on the outside of the joints. The specimen was clamped at both ends to assure pressure during the curing period and a 100 μ m thick teflon

spacer was placed along one edge to create a difference of thickness in the joint. Sensor #1 was glued on the area where the bond was thick with many air bubbles whereas sensor #2 was glued on the area where the bond was thin with few air bubbles to see if it was possible to detect any difference (see fig. 16). Indeed an incident pulse of ultrasound will be reflected and transmitted at each interface of the joint. The amplitudes of the reflected and transmitted pulses are dependent¹ on the reflection coefficient of the interface which may be calculated from

$$R = \left| \frac{Z_1 - Z_2}{Z_1 + Z_2} \right|$$

$$T = 1 - R$$

where R = reflection coefficient
 T = transmission coefficient
 Z = ρV = acoustic impedance

If a defect is assumed to contain air or any other low density substance, then it will have a very low acoustic impedance relative to the adherend or the adhesive. At a boundary between either an adherend or the adhesive and a defect, the reflection coefficient approaches unity. An incident pulse at the defect is then practically totally reflected leaving negligible energy to be transmitted through

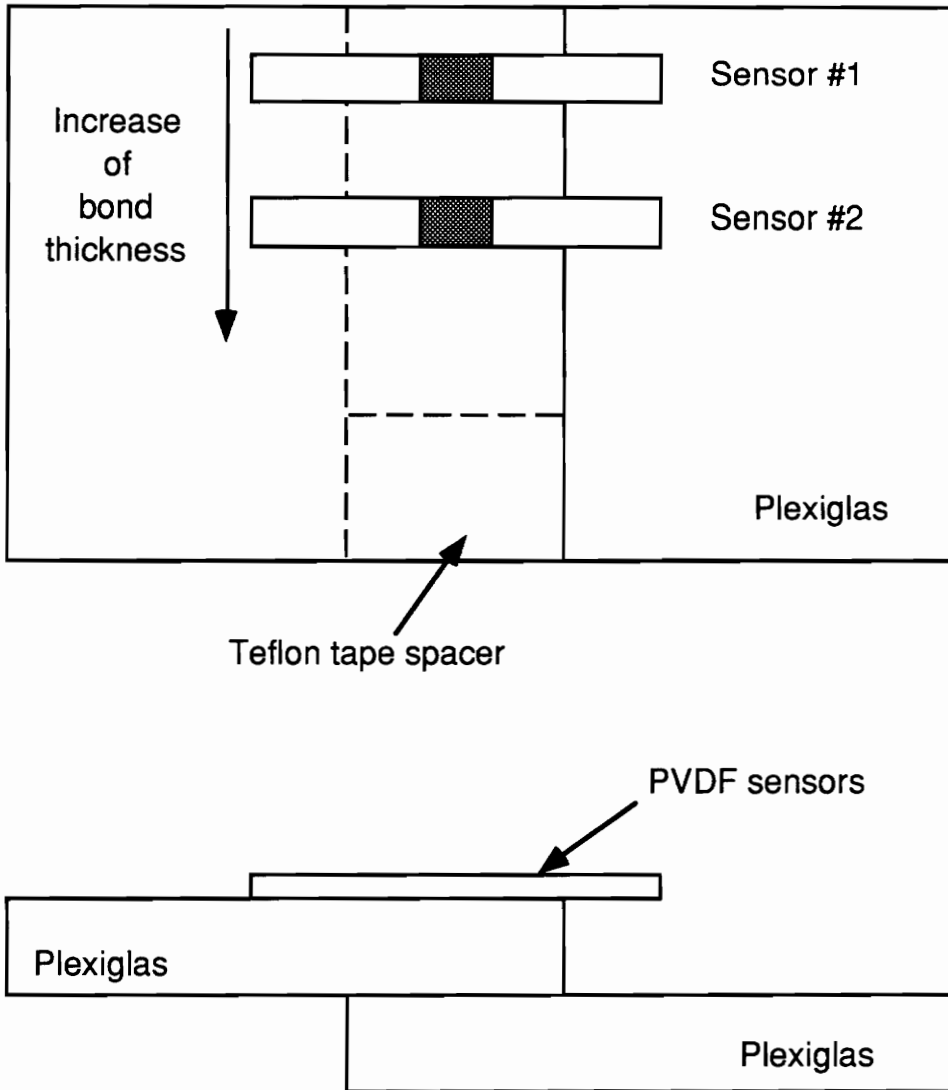


Figure 16. Schematic diagram of the specimen.

the defect. Measurement of the reflected or transmitted energy may therefore be used to indicate the presence of a defect.

Ultrasonic pulses were sent from the opposite side of the joint by a 12.7 mm (0.5 in.) dia., 2.25 MHz PZT ceramic transducer in a through-transmission mode. The signals sent by the ceramic transducer through a pulser-receiver ACCU-TRON model 1010PR and received by the PVDF films were observed using an oscilloscope (Tektronik 2230) (see fig. 17).

Figures 18 and 19 show the ultrasonic signals for urethane bonded joints with many air bubbles and few air bubbles in the adhesive bond respectively. These diagrams were not traced from actual data but represent the signal which was visually observed on the oscilloscope.

In the case of receiver #1, the glue was so thin, due to the applied pressure, that there were few air bubbles (see micrograph of the bond in fig. 20). As the acoustic impedance of urethane is close to that of plexiglas, there was almost no acoustic impedance mismatch at the interface and thus there was very little reflection of the signal by the joint (the oscilloscope didn't detect it); the main part of the signal was transmitted (see fig. 18).

In the case of receiver #2, the glue was much thicker and contained a lot of air bubbles (see micrograph of the bond in fig. 21). Because of them, part of the signal sent by the crystal went through

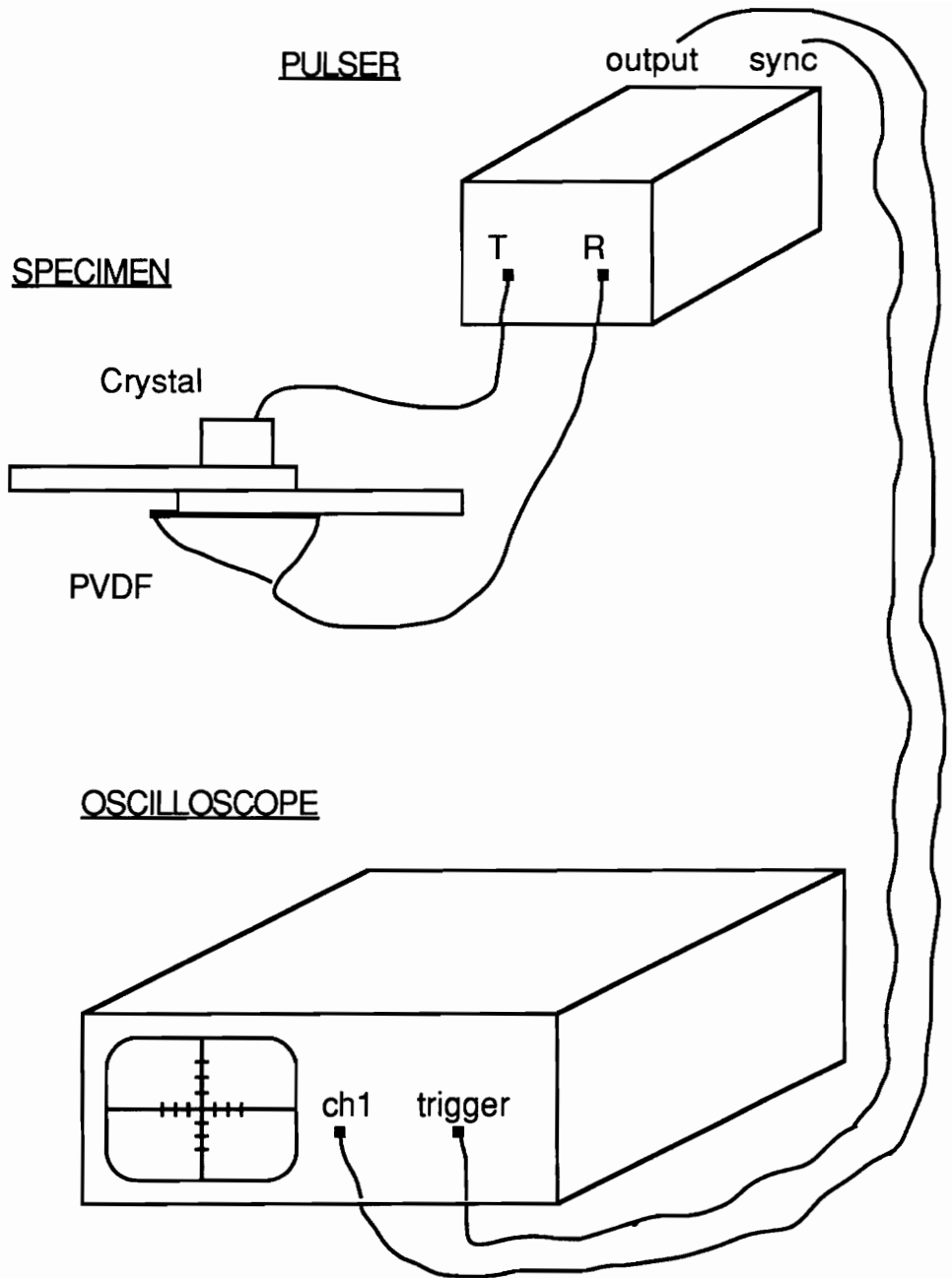


Figure 17. Schematic diagram of the experiment.

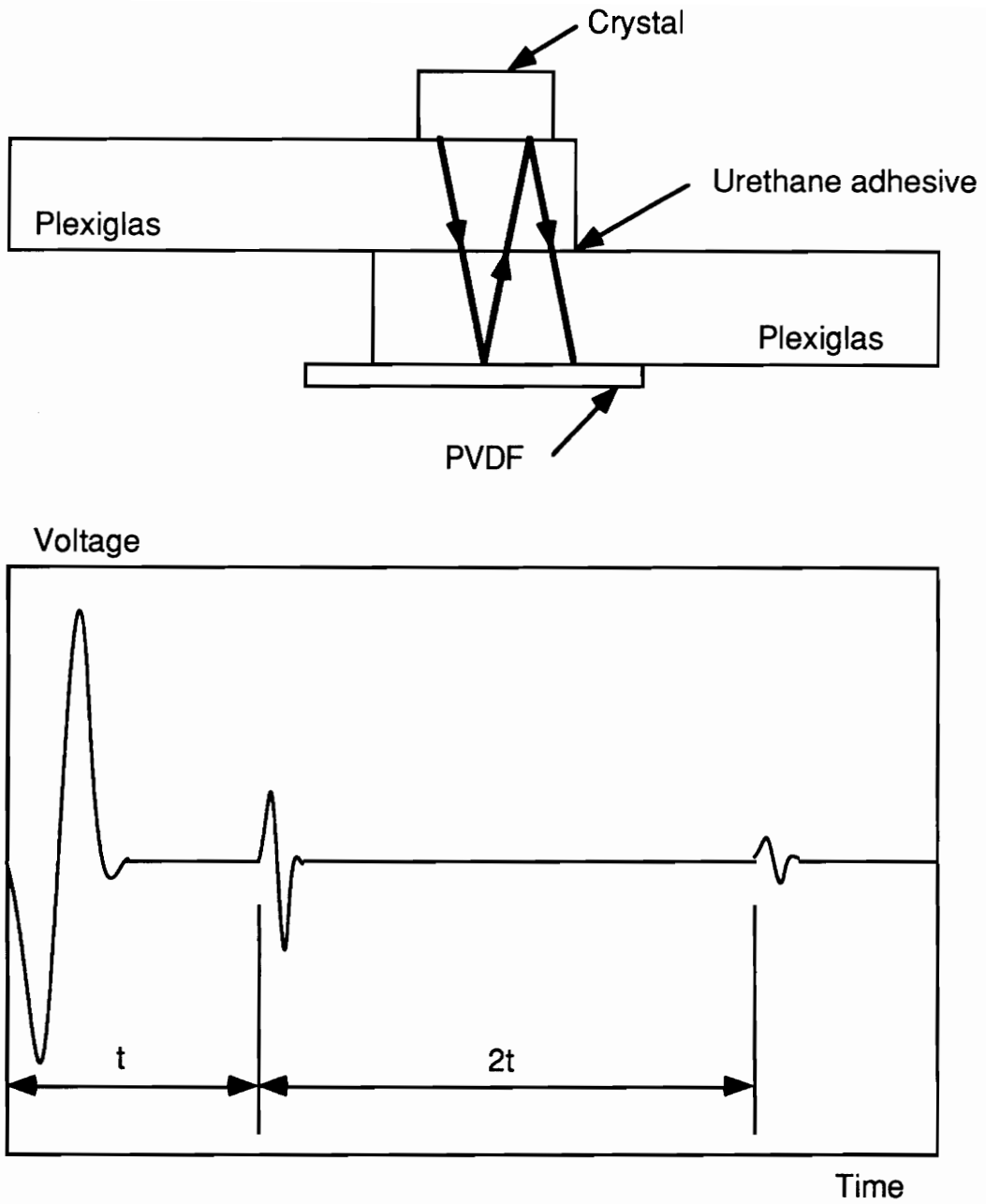


Figure 18. Schematic diagram of the ultrasonic signals for urethane bonded joints with few air bubbles in the adhesive bond.

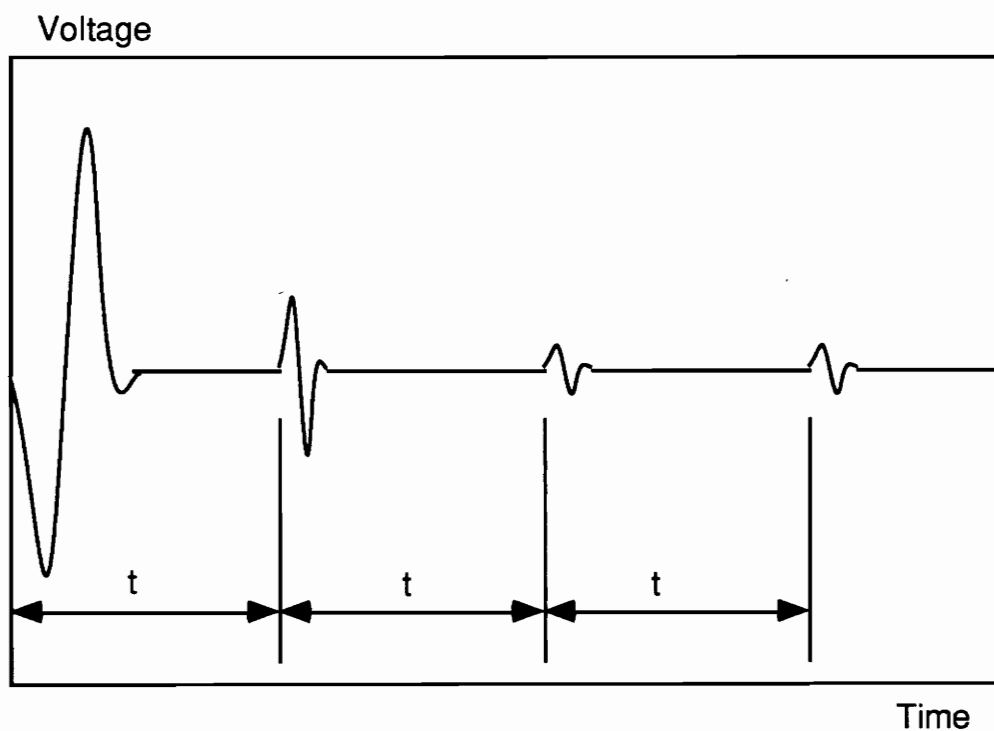
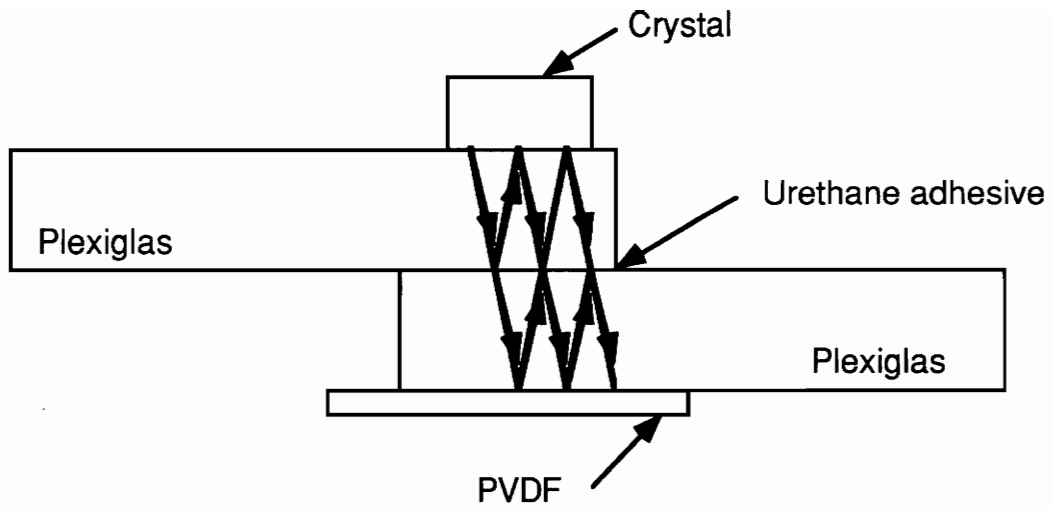


Figure 19. Schematic diagram of the ultrasonic signals for urethane bonded joints with many air bubbles in the adhesive bond.

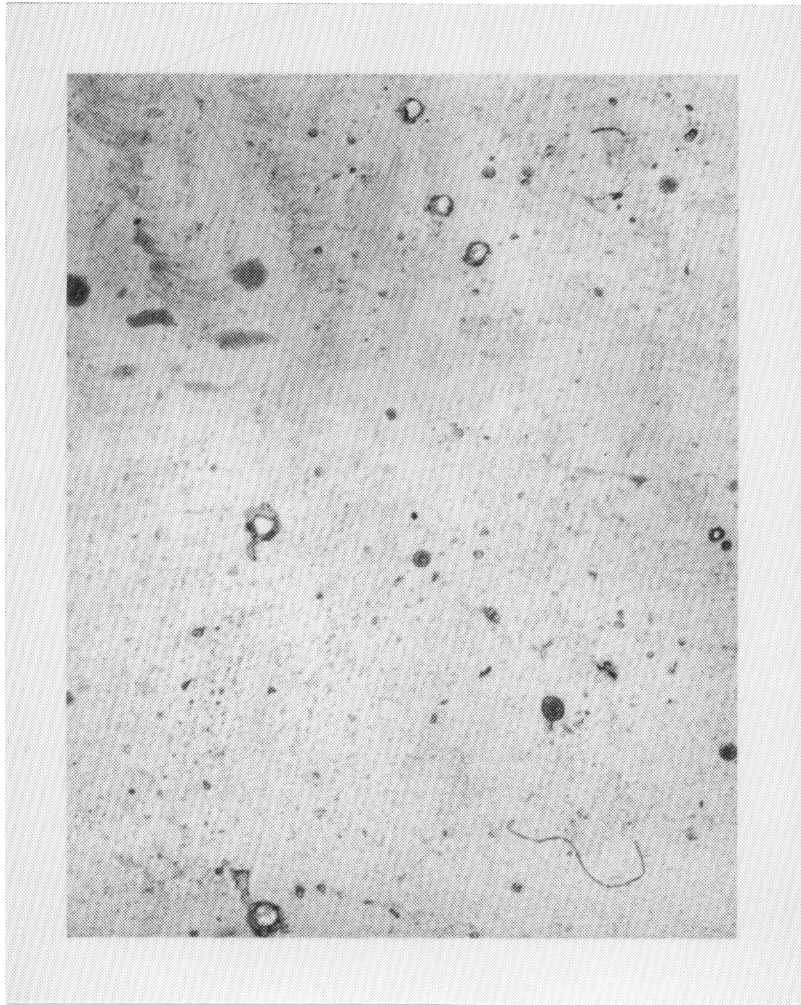


Figure 20. Micrograph of the urethane adhesive bond with few air bubbles.

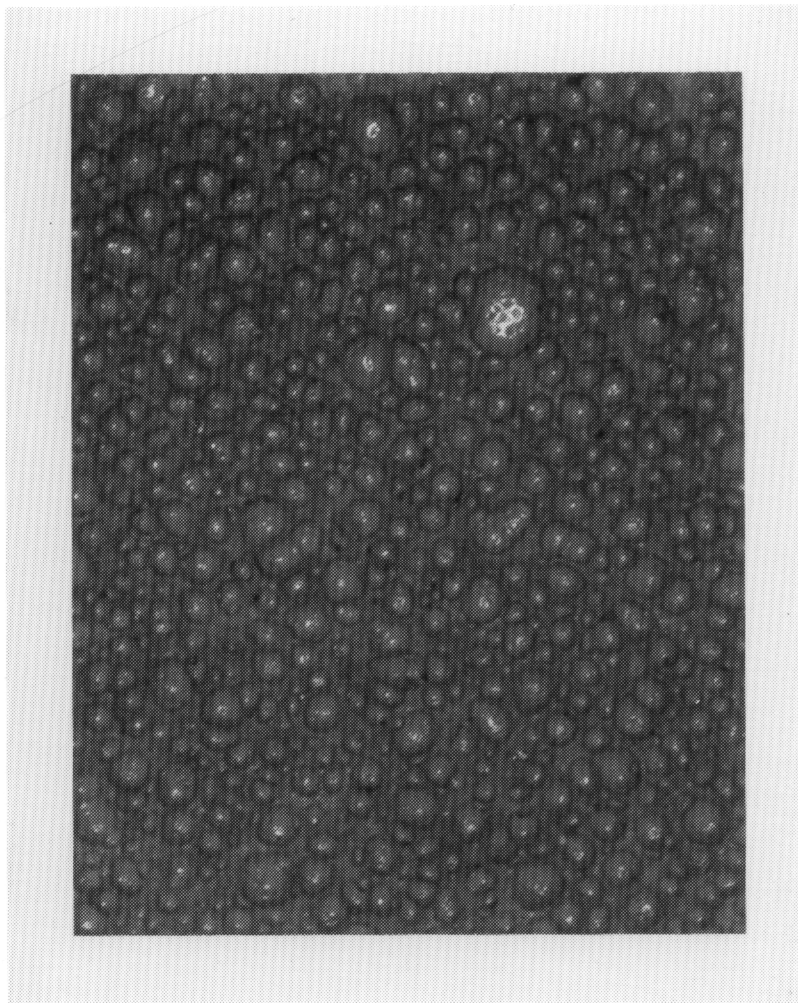


Figure 21. Micrograph of the urethane adhesive bond with many air bubbles.

the joint and the other part was scattered by the air bubbles which created an acoustic impedance mismatch (see fig. 19).

This experiment showed that PVDF could detect the porosity of a bond. Since PVDF transducers are very cheap compared to ceramic ones and since they give good results in pulse-echo mode according to other experiments described later, PVDF sensors could be permanently attached during manufacture of the structure and thus check the quality of numerous joints before and during service. It would be a simple, and quick nondestructive evaluation: the operator would just have to connect some cables from a data acquisition system which would analyse the quality of the bond. In this technique, drawbacks relative to ceramic transducers such as special set-up, the use of weights and couplants are avoided.

4.2 Setting of adhesive

Many defects occurring in an adhesive bonded joint can be due to problems with curing such as overcure/undercure, mix ratio variations and incorrect formulation. These defects are often quite subtle and are difficult to find using conventional techniques. Yet they can influence performance considerably. It then becomes necessary to control the quality of viscoelastic properties of the adhesive in the course of curing and to perform real-time continuous monitoring over the entire range of variation of adhesive properties. The use of ultrasonic velocity and attenuation measurements for cure monitoring has been already investigated³⁷⁻³⁹ using regular piezoelectric transducers. The authors showed the success of these techniques and their possible applications for the characterization of adhesives.

The purpose of our experiment was to monitor the curing of a 5 minute epoxy (Tru Bond 5-Minute Epoxy, Devcon Corporation, Chicago, IL.) using PVDF sensors in pulse-echo mode. The specimen used was constructed using two 50 mm X 50 mm X 6 mm pieces of plexiglas on which one 5 mm X 5 mm PVDF sensor was glued as shown in fig. 22.

A Sonotec STR*825 data acquisition board was used to store the signal (see fig. 23). The signals were analysed later by an acousto-ultrasonic evaluation program ("Signal") developed at VPI & SU²⁷. Ultrasonic pulses in the pulse-echo mode were sent and received by

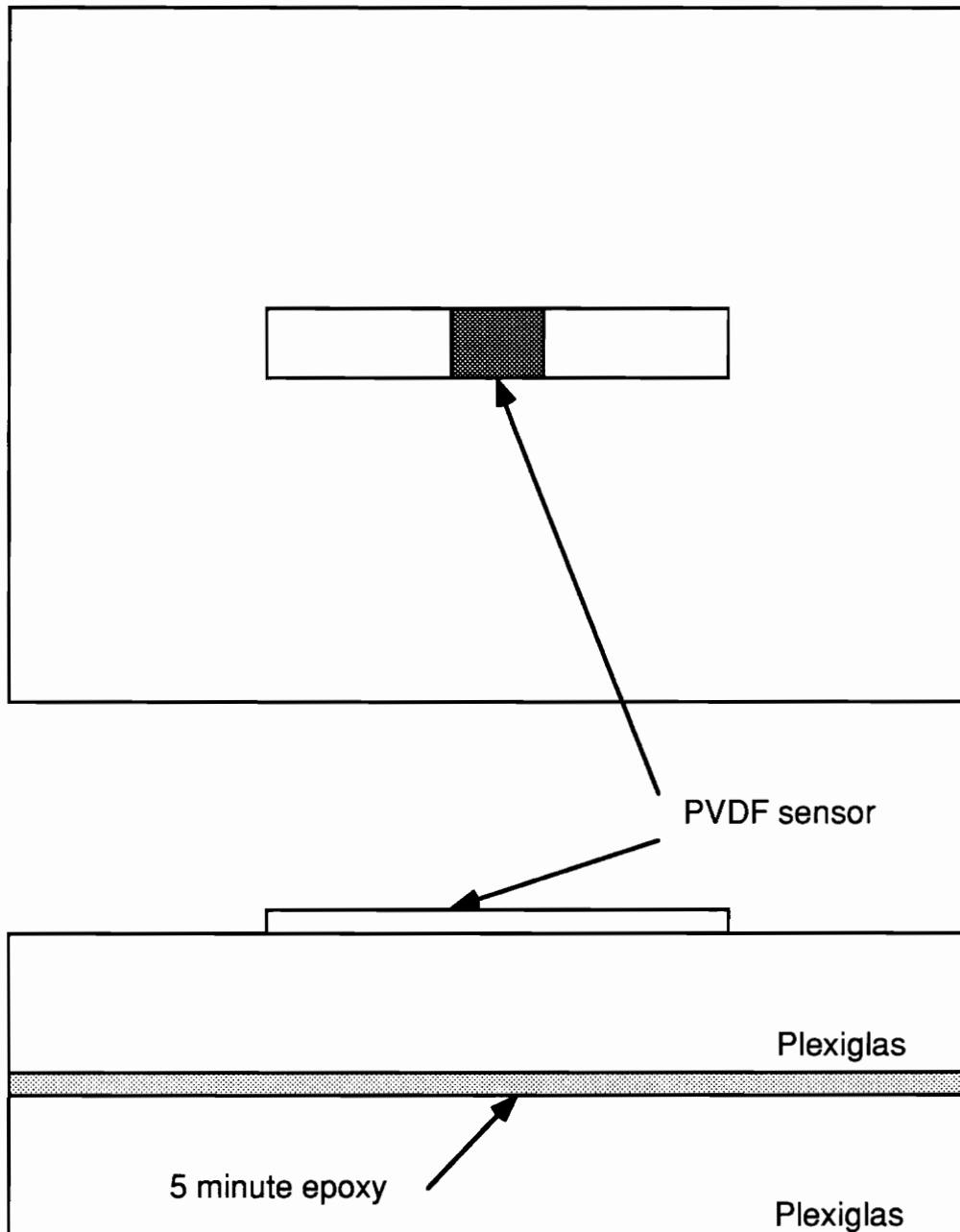


Figure 22. Specimen used for the setting of a 5 minute epoxy .

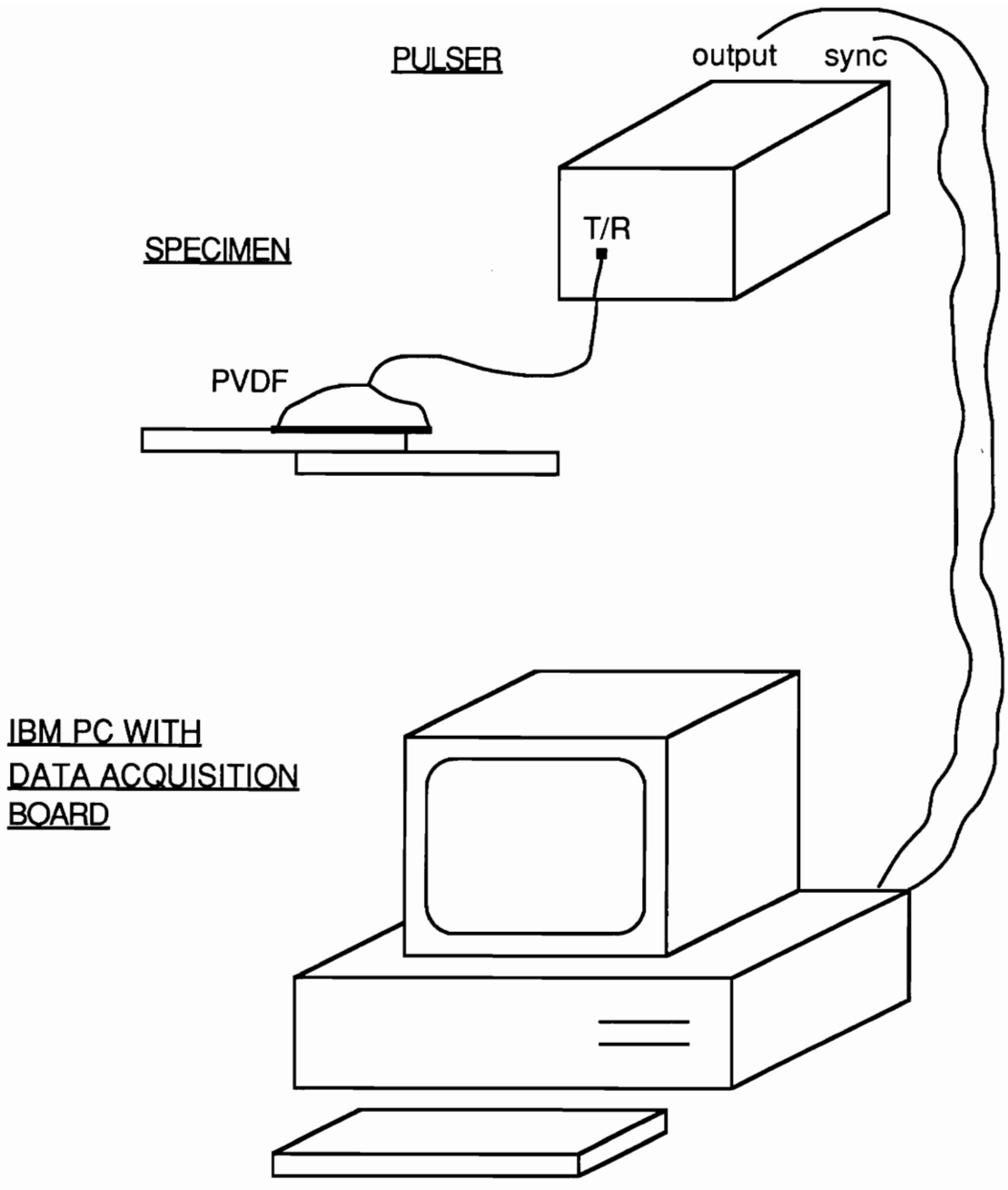


Figure 23. Schematic diagram of the experiment.

the sensor. Two different ultrasonic signals were monitored as shown in fig. 24 and fig. 25.

Fig. 26 shows the amplitude of the first signal (path #1) versus time. It decreased versus time showing the change of properties of the epoxy. Indeed during curing, the properties of the adhesives are modified leading to a change in the acoustic impedance since "Z" is a function of the Young's modulus (E), the density of the material (ρ), and the Poisson's ratio (ν). Once set, the epoxy had almost the same acoustic impedance as the plexiglas, therefore its coefficient of reflection (R) approached zero leading to almost total transmission of the energy and little reflection.

On the other hand, the amplitude of the second signal (path #2 and #3) monitored in another experiment, shown in fig. 27, increased versus time since most of the energy was due to transmission (path #2) which increased as the adhesive set. Nevertheless, the graph of the amplitude of the second signal versus time was not as perfect as the previous one due to the decrease of energy of the double reflection (path #3) (see fig. 25). The analytical explanation of this phenomenon is given in appendix C. Since the amplitudes of signal #1 and #2 haven't been monitored in the same experiment, there can be a shift in the time scale between the two curves.

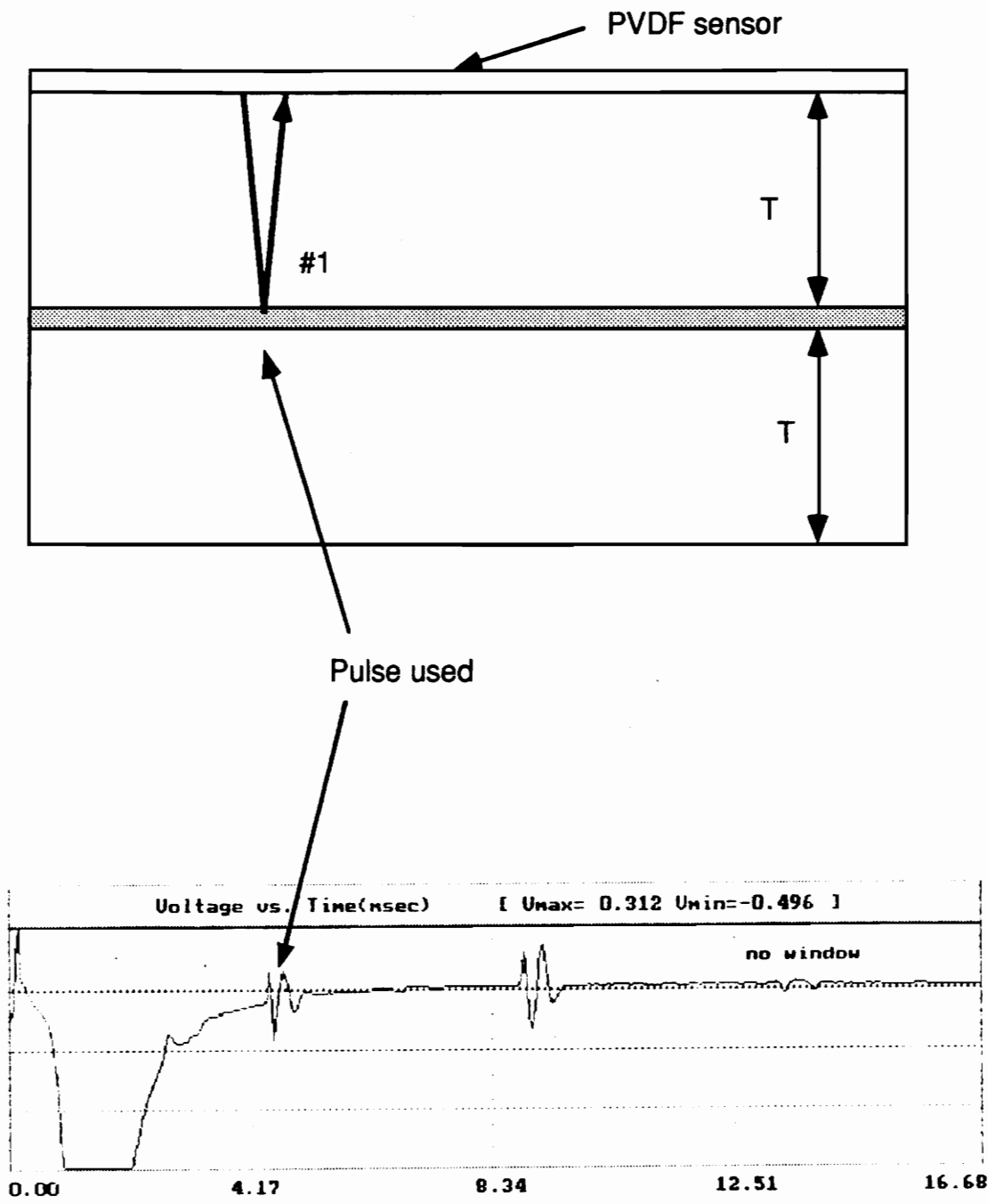


Figure 24. Pulse-echo signal (path #1) for the setting of a 5 minute epoxy.

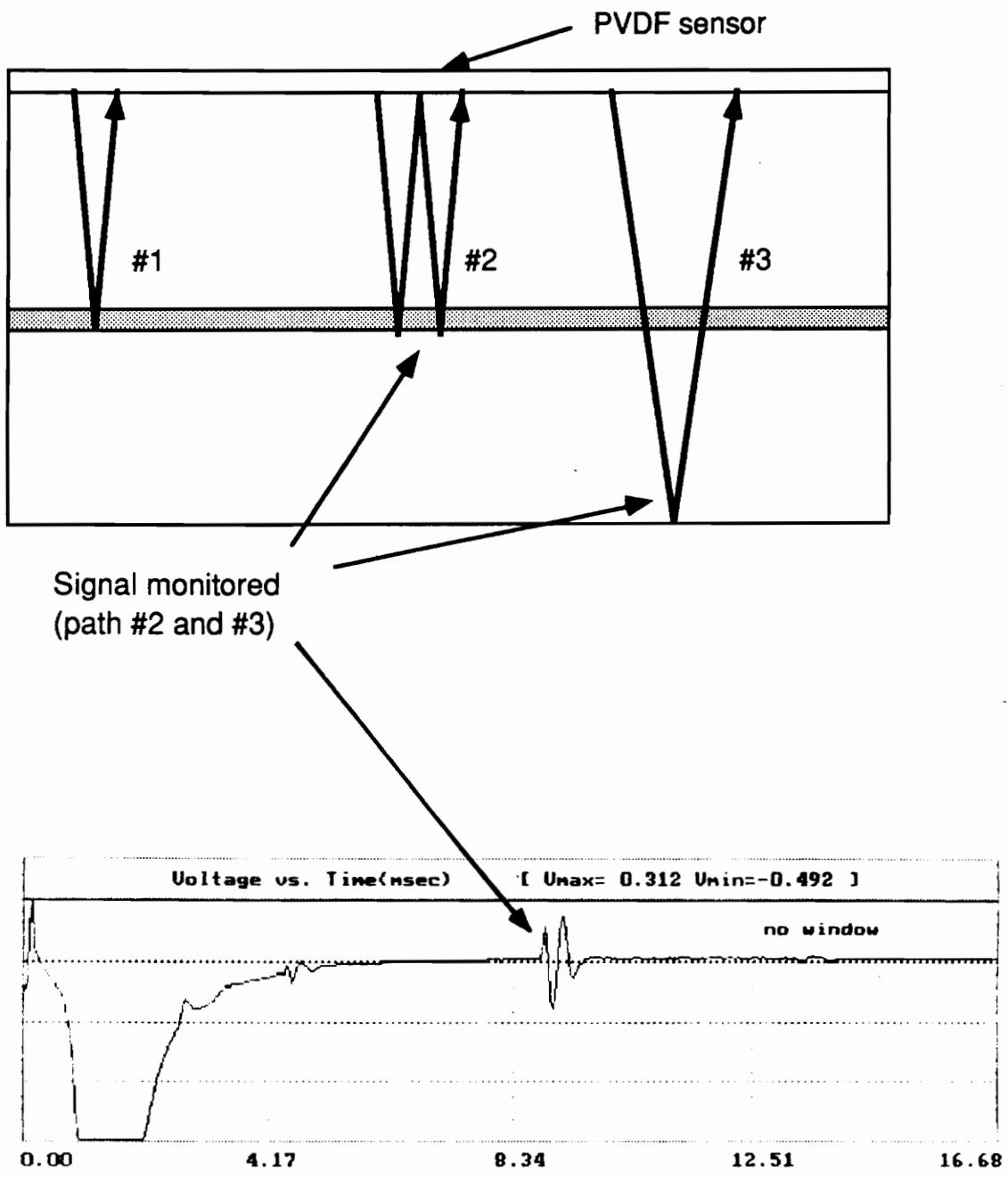


Figure 25. Pulse-echo signal (path #2 and #3) for the setting of a 5 minute epoxy.

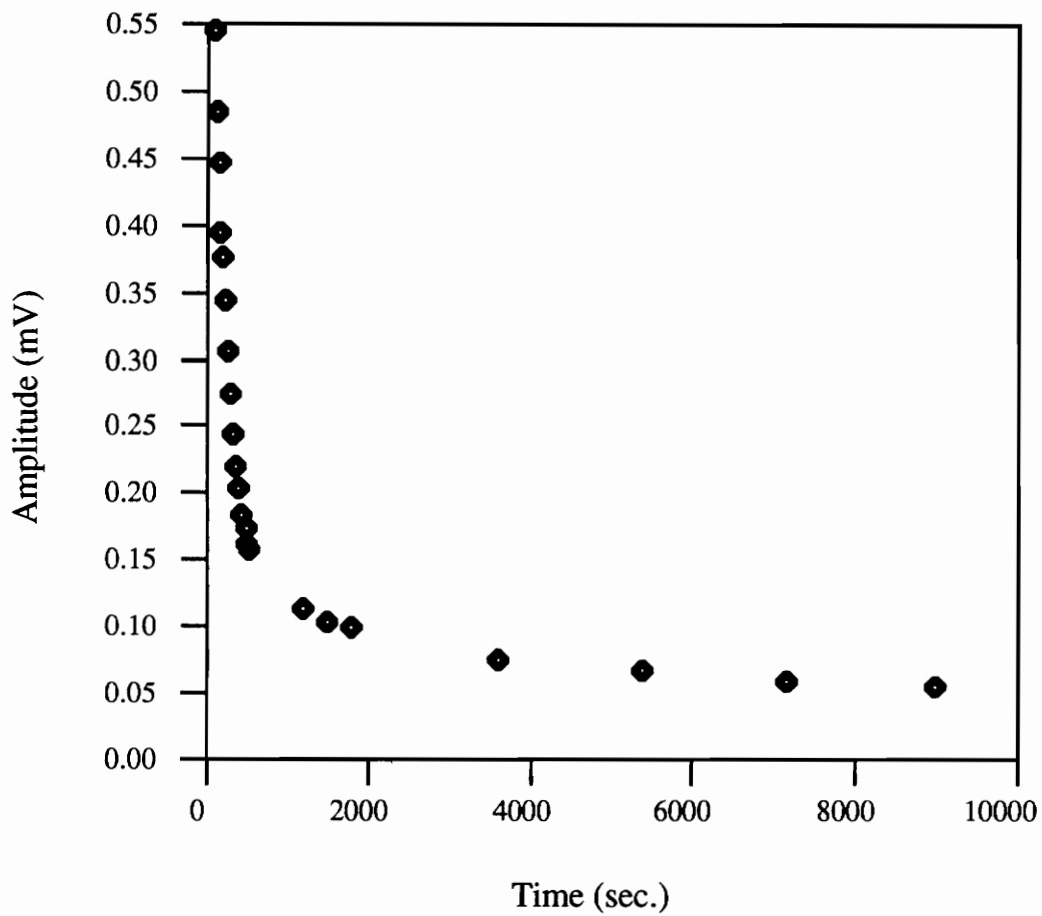


Figure 26. Amplitude of the first signal (path #1) versus time for the setting of a 5 minute epoxy.

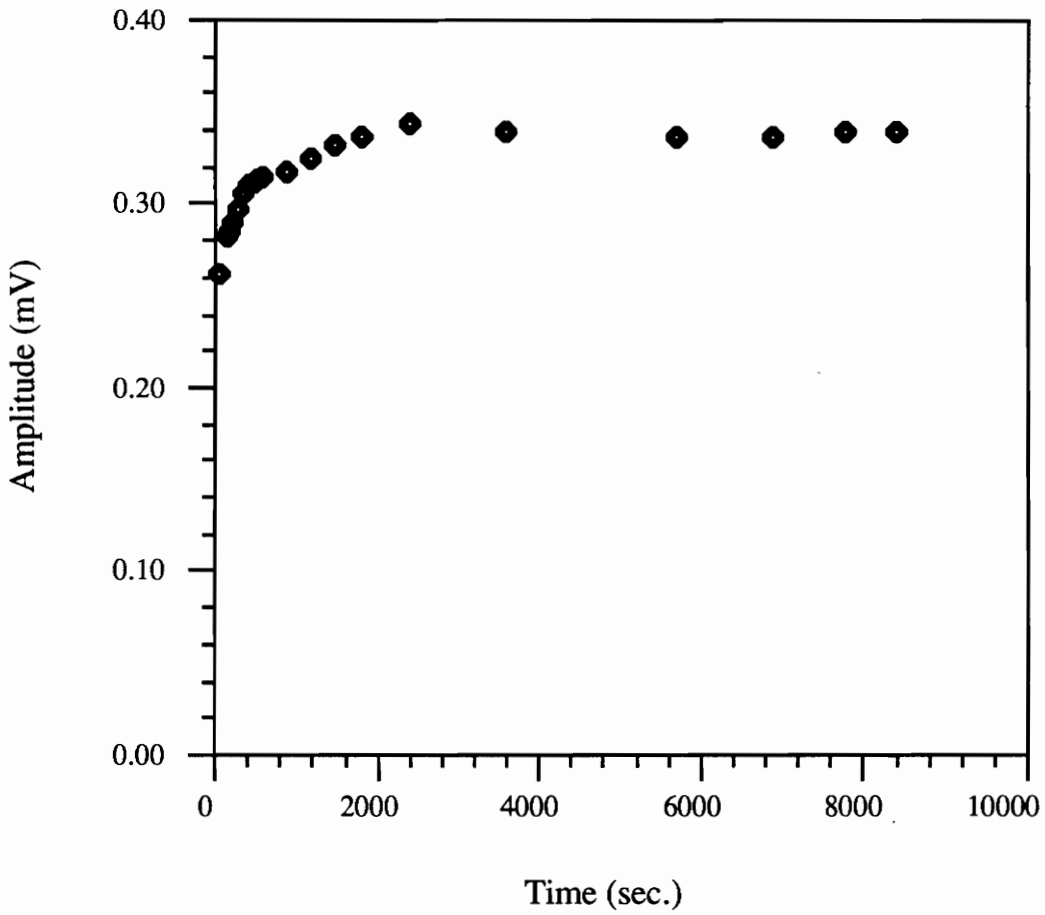


Figure 27. Amplitude of the second signal (path #2 and #3) versus time for the setting of a 5 minute epoxy.

As discussed earlier, it would be of great interest to know the properties of an adhesive during its curing. This technique would moreover enable the operator to know when the adhesive is cured and then when the structure can be removed, it would also detect if the adhesive is properly set over the entire surface and not just on the edge. The change of signal as a consequence of cure indicates that this technique has a great potential for the monitoring of cure in adhesive joints. The advantage of this technique over conventional techniques such as Differential Scanning Calorimetry (DSC) is that the adhesive is examined in situ rather than as the neat resin. Sensors could be attached on structures to monitor the cure of the assemblies which would then be compared to the cure monitoring of good bonds. One problem with PVDF film is that it loses its piezoelectric properties when exposed to high temperatures. The film cannot be used above 100°C and exhibits a time-dependant loss of properties²⁰ at temperatures as low as 60°C. However this problem could be overcome by adding ceramic particles⁴⁰ during the manufacture of PVDF which has the effect of increasing its limit of service temperature.

5.0 MONITORING DAMAGE IN SEVERAL JOINT GEOMETRIES

The bond integrity of several joint geometries affected by loading or environmental conditions has been monitored by PVDF sensors used in pulse-echo mode, through-transmission mode or acousto-ultrasonic technique. Emphasis has been placed on the pulse-echo mode since it is a generally accepted method¹⁻² and requires access to only one side of the structure. Hence it is possible to apply this technique to existing in-service materials where two-side accessibility may not be possible from access or exposure problems.

Many experiments used model joints made with plexiglas as an adherend and silicone rubber as an adhesive. Indeed plexiglas is transparent and thus allows defects in the bondline to be seen. Silicone rubber can be considered as an appropriate model adhesive since cracks can be easily produced in a controlled manner at relatively low loads.

All the results have been monitored by the data acquisition system shown in fig. 23.

5.1 Single lap shear joint

Crack propagation due to mechanical loading has been detected in single lap shear joints by PVDF sensors used in through-transmission mode and acousto-ultrasonic technique. Loading has been performed by the introduction of a screwdriver into the bondline in the first specimen and by a tensile test in the second specimen.

5.1.1 Loading by prying

A lap joint composed of plexiglas adherends (90 mm X 100 mm X 5 mm) and a silicone rubber adhesive was fabricated with two 3.5 mm X 3.5 mm PVDF sensors located on the outside of the joints. PVDF films were glued on the specimen as shown in fig. 28. Two different thicknesses of plexiglas were used for this experiment and teflon tape was put on both ends of the sample in order to have the same thickness of adhesive (0.15 mm).

Ultrasonic pulses were sent from the opposite side of the joint by using a 12.7 mm dia., 2.25 MHz PZT ceramic crystal in a through-transmission mode.

Finger-like micro-cracks developed at the crack tip during loading as shown in fig. 29. The specimen was loaded until the crack front reached the surface of sensor #1 (fig.28)

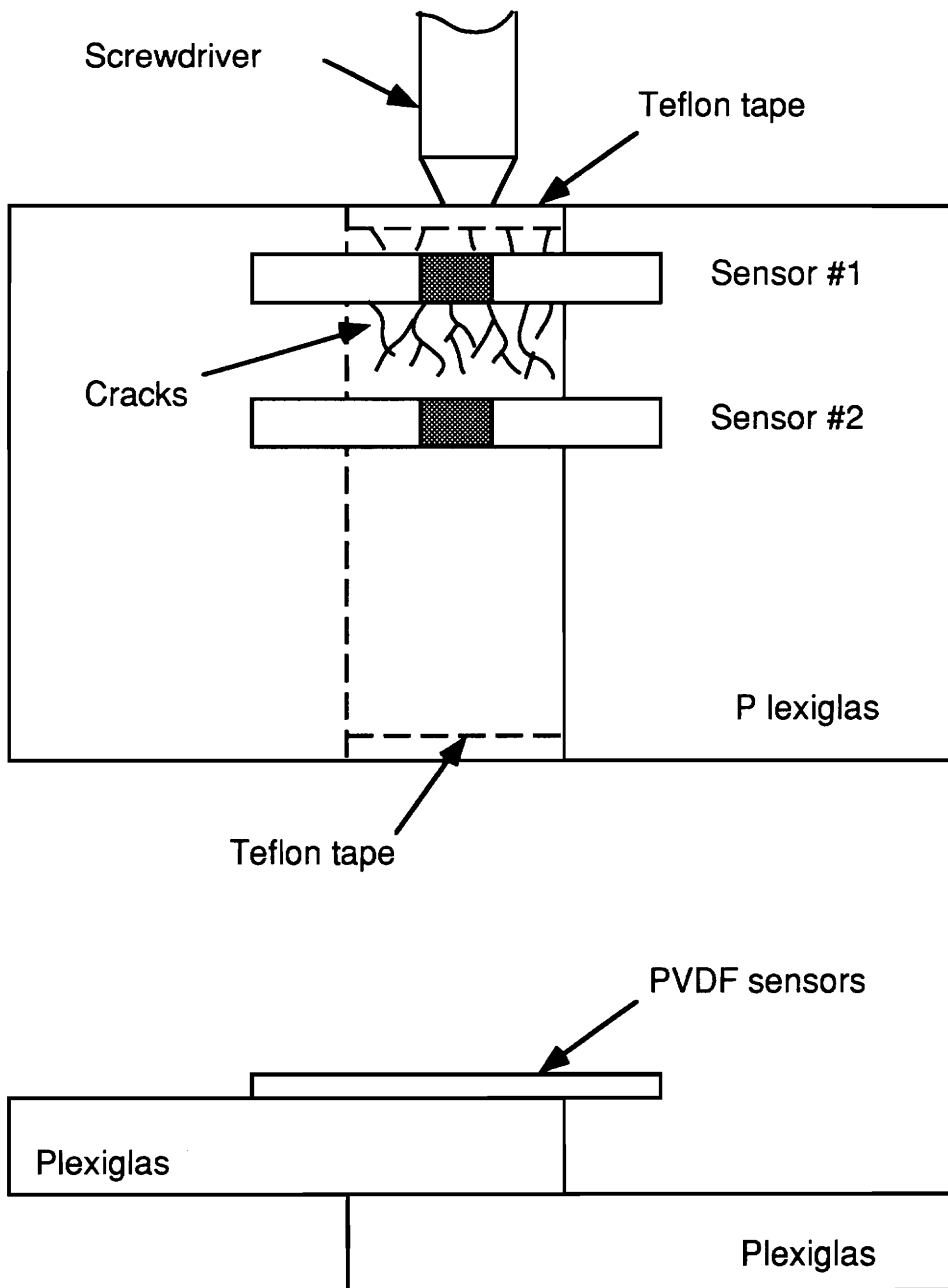


Figure 28. Schematic diagram of the specimen.

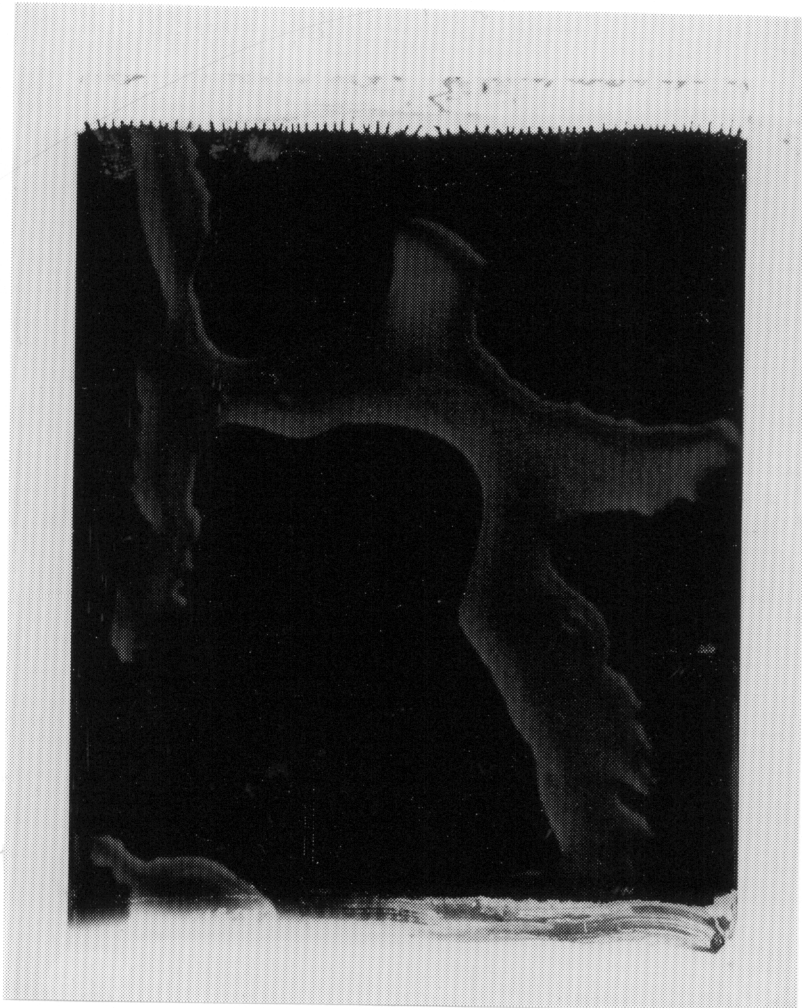
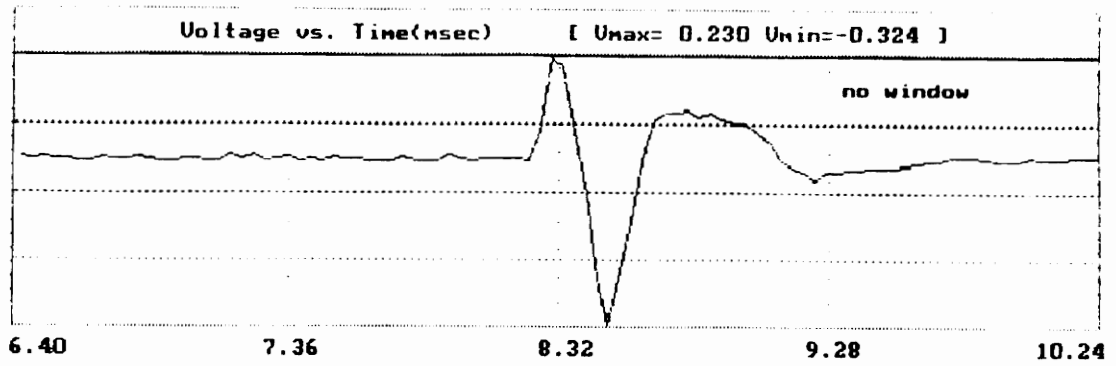


Figure 29. Micrograph of the finger-like cracks in the silicone rubber adhesive bond.

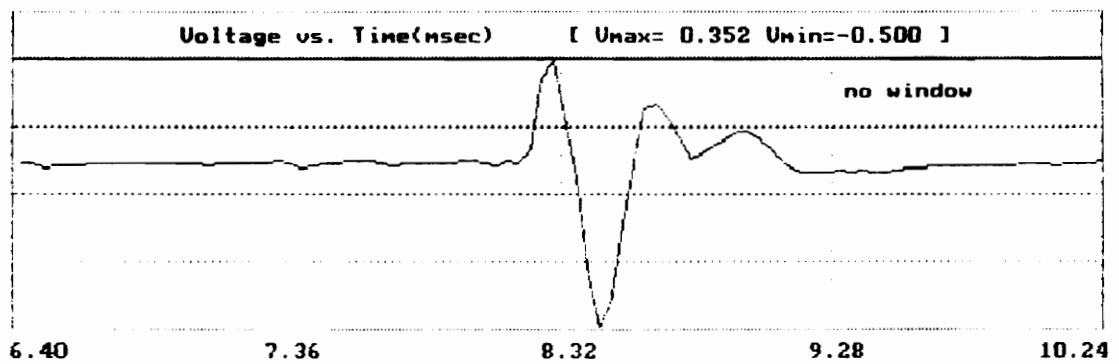
First of all, comparison was made between the signals received by sensor #1 (with cracks) and sensor #2. Results showed that the cracks attenuated the signals and filtered out high frequency components as shown in fig. 30. In Fig. 30, results for sensor #1 and sensor #2 are not at the same scale. For comparison, the FFT spectrum of sensor #1 (cracks) has been drawn in dashed line on the graph of sensor #2 (fig. 30(b) ii). No signal received by sensor #1 was taken before crack propagation. Thus, it was not possible to make comparison before and during crack propagation for this sensor.

Signals of sensor #2 were monitored while propagating the micro-cracks inside the rest of the joint. Results were similar to those above and are shown in fig. 31 (the signal gain was adjusted to show a good signal on screen). No signal was detected after the crack grew totally through the PVDF sensor region.

These experiments showed that PVDF sensors could be used with success in through-transmission mode to detect cracks in the bondline. However this technique has been abandoned in the next experiments since pulse-echo mode and acousto-ultrasonic technique are preferred to through-transmission technique except for the inspection of honeycomb structures² or bonded assemblies where both adherends have the same thickness. Indeed pulse-echo mode and acousto-ultrasonic techniques require access to only one side of the structure and don't need any alignment of the transducers which can be laborious in the through-transmission technique.

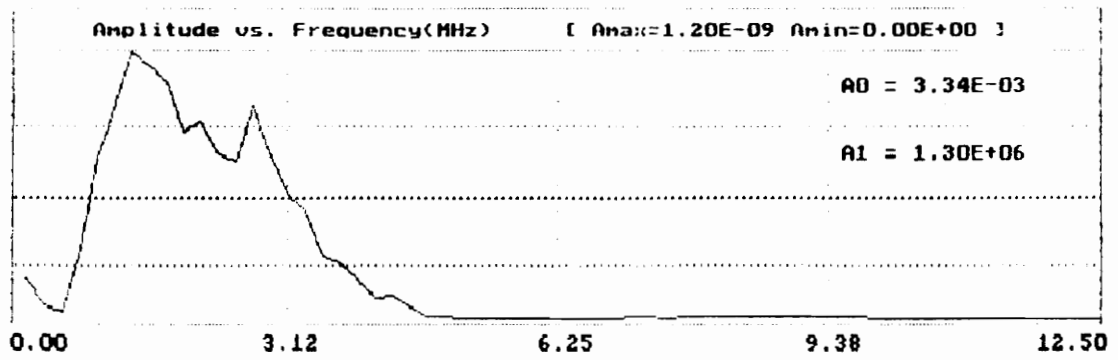


(i)

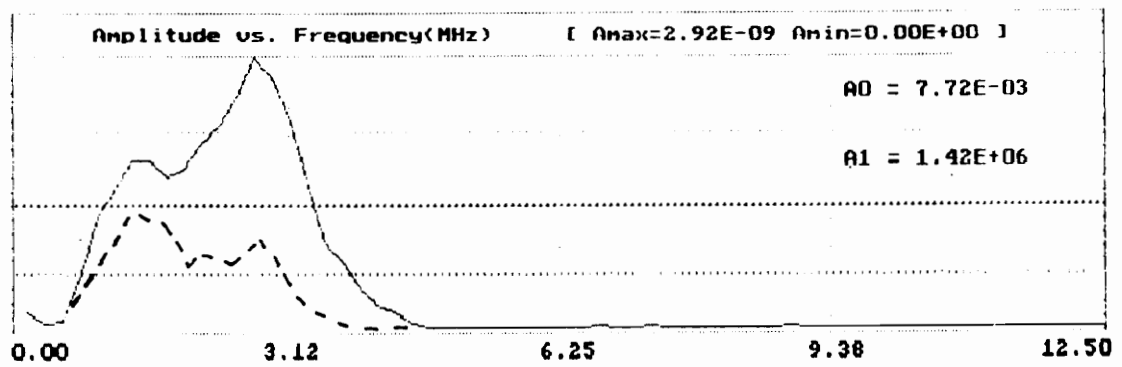


(ii)

Figure 30 (a). Signals received by PVDF (i) sensor #1 (micro-cracks)
(ii) sensor #2

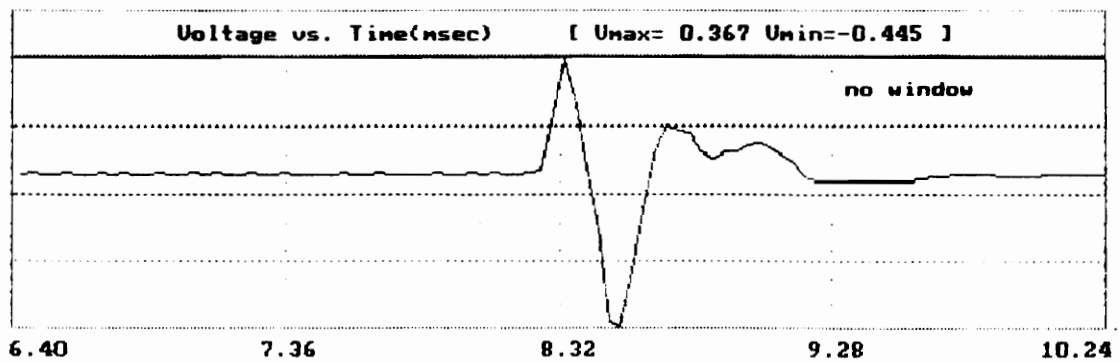


(i)

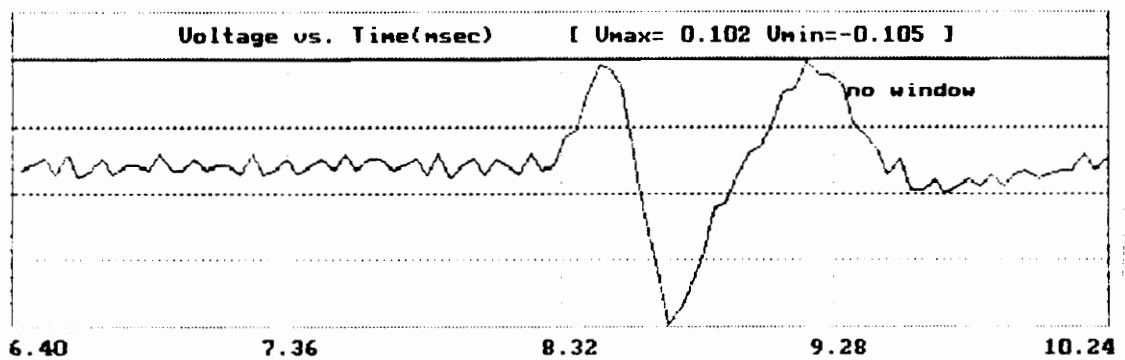


(ii)

Figure 30 (b). FFT spectra for (i) sensor #1 (micro-crack)
(ii) sensor #2

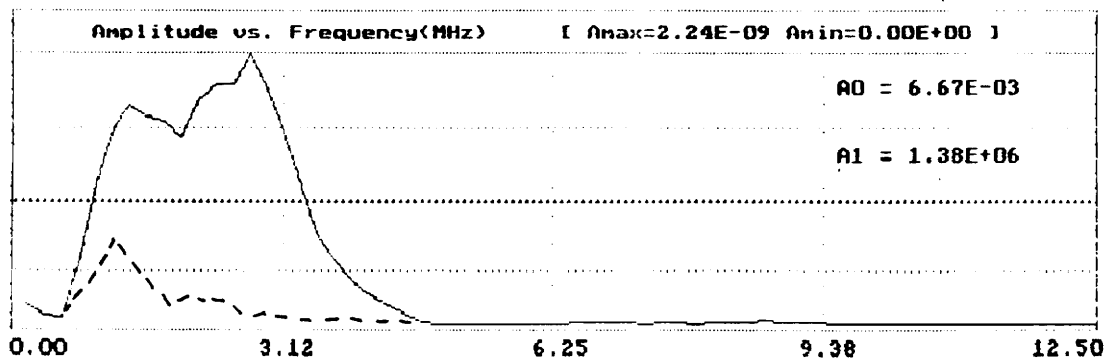


(i)

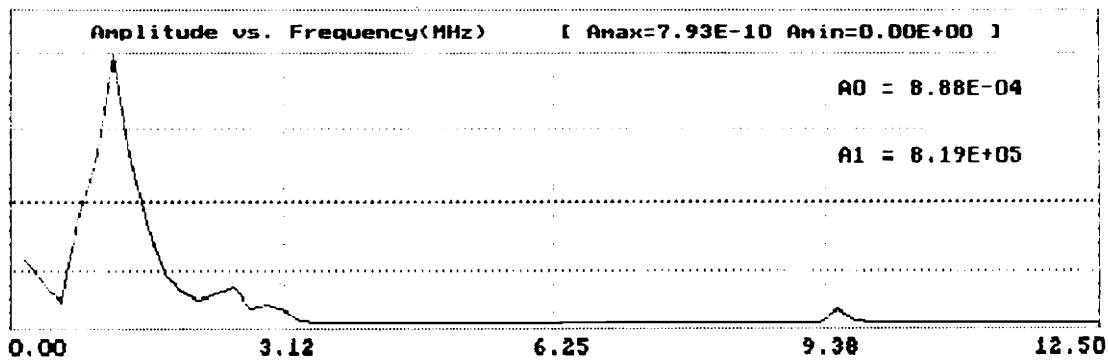


(ii)

Figure 31 (a). Signal received by sensor #2 (i) without cracks at 40dB
(ii) with cracks at 60 dB .



(i)



(ii)

Figure 31 (b). FFT spectra of the signal received by sensor #2

(i) without micro-cracks

(ii) with micro-cracks

5.1.2 Tensile test

The acousto-ultrasonic method has been successfully used with ceramic transducers to estimate the strength of adhesively bonded structures¹²⁻¹⁴. The purpose of the following study was to show that PVDF sensors would have the same results as the ceramic transducers in characterizing a lap shear joint by the acousto-ultrasonic method. The advantage of using PVDF rather than ceramic transducers is that PVDF would be permanently attached on the structure so that it could measure bond integrity in service and with a better reproducibility. Indeed there is no need for couplant or weights in this technique and the distances between the different sensors are fixed. Moreover the use of ceramic sensors requires a specific set-up which can damage the structure³.

The acousto-ultrasonic (AU) method was used on adhesively bonded single lap shear joints fabricated from plexiglas with sensors located on the outside of the joint (fig. 32). Three different sensor configurations were used:

- 1 - two 6.7 mm dia., 2.25 MHz crystals,
- 2 - one crystal as a sender and one 20 mm X 3.3 mm PVDF sensor as a receiver, and,
- 3 - two 20 mm X 3.3 mm PVDF sensors.

The specimens were loaded in tension. Figs. 33-35 show the value of M_0 for the different configurations. M_0 decreased during the loading of the structure showing a decrease of the energy propagating through the bonded joint. Indeed developments of cracks were observed which effect was to attenuate the energy. The difference in the three diagrams may be due to the different damage modes. The results for the three configurations are consistent and lead us to believe that PVDF sensors can be used in an AU configuration to detect damage in adhesive joints. On the other hand, the mechanism responsible for the increase of the central frequency (M_1/M_0) versus load, shown in figs. 36-38, is not fully understood. M_1/M_0 was expected to decrease after reaching the maximum load since damage in the bondline should have filtered out high frequencies and, thus, made the central frequency decrease. The increase of the central frequency may be due to the surface waves propagating on the exterior of the surface which shouldn't be affected by damage in the bondline. Therefore their frequency content which was negligible when the energy due to longitudinal waves went through the bond, became preponderant once signals were scattered, and increased the central frequency.

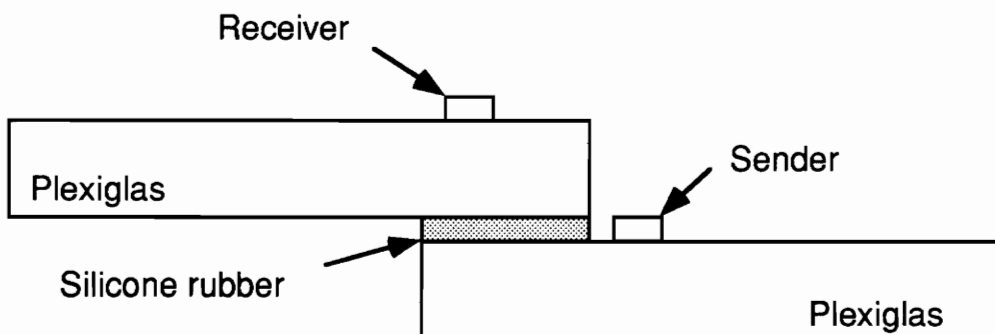
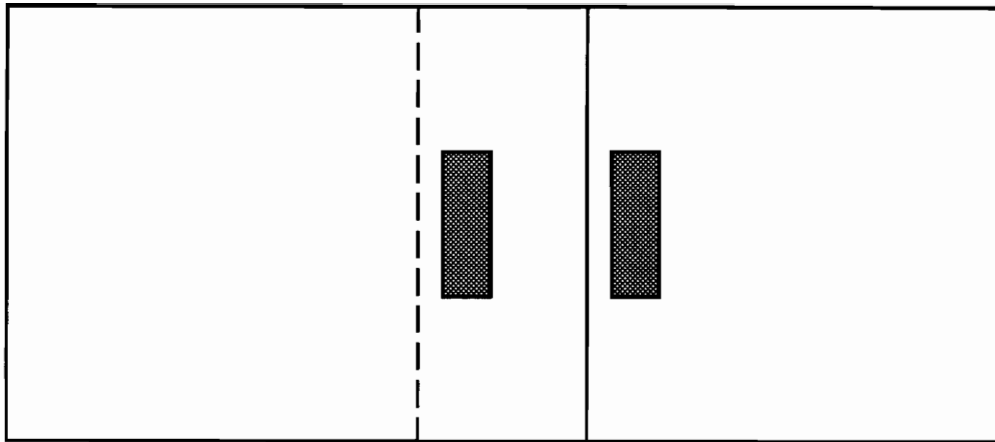


Figure 32. Adhesively bonded lap shear joint with PVDF sensors.

M₀ versus Load (crystal)

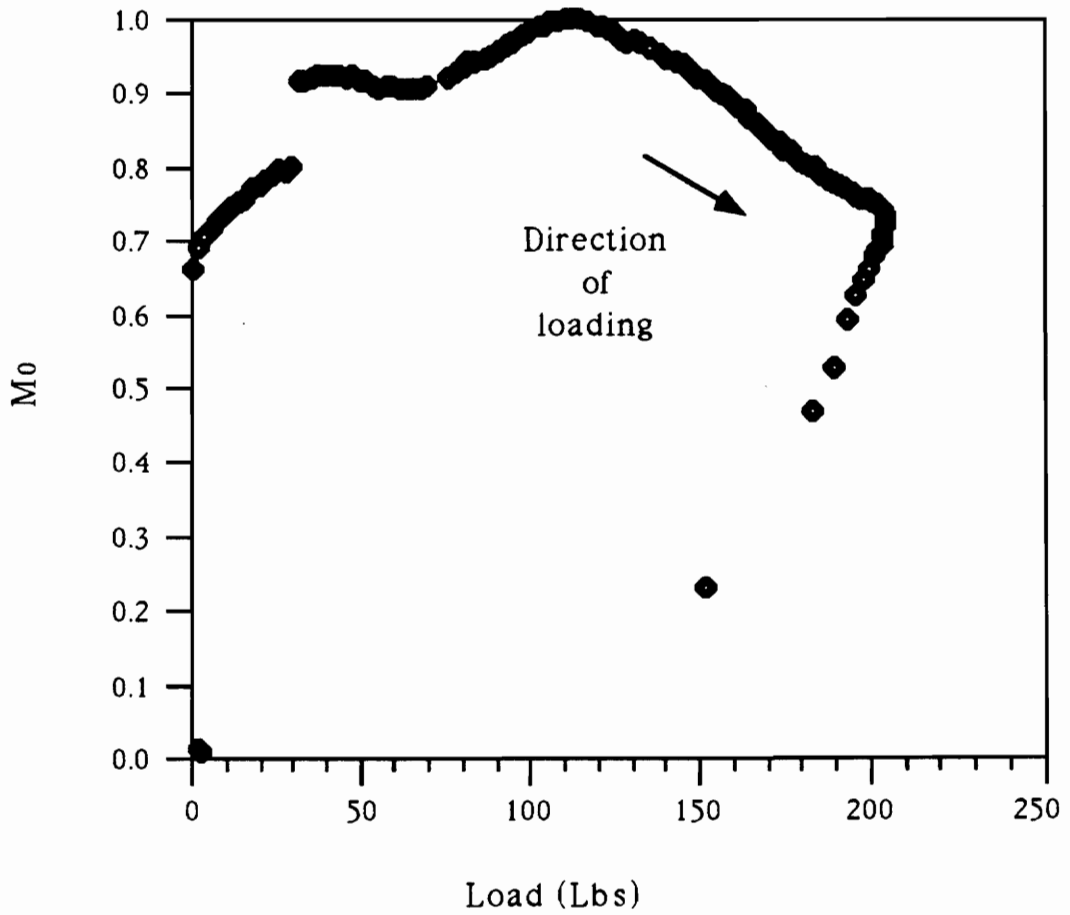


Figure 33. Results for the shear lap joint with two crystals.

M0 versus Load (crystal & PVDF)

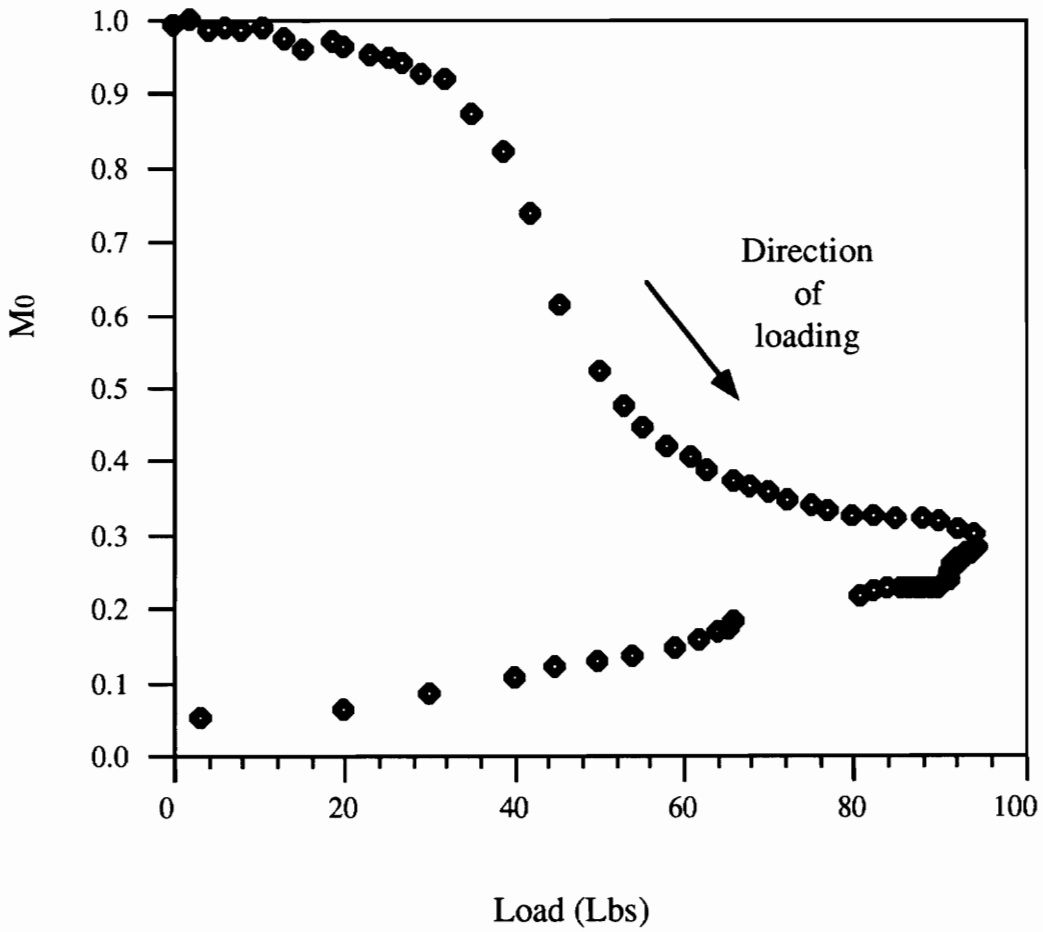


Figure 34. Results for the shear lap joint with one crystal and one PVDF sensor.

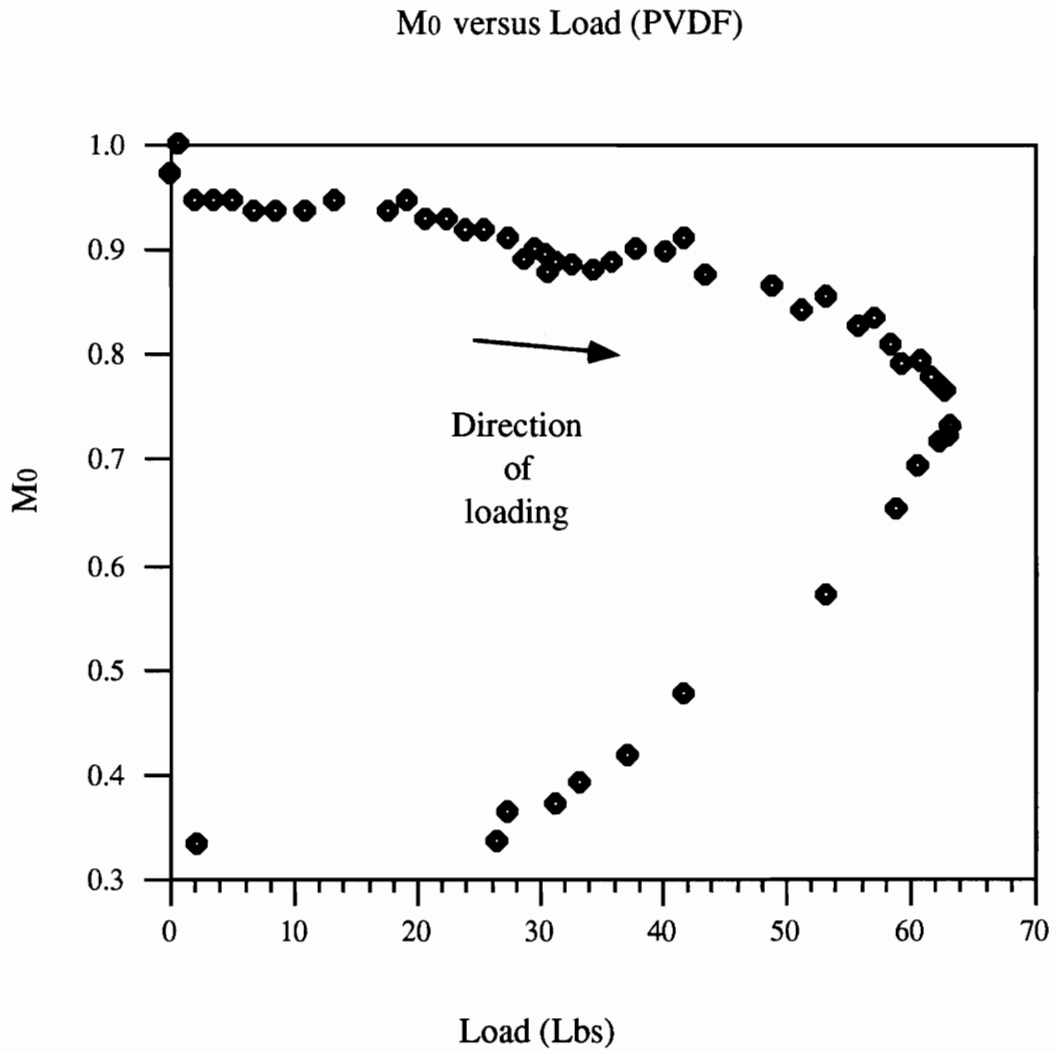


Figure 35. Results for the shear lap joint with two PVDF sensors.

M_1/M_0 versus load (crystal)

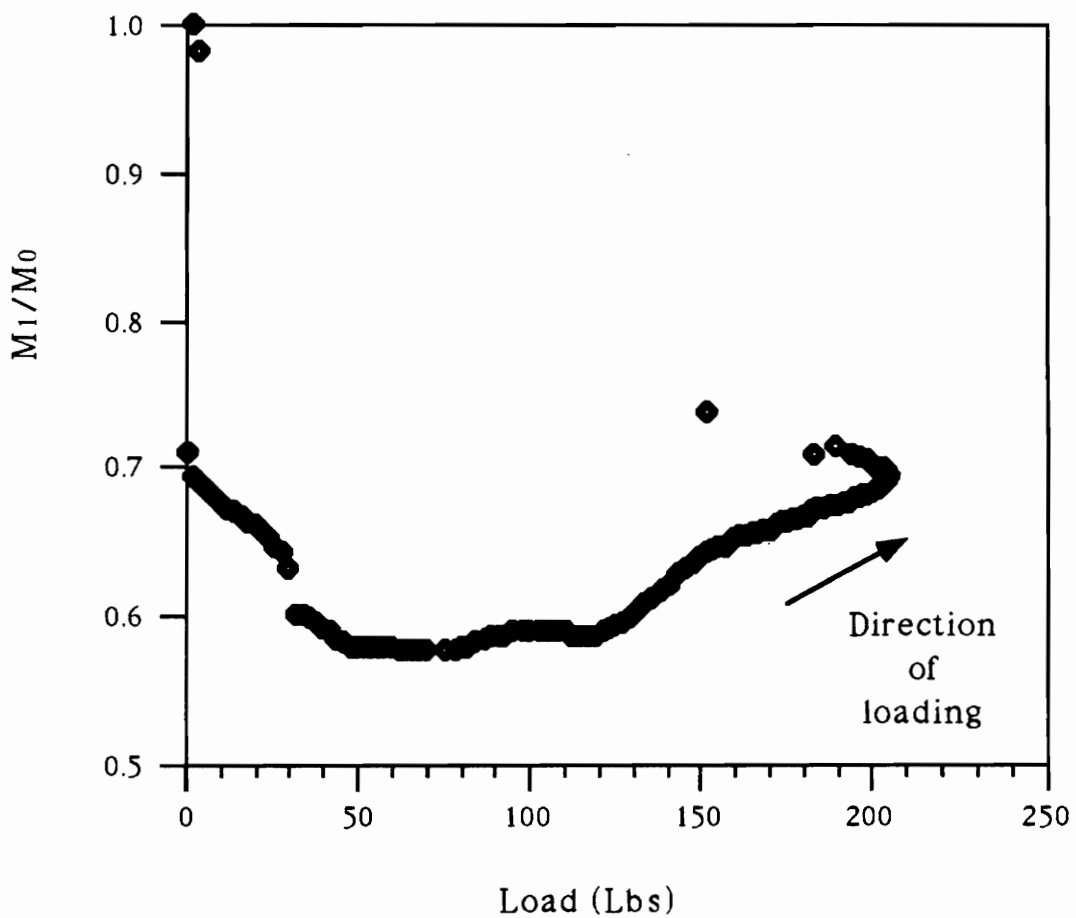


Figure 36. Change of central frequency for the specimen with 2 crystals.

M₁/M₀ versus load (crystal & PVDF)

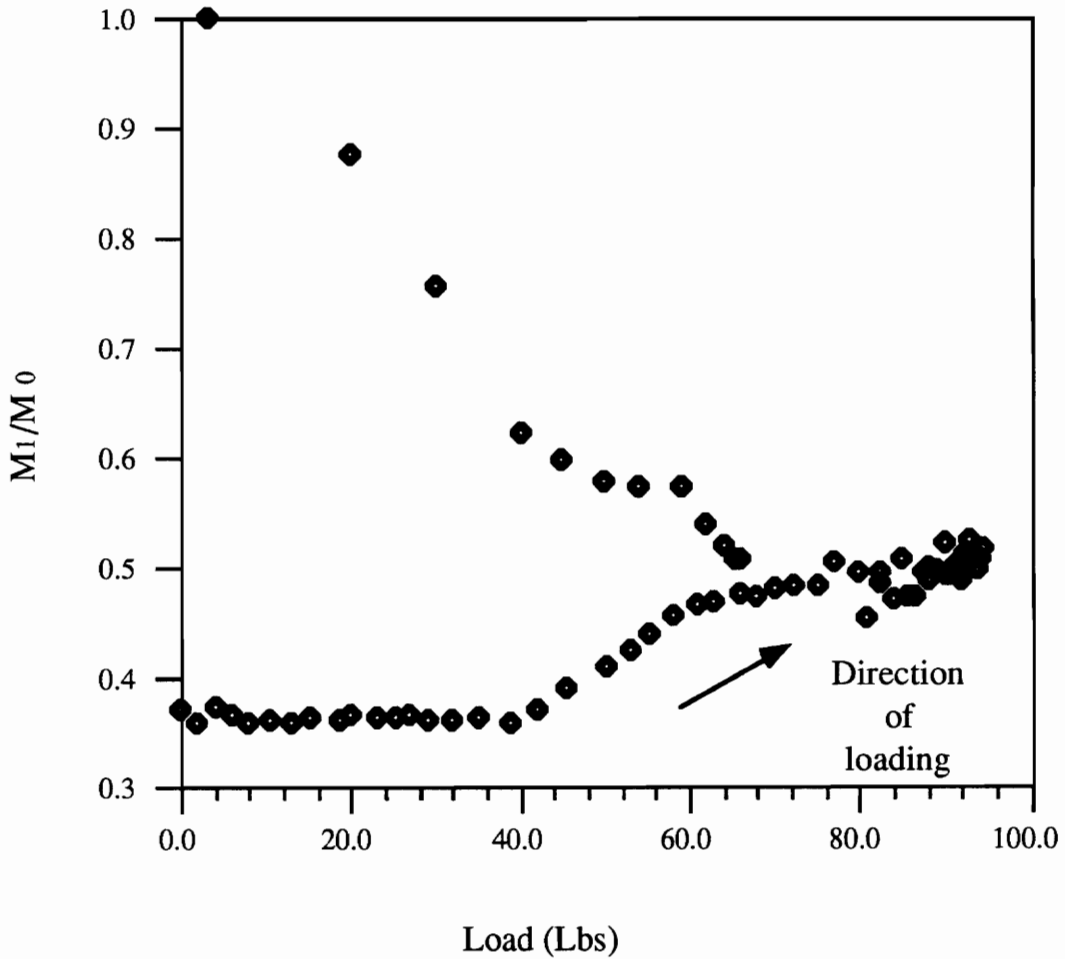


Figure 37. Change of central frequency for the specimen with one crystal and one PVDF sensor.

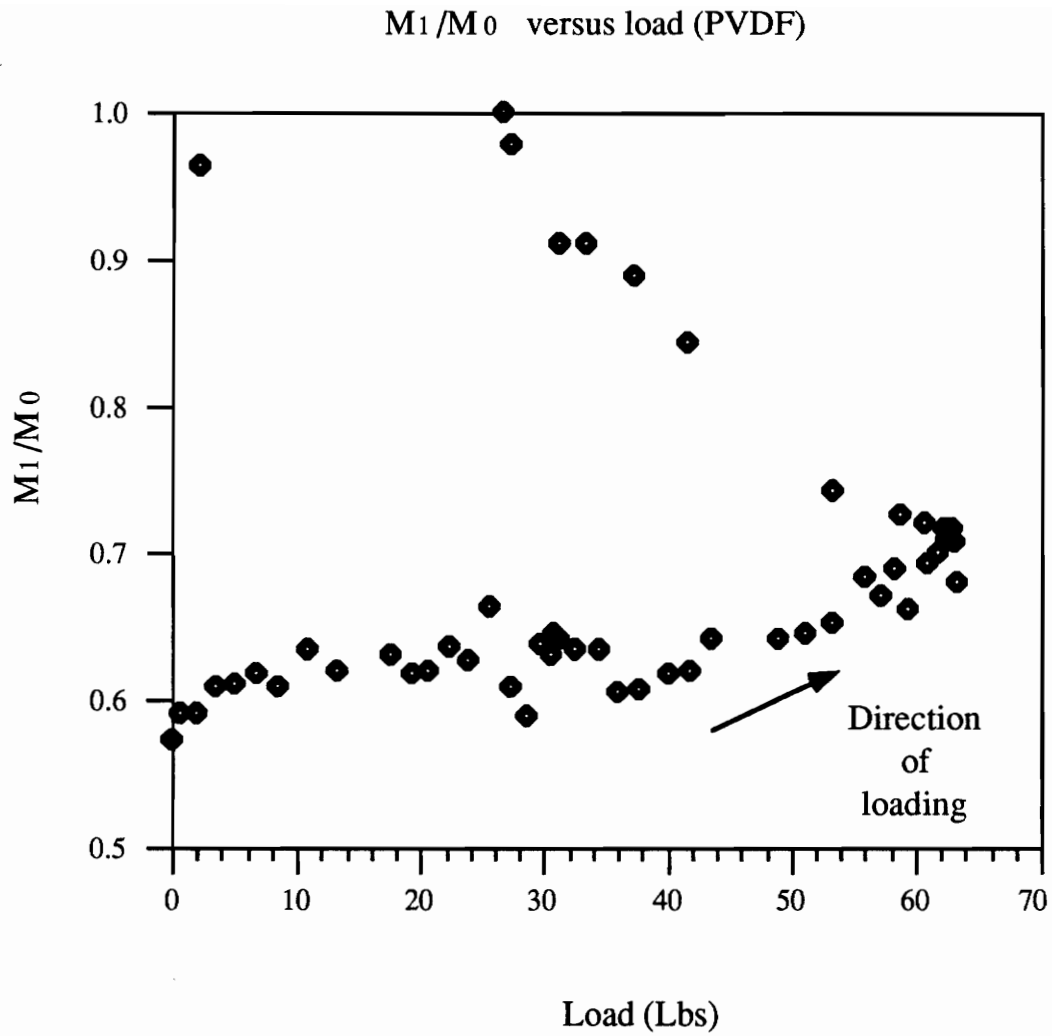


Figure 38. Change of central frequency for the specimen with two PVDF sensors.

5.2 Mechanically loaded blister

A mechanically loaded blister was designed to propagate cracks in the bond and show that PVDF could detect them in pulse-echo mode.

5.2.1 Monitoring of debonding area

The purpose of this experiment was to measure the debonding area. The specimen was constructed using two 50.8 mm X 44.5 mm plexiglas adherends of different thicknesses (5 mm and 9 mm), one of which contained a threaded hole to accommodate a 6.3 mm (1/4 in.) screw. These pieces were bonded together by a silicone rubber adhesive. A 37.5 mm X 37.5 mm large PVDF sensor, with a 9 mm X 9 mm cutout to permit the introduction of the screw, was glued on the surface of the joint (fig. 39). Debonding of the specimen was achieved by loading the interface of the bonded joint by the advancement of the screw. Debonding was monitored by a video camera while the ultrasonic pulse-echo data were taken intermittently. The debonding areas were later measured from the replay of the video-tape.

Fig. 40 shows that the amplitude of the ultrasonic signals (path shown in fig. 39) decreased with the increase of the debonded area. These results are interesting but this technique does not locate the

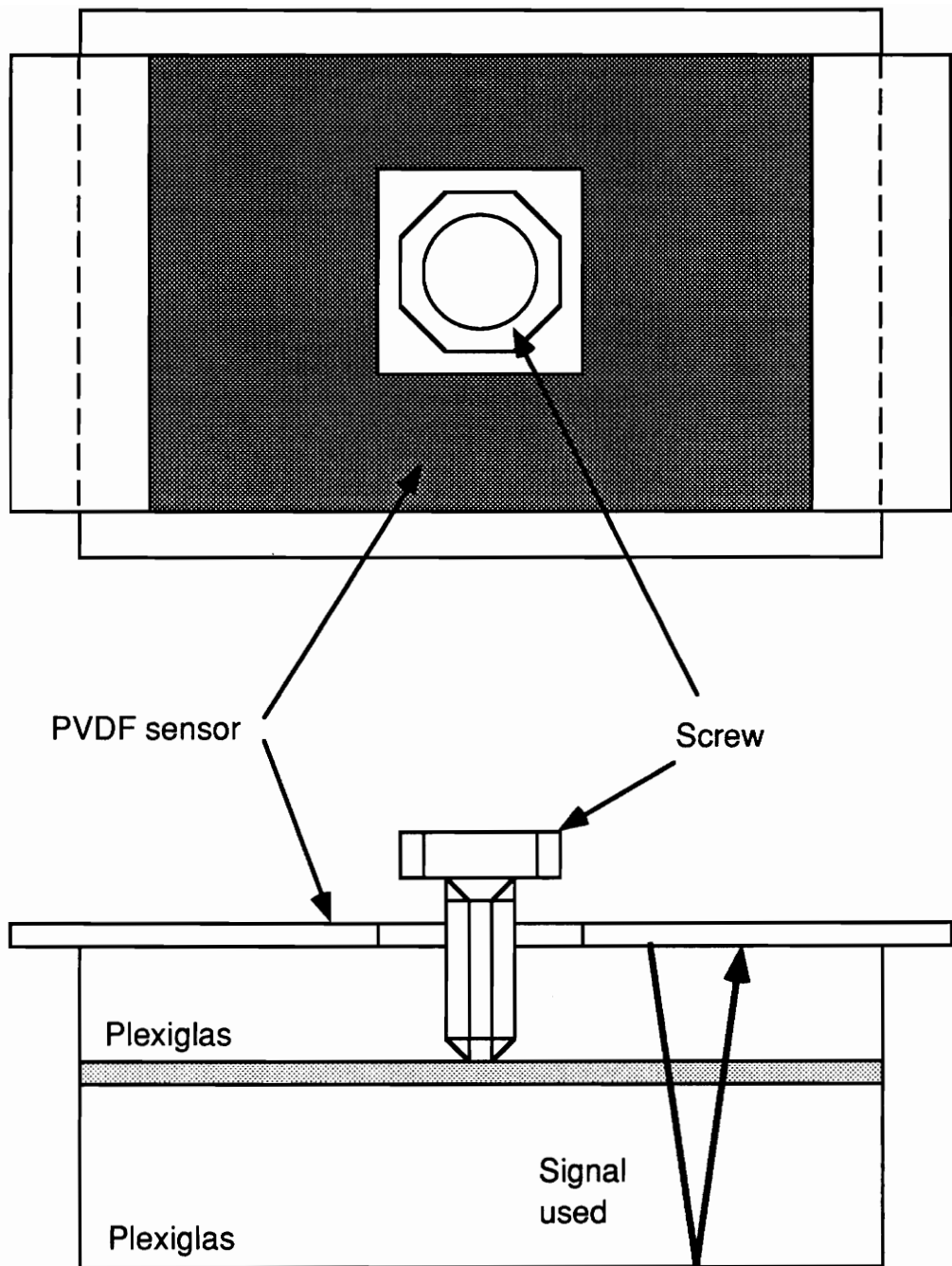


Figure 39. Bonded specimen with a large PVDF sensor for monitoring of debonding.

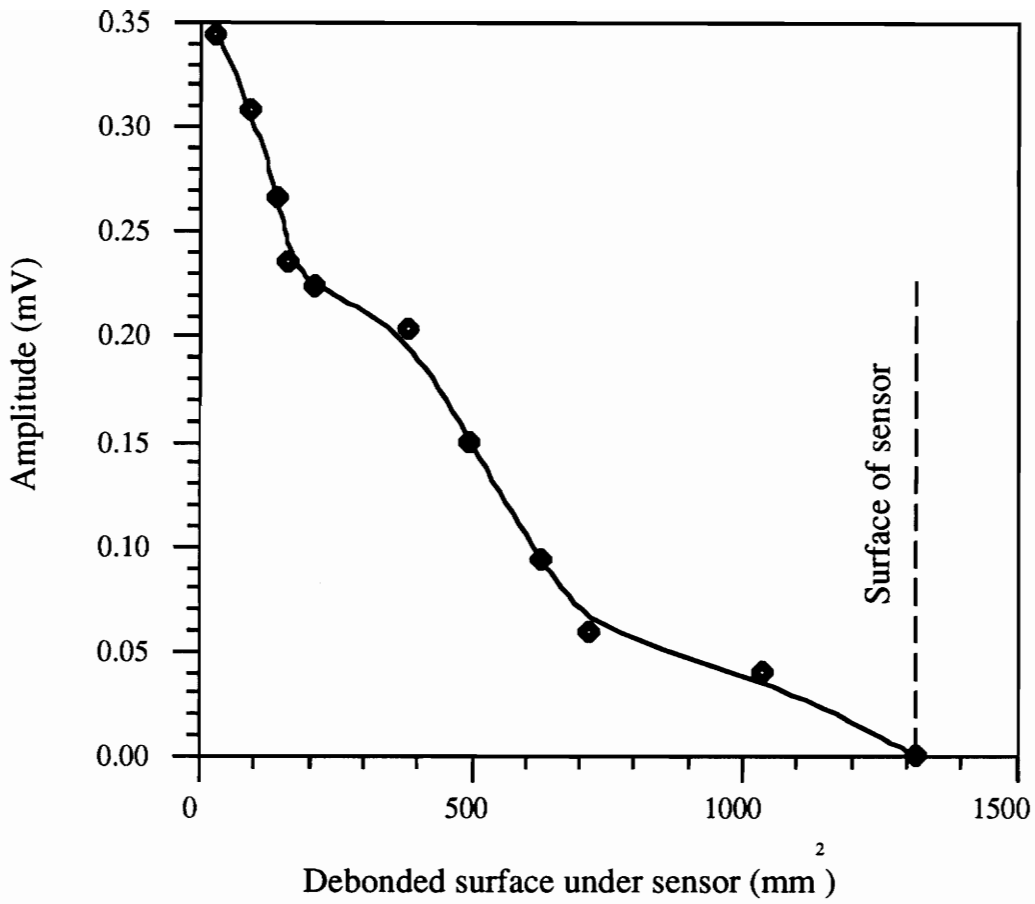


Figure 40. Results for the monitoring of debonding area.

cracks and does not give any information on the shape of the cracks because of the large surface of the sensor. Nonetheless, the good correlation between remaining bond area and output signal suggests possible applications, especially for large bond areas such as rocket propellant to motor cases.

The amplitude of the signal is proportional to the size of the sensor as shown in fig. 11. However, the graph showing the debonding area (fig. 40) was not linear. This can be explained by several facts:

- once debonding occurred, it created a passive area of film (sensor's area which didn't receive any ultrasonic signal) which acts as a capacitor in parallel with the active film. This effect was to lower the voltage and cause substantial loss of energy²⁰. A way to prove this effect would be to design another identical sensor which wouldn't have the area corresponding to the crack surface, glue it on the other side of the specimen and compare both signals.
- some parts of the large sensor were probably not bonded perfectly to the plexiglas so that the active surface of the sensor was not the one expected. It should be possible to check it by using an acoustic microscope.
- the way to calculate the debonding area from the video tape was not accurate enough. This effect should be negligible because the error was of the order of 2%.

- the debonding area shown on the monitor could have been less than the real debonding area. This effect should also be negligible because these attenuations should be very small compared to the ones due to large surfaces of debonding.

5.2.2 Detection of crack propagation

Whereas the previous experiment measured the debonding area, the purpose of this experiment was to detect the crack front by using several spatially separated sensors. Two 1.6 mm X 1.6 mm PVDF sensors were glued outside of the bonded joint as shown in fig. 41. Indeed, as the crack was known to be circular, the only way to detect the crack front was to have small area sensors.

A crack was propagated by loading the interface of the bonded joint with advancement of the screw. Ultrasonic pulses, traveling through the bond as shown in fig. 42, were sent and received by the same sensor. The ultrasonic data were taken after each increment in the circular crack area.

Fig. 43 and 44 show the amplitude of the signal for each measurement for two different specimens (the thickness of the adhesive was 0.5 mm). The cracks reached sensor #1 before reaching sensor #2 (signal of sensor #1 was the first to decrease significantly). But there was still a signal from sensor #1 when the crack reached sensor #2 since the cracks developed in small bubbles (see fig.41 (b)) letting part of the signal going through the adhesive.

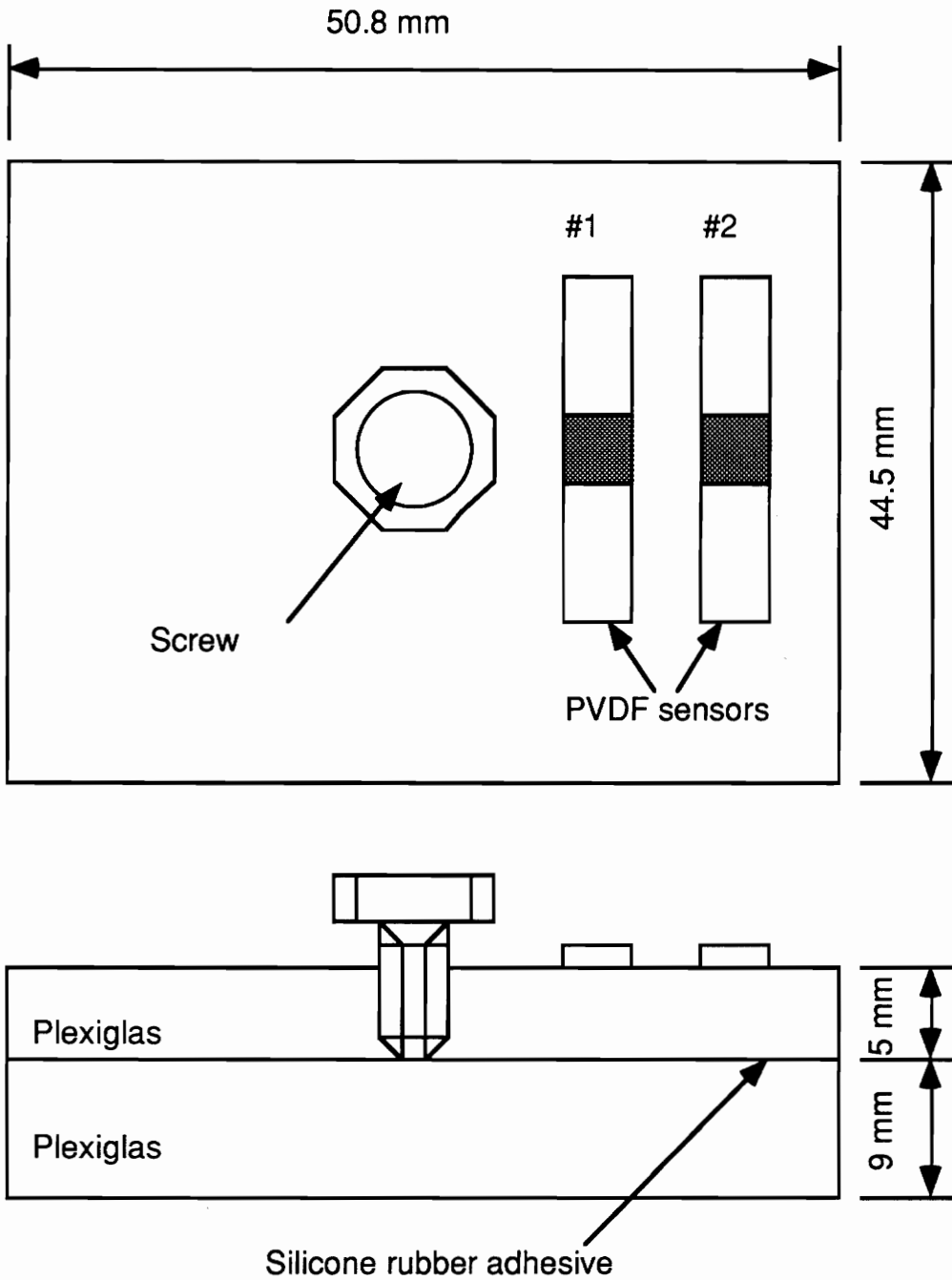


Figure 41 (a). Specimen before crack propagation.

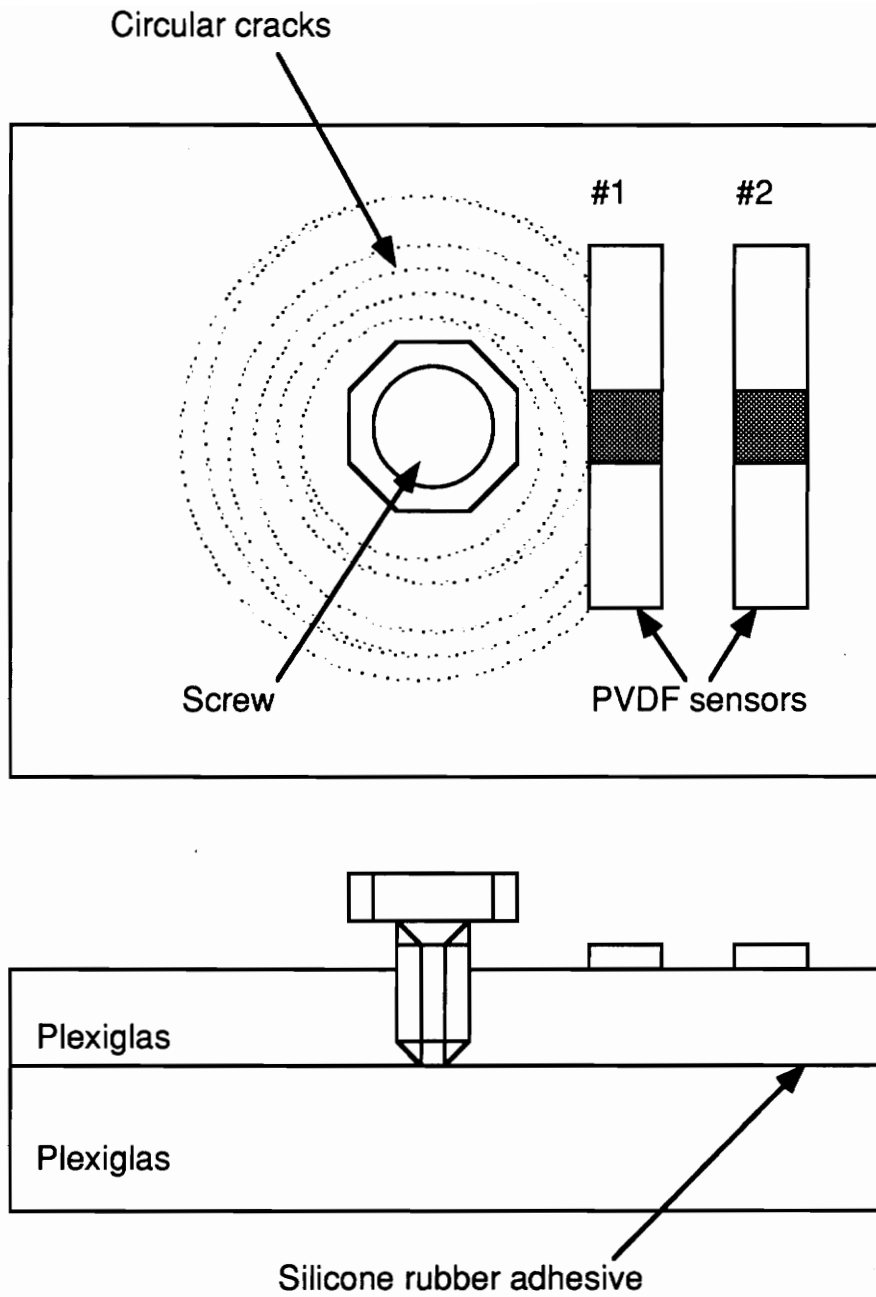
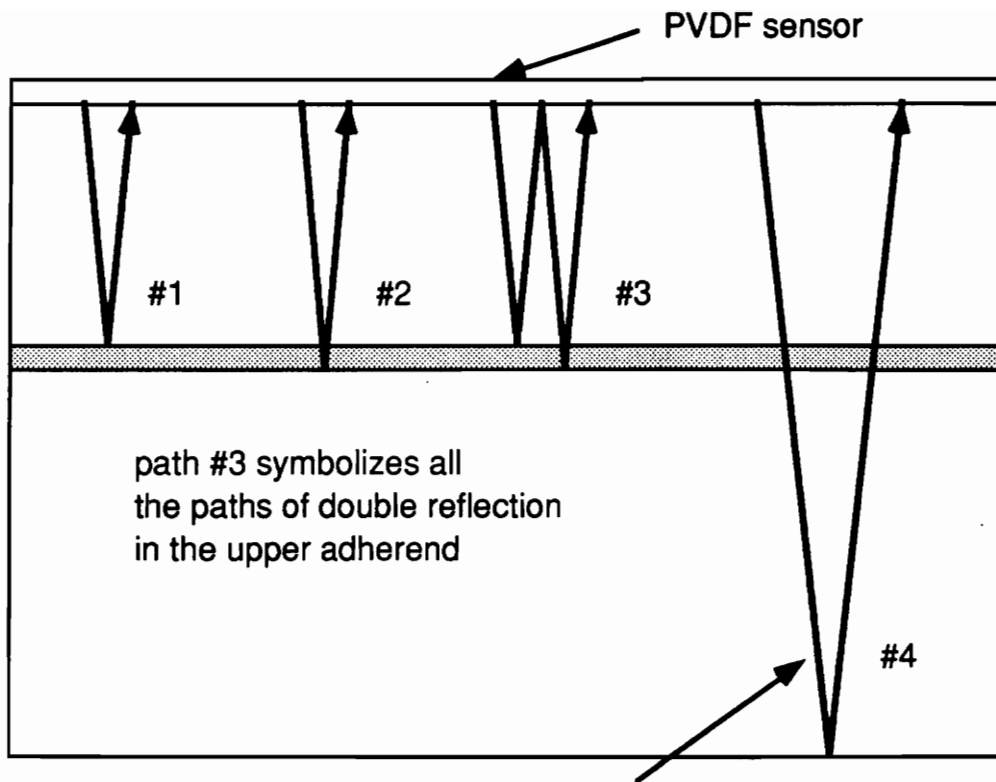


Figure 41 (b). Specimen during circular crack propagation.



Pulse traveling through the bond

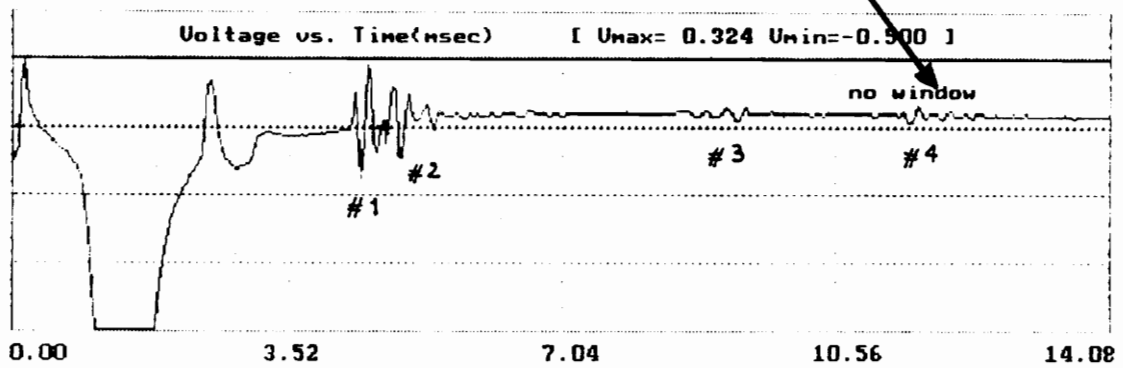


Figure 42. Pulse-echo signal for crack propagation.

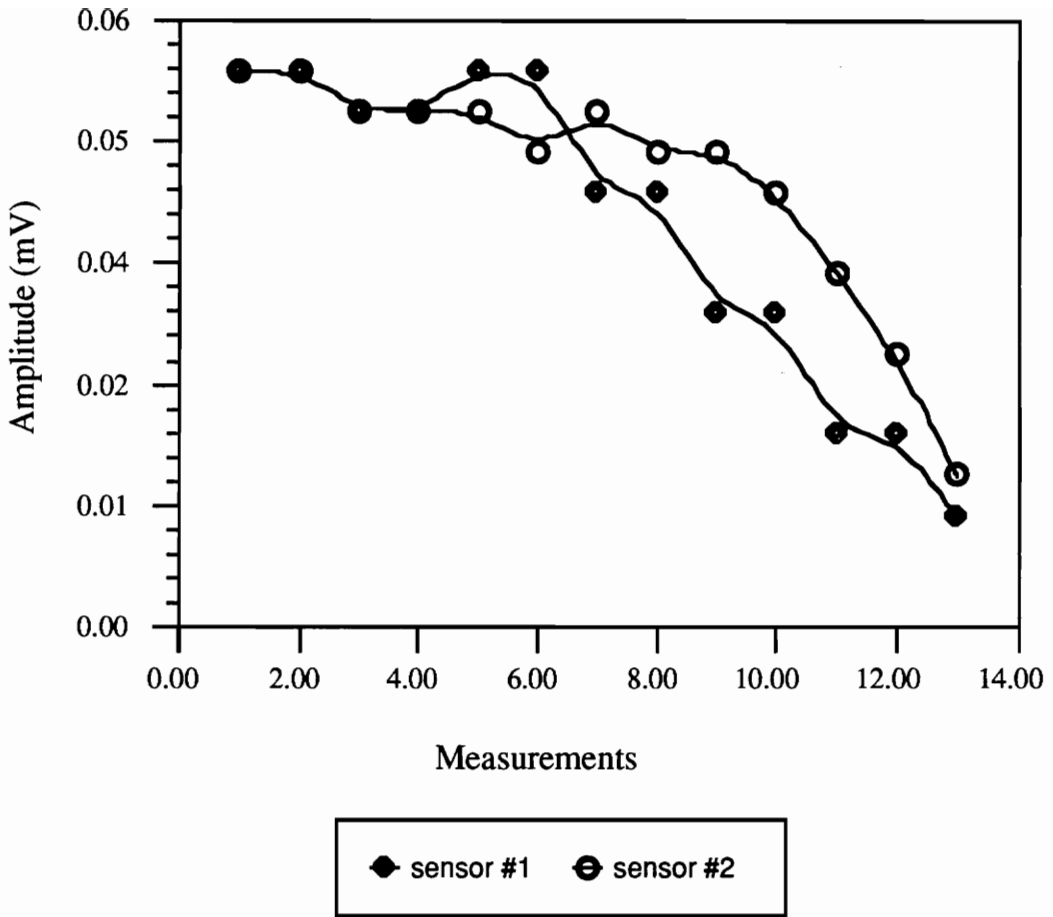


Figure 43. Amplitude of signals for each increment of the circular crack area (bond thickness = 0.5 mm) for specimen 1.

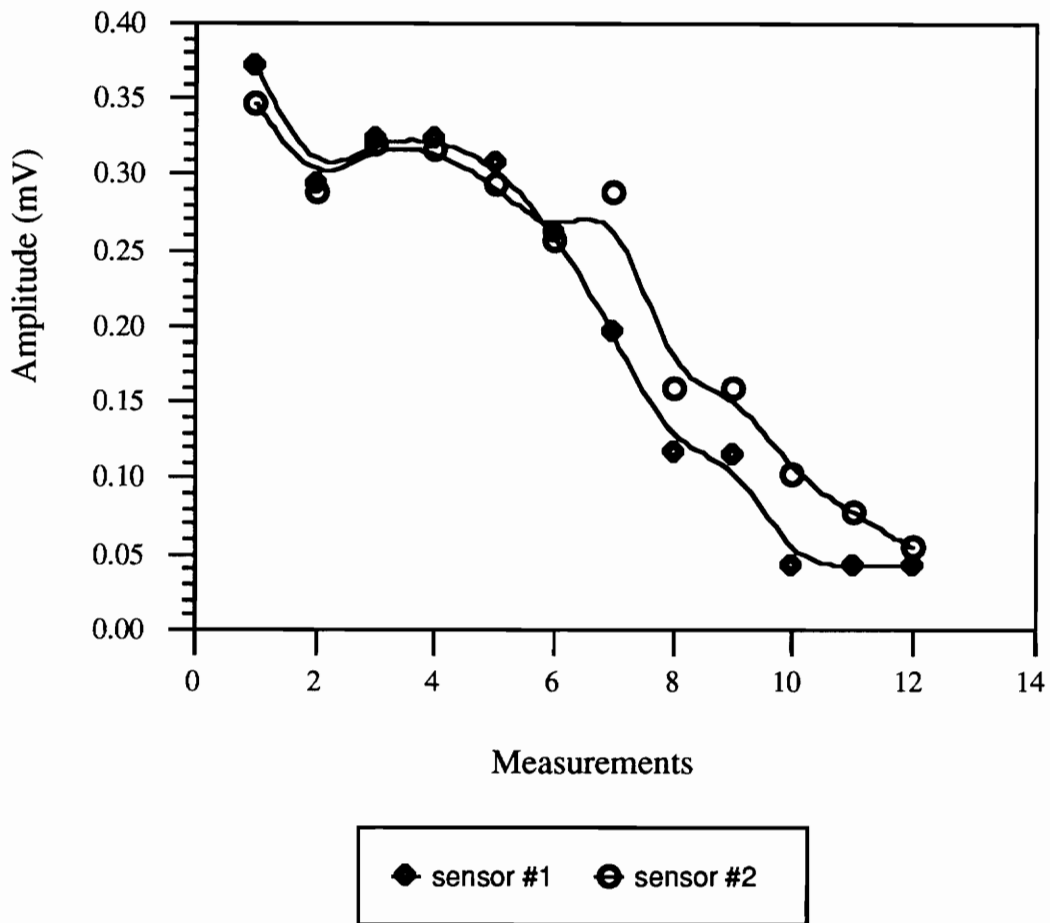


Figure 44. Amplitude of signals for each increment of the circular crack area (bond thickness = 0.5 mm) for specimen 2.

A thicker bonded joint (thickness = 0.9 mm) was also used. The way the crack propagated was no longer circular but random (see fig. 45). Fig. 46 shows the amplitude of the signal for each measurement. As the crack propagated randomly, it was not easy to control its propagation and cracks reached both sensors in the same time so that the decreasing of the amplitude of both sensors happened during the same measurement.

The results were satisfactory because it was shown that the technique could detect development of porosity under a small PVDF sensor (1.6 mm X 1.6 mm) used in pulse-echo mode and, led us to the conclusion that PVDF transducers can be used to monitor the crack propagation. Because of the ease with which intricate patterns may be etched on PVDF films, multi-point arrays can easily be fabricated. By individually sending a pulse to each grid point of the array, and then processing the received signal from the same point, a discrete "C-scan" of the bond would result. These arrays could also be used in acousto-ultrasonic technique by using different grid points as sender and receiver. This technique has the advantage of being used without removing the structure from its environment. Moreover it doesn't require access to the location where bond integrity is to be checked: the remote PVDF sensors are already fixed and the operator only needs to connect cables.

Cracks propagating randomly

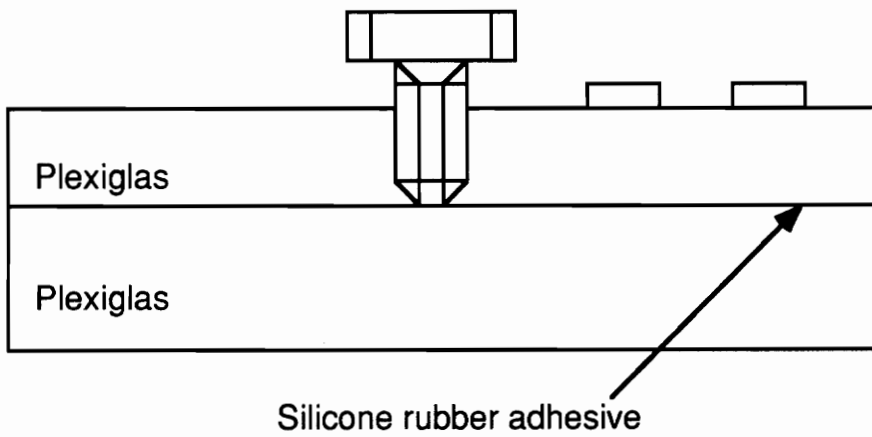
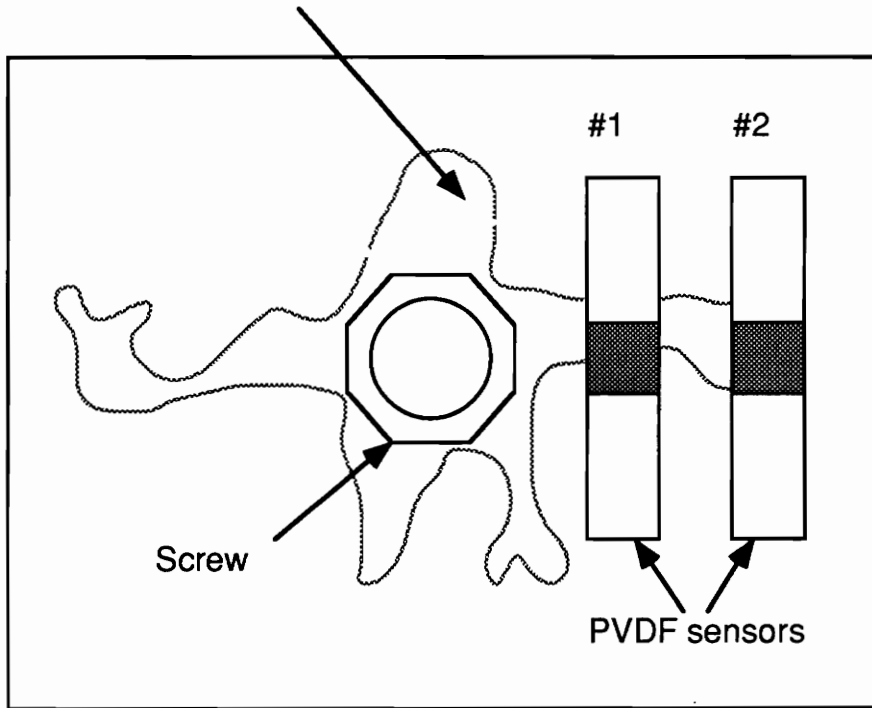


Figure 45. Specimen during non circular crack propagation .

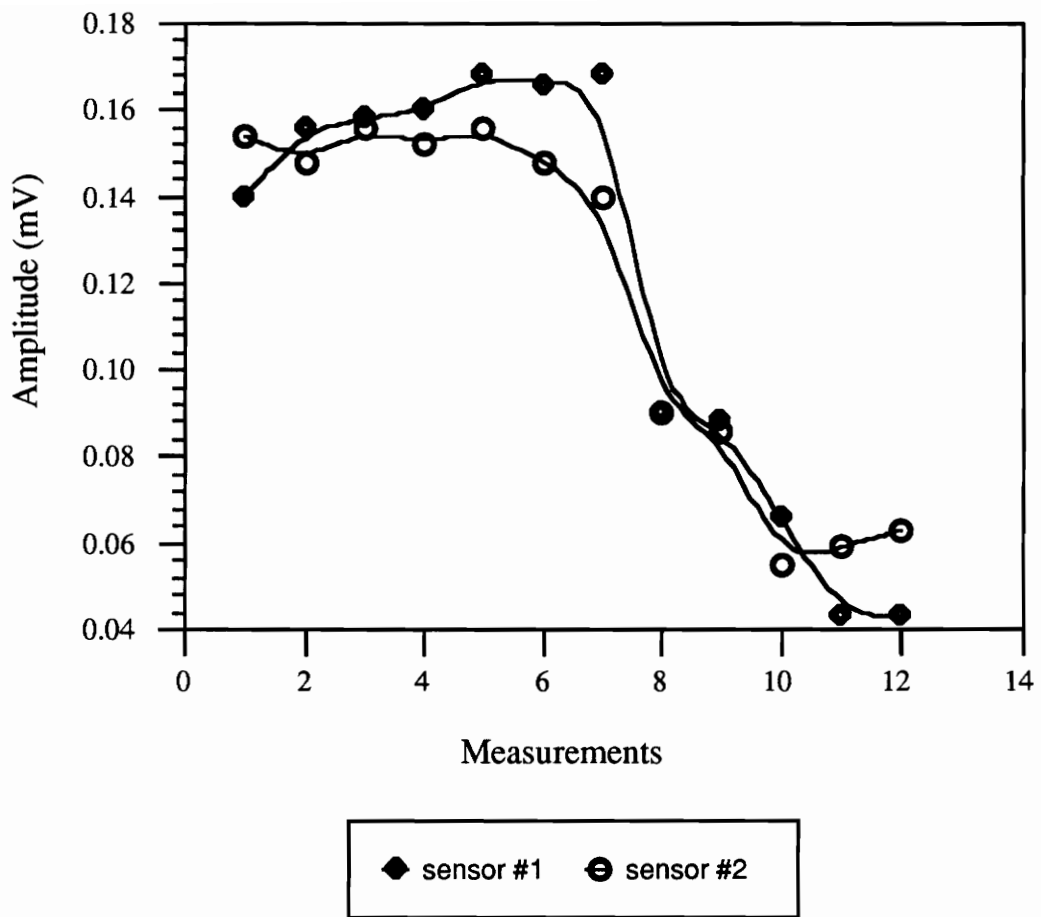


Figure 46. Amplitude of signals for each increment of crack area with arbitrary shape (bond thickness = 0.9 mm).

5.3 Double cantilever beam

In order to have better control of the propagation of cracks, double cantilever beams were used on which 1-D arrays of PVDF sensors were glued. Once it was shown that there was a good qualitative correlation between the amplitude of the sensors and the crack front, the technique was used on a composite material to detect delamination.

5.3.1 Crack propagation

The specimen used in this experiment was constructed using two 100 mm X 35 mm pieces of plexiglas, one of which contained a threaded hole to accommodate a 6.3 mm screw. These pieces were bonded together by a silicone rubber adhesive (thickness = 0.75 mm) and five 4.8 mm X 4.8 mm PVDF sensors were glued outside of the bonded joint as shown in fig. 47. A crack was propagated by loading the interface of the bonded joint with the advancement of the screw.

Two different experiments were done:

- one experiment with the same thickness adherends.

$$(t = t' = 8 \text{ mm})$$

- one experiment with two different thickness of adherends.

$$(t = 8 \text{ mm} ; t' = 6 \text{ mm})$$

5.3.1.1 same thickness of adherends

Ultrasonic pulses in the pulse-echo mode, traveling through the bond were sent and received by the same sensor. The signal traveling through the bond and the upper piece of plexiglas only was gated in this experiment as shown in fig. 48, in order to take account in both interfaces of the bond. The ultrasonic data were taken after each increase in crack length which was detected by visual observation.

Fig. 49 shows the amplitude of the signal for each sensor versus the crack front. Contrary to the experiment with circular cracks, the amplitude of the signal increased when the crack reached the surface of the sensors. This was due to the fact that the failure was adhesive and occurred at the bottom of the bond. In this case indeed, the signal couldn't transmit from the bond to the bottom piece of plexiglas and thus more energy was reflected. (see explanation in fig. 50). Fig. 51 shows what happens when the crack occurs at the upper side of the bond.

In real structural materials, it won't be possible to isolate signal #2 (fig. 49) if the thickness of the adhesive is too thin. Therefore the signal traveling through the bond and both adherends must be gated. But then the experiment must be performed with two different

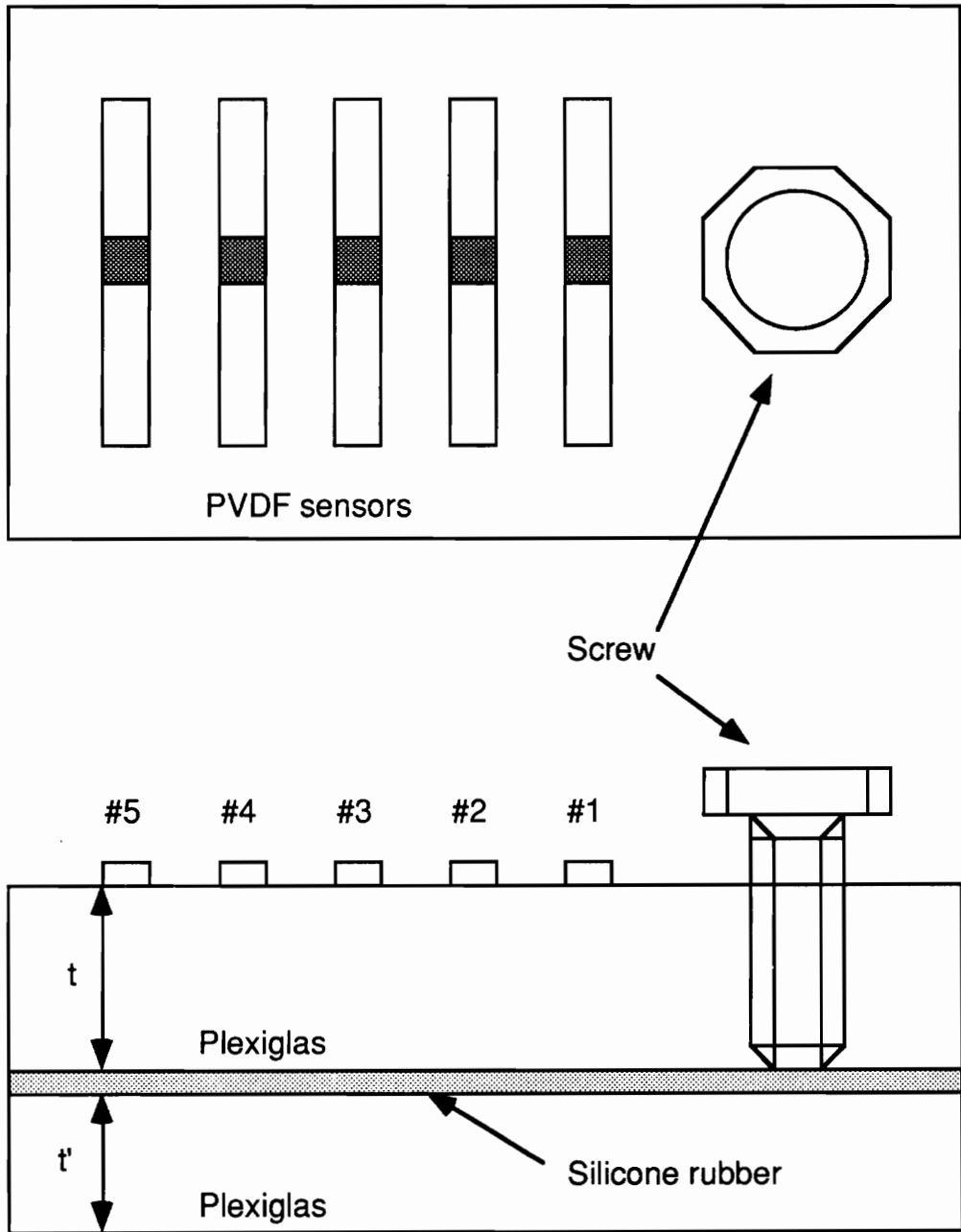


Figure 47. Double cantilever beam used for crack propagation.

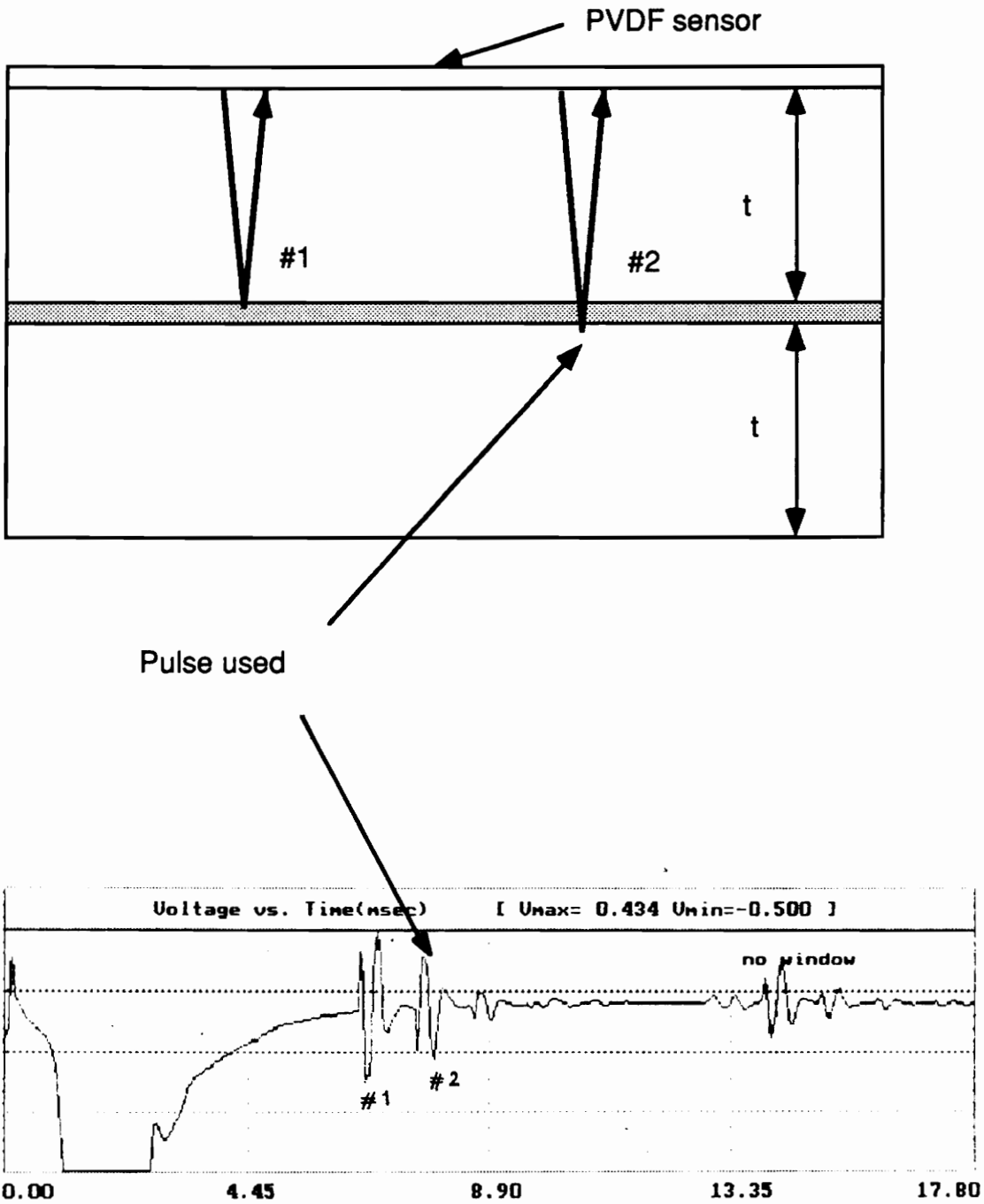


Figure 48. Pulse-echo signal for crack propagation (path #2)

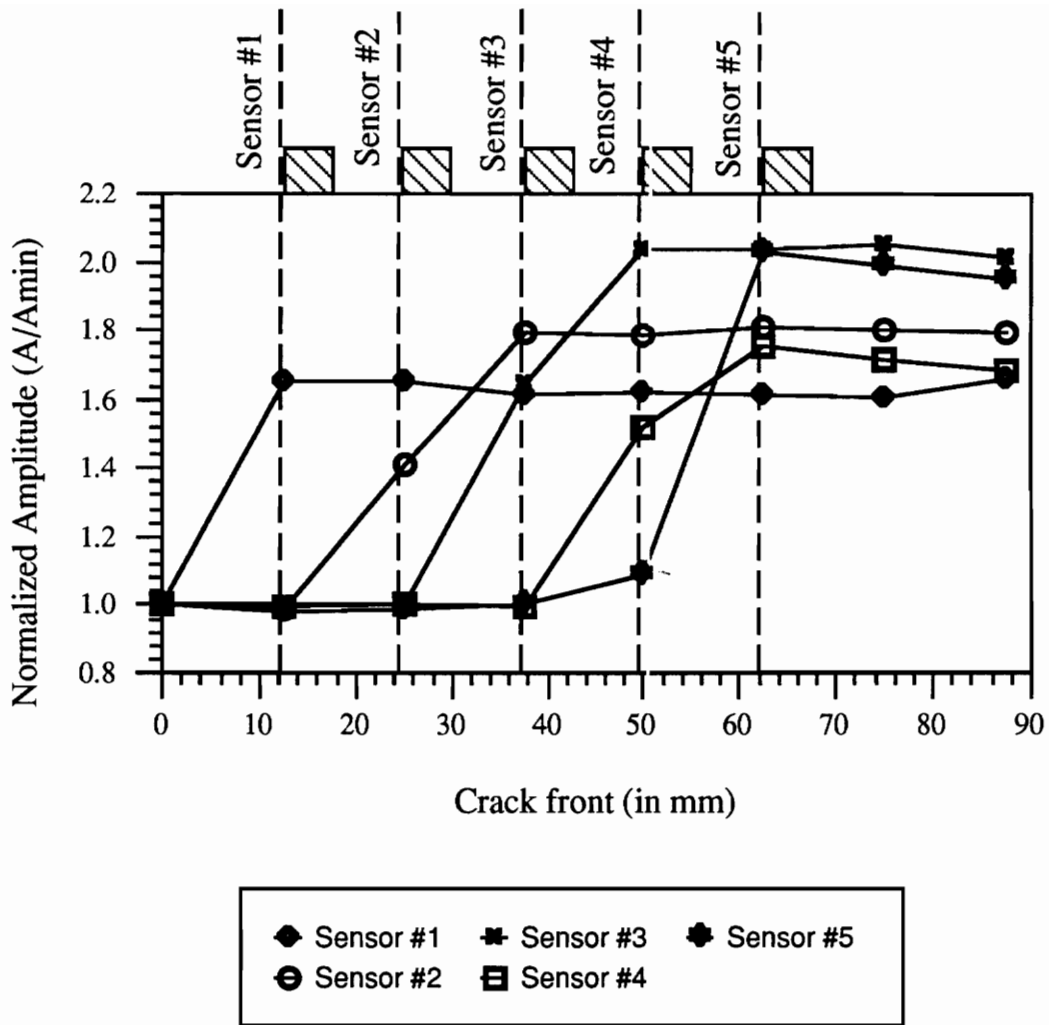


Figure 49. Amplitude of the signal versus the crack front.

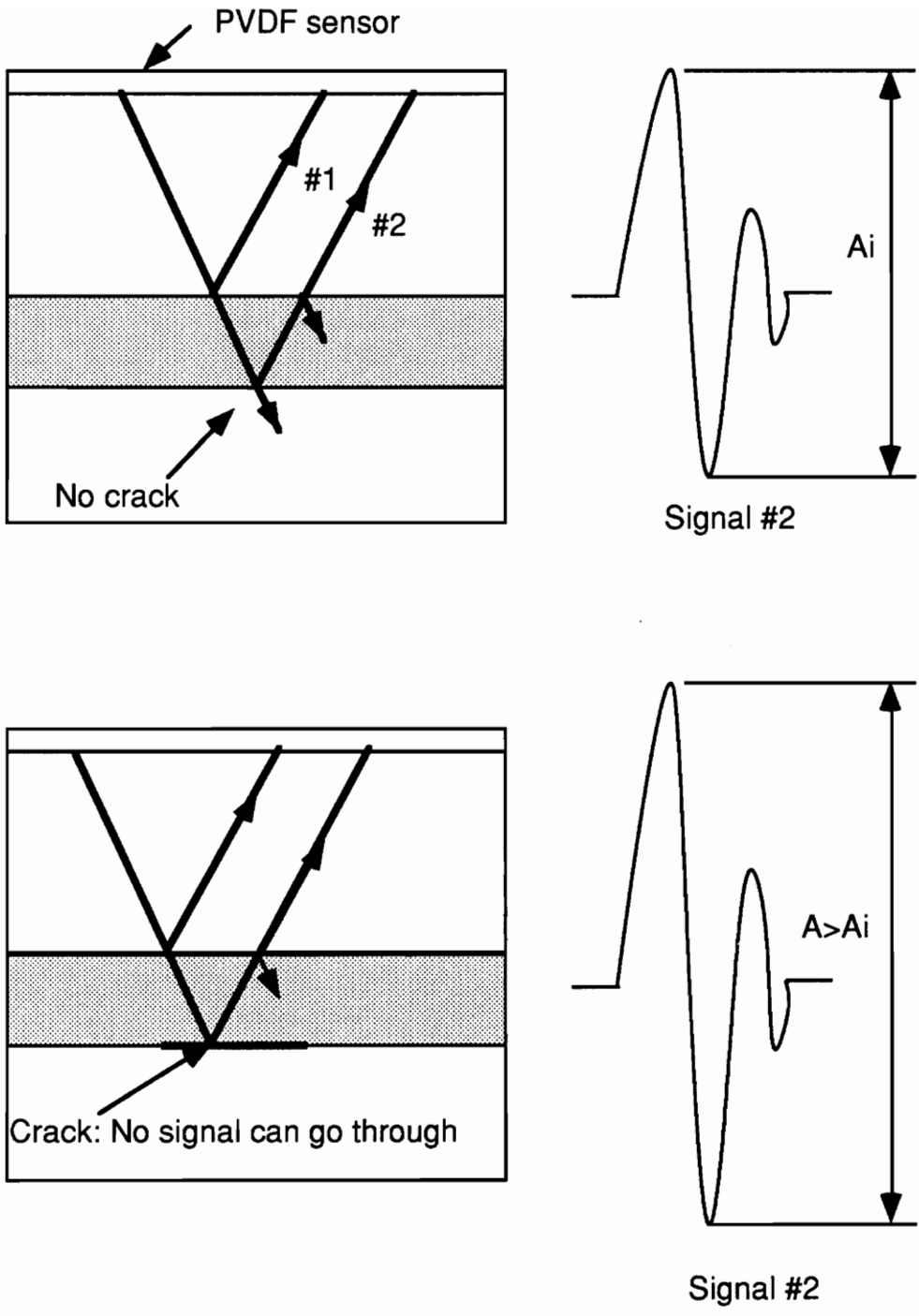


Figure 50. Amplitude of the signal when a failure occurs at the bottom of the bond.

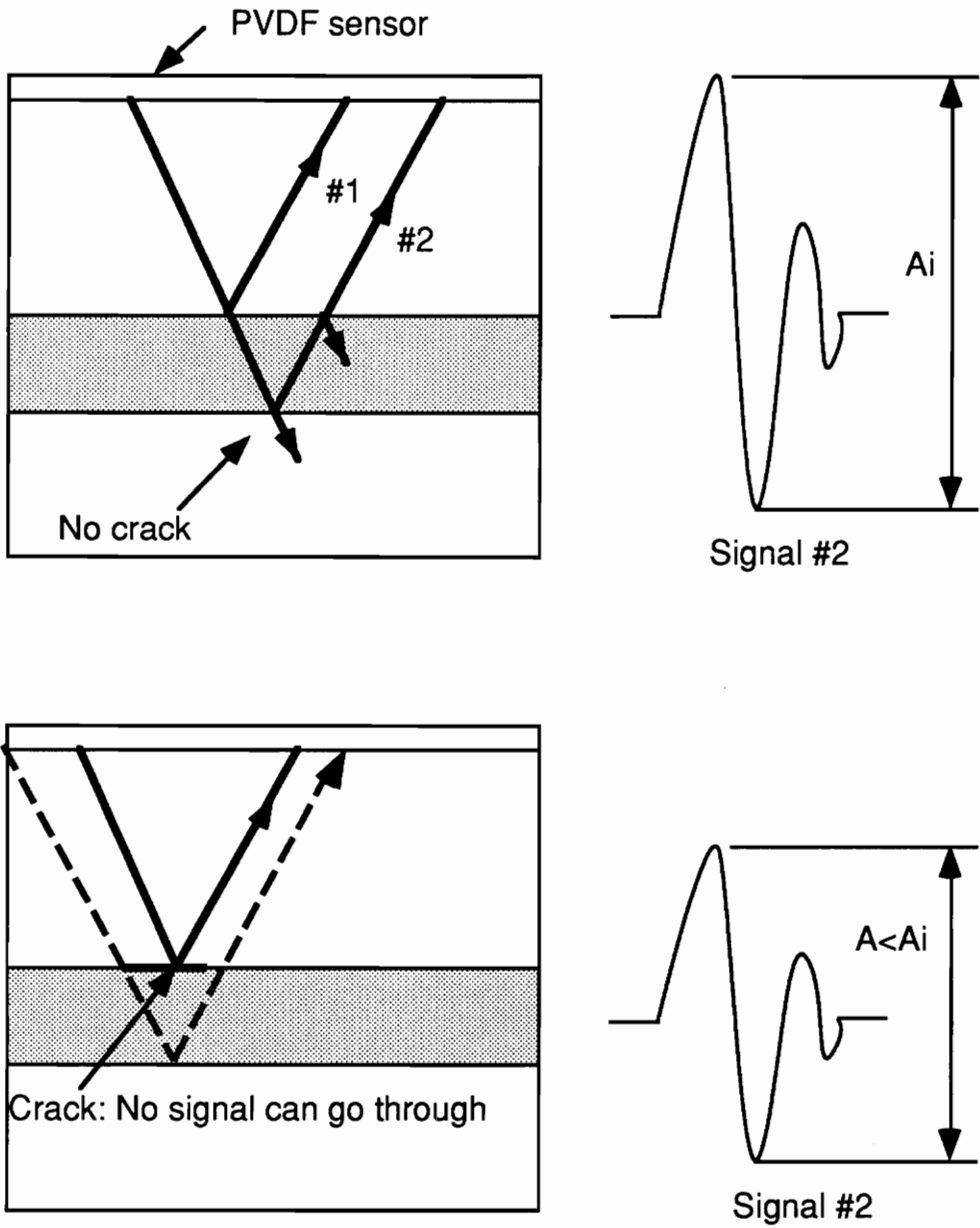


Figure 51. Amplitude of the signal when a failure occurs at the upper side of the bond.

thicknesses of adherends in order not to superpose the double reflection of the signal in the upper adherend with the signal studied.

5.3.1.2 Different adherend thicknesses

Ultrasonic pulses in the pulse-echo mode, traveling through the bond and both pieces of plexiglas as shown in fig. 52 were sent and received by the same sensor. The ultrasonic data were taken after each increase in the crack length.

Fig. 53 shows the amplitude of the signal for each sensor versus the crack front. In this experiment, the amplitude of the signal decreased when the crack reached the sensor because the signal gated traveled through both pieces of plexiglas and because the thickness of the two adherends were different so that there was no addition of unwanted signals.

These experiments on crack propagation showed that PVDF sensors could be used with success in pulse-echo mode to detect damage in the bond. Their advantage over ceramics is that they could be designed in 2-D arrays composed of multi-point sensors which could show the size of the cracks, their location and how they propagate versus time during service. Nevertheless all these experiments have been performed on model structures which are not realistic in industrial applications.

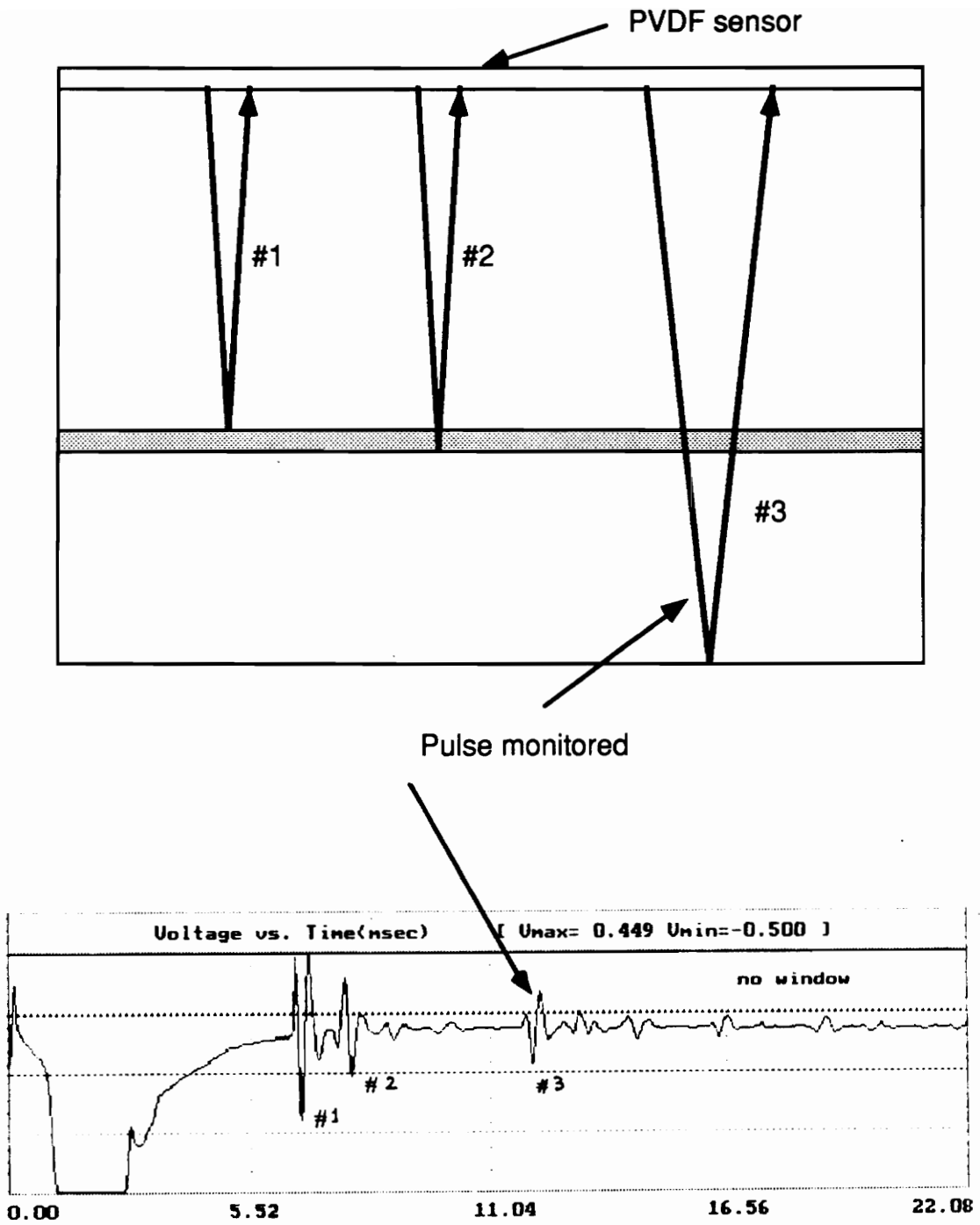


Figure 52. Pulse-echo signal for crack propagation.

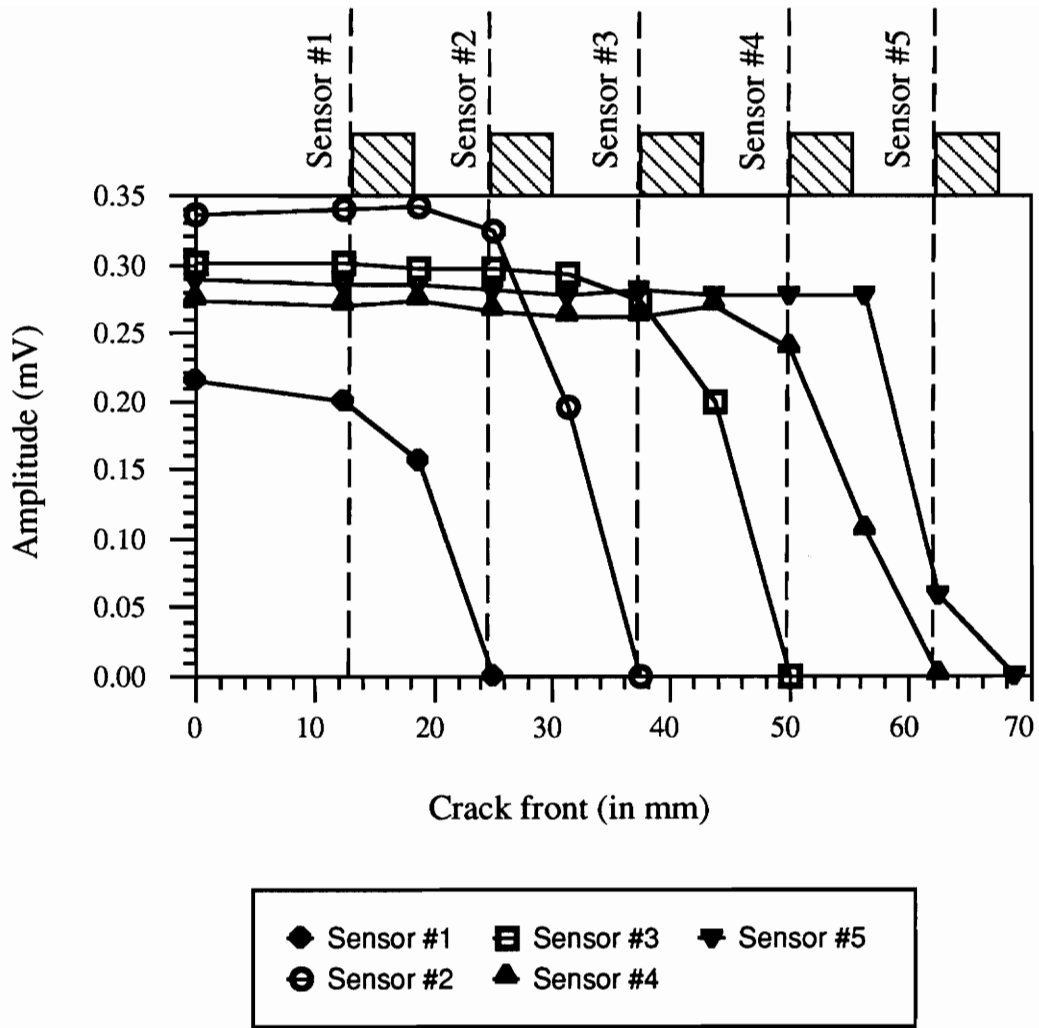
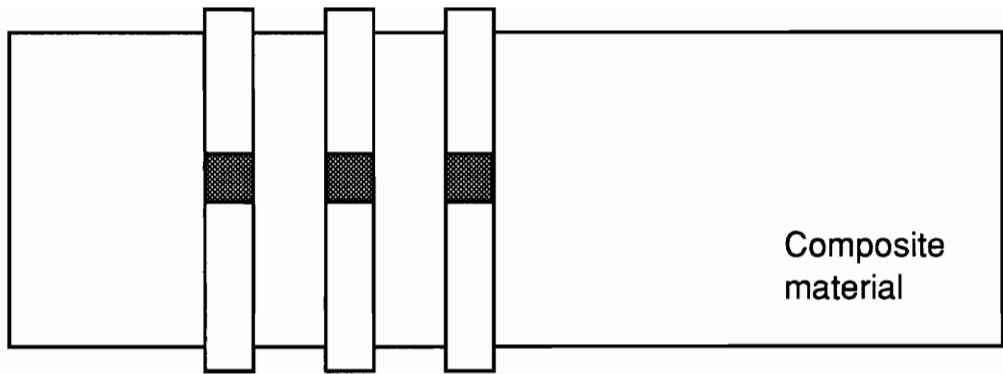


Figure 53. Amplitude of the signal versus the crack front.

5.3.2 Delamination of composites

An experiment was needed to show the success of the technique in a more realistic application. The specimen used was a 1.52 mm thick AS4/J2 composite material (graphite epoxy) made of 12 0° plies. A crack was propagated in its middle and three 3 mm X 3 mm PVDF sensors were bonded on the surface of the specimen in the area where the crack was supposed to be (fig. 54). Because of the shape of its pulse-echo signal (fig. 55), it was predicted that the crack was under the area of sensor #1. Indeed once delamination reached the area located under sensor #1 (fig. 54), the first signal received by the sensor occurred sooner ($t = 0.6 \mu\text{s}$) since the signal went through a thinner layer (fig. 55). In the case of sensor #2 and #3, the first signal occurred at $t = 1.1 \mu\text{s}$ because the composite was not delaminated. Anyhow, the signals were small and the minimum size of PVDF sensors for this material was reached. Therefore two 5 mm X 13 mm bigger PVDF sensors were glued on the other side of the specimen, one of them (sensor #4) on the predicted delaminated area and the other one (sensor #5) on the non damaged area (fig. 56). The results were much better than the previous experiment: sensor #4 detected the first reflection in the delaminated composite at time $t = 0.60 \mu\text{s}$ and its second reflection at time $t = 1.1 \mu\text{s}$ (fig. 57). Sensor #5 seemed to detect a very small signal at time $t = 0.6 \mu\text{s}$ which was thought to come from partial delamination under the area of sensor #5, and a larger signal at time $t = 1.1 \mu\text{s}$ (fig. 57) due to the reflection



PVDF sensors

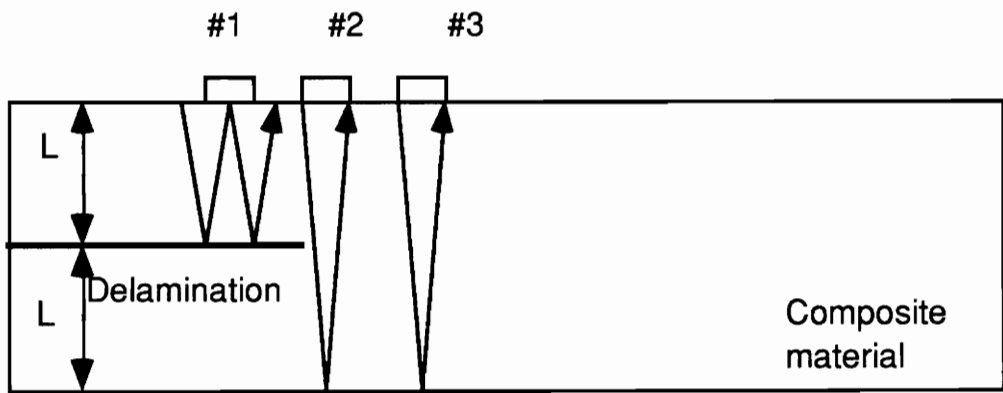
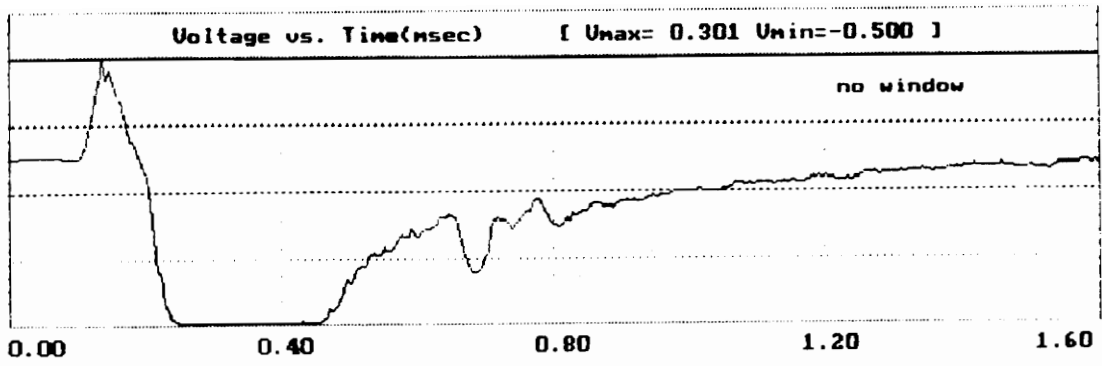
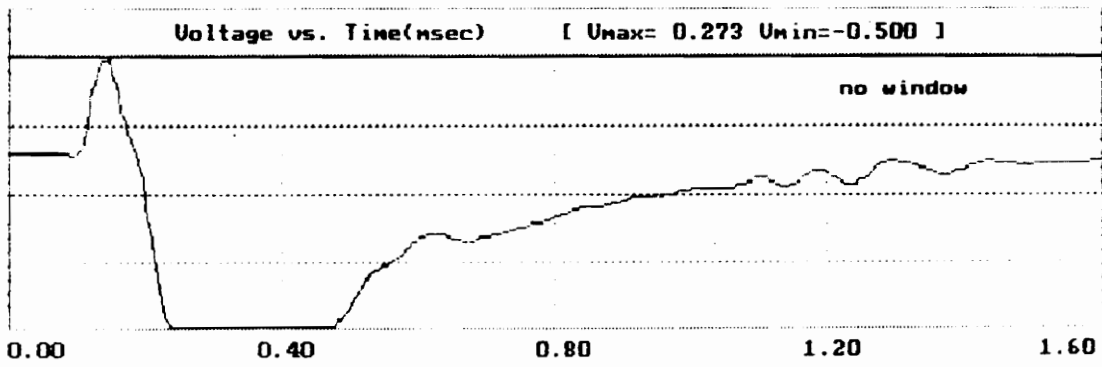


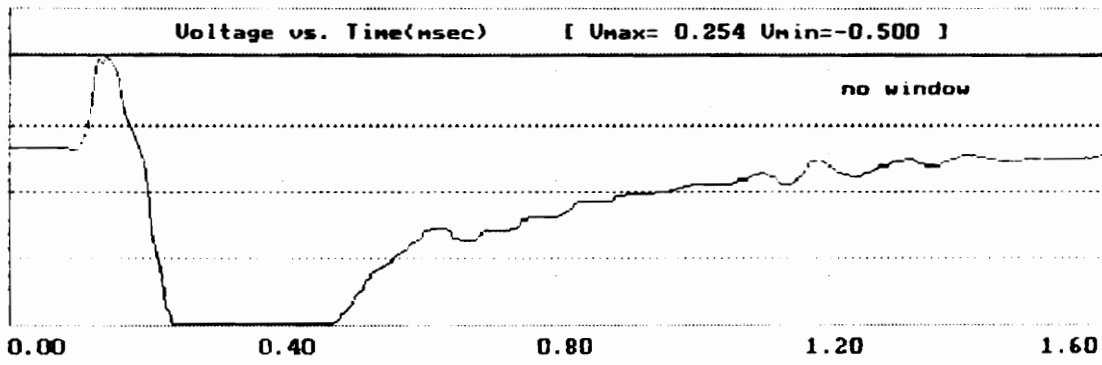
Figure 54. Specimen used to detect the delamination of a composite (not to scale).



(i)



(ii)



(iii)

Figure 55. Pulse-echo signal for (i) sensor #1.

(ii) sensor #2

(iii) sensor #3

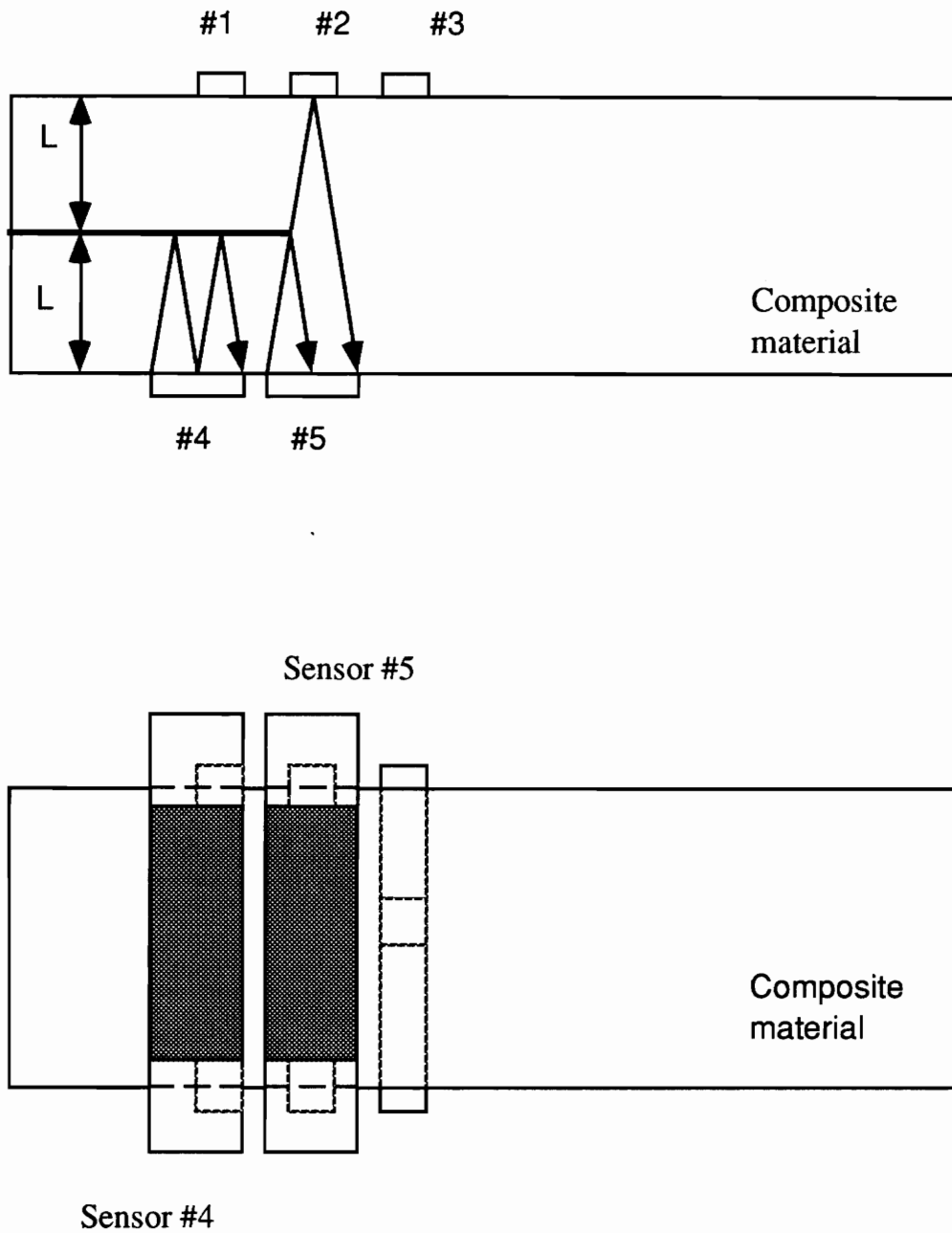
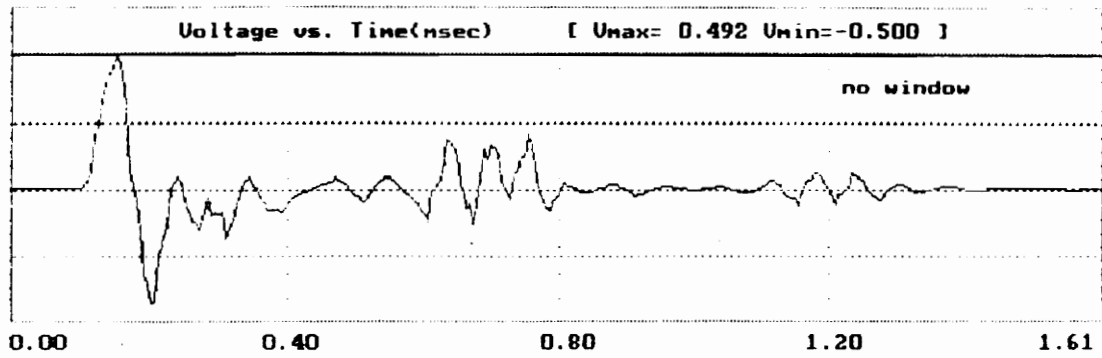
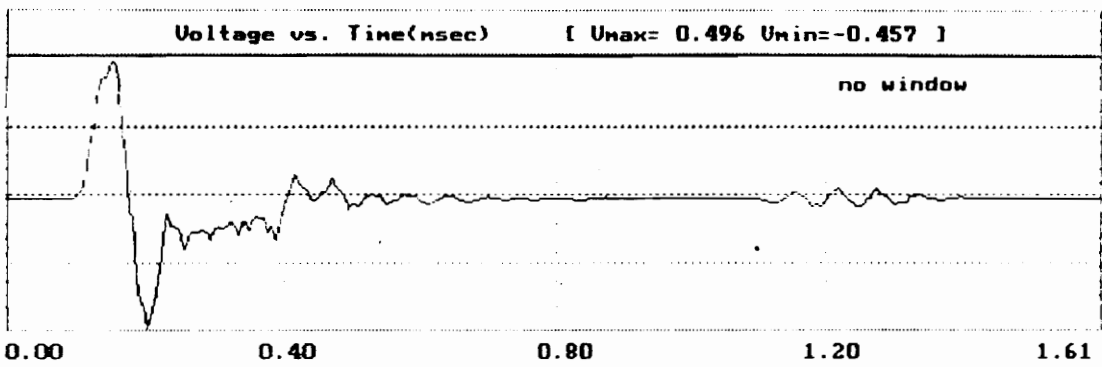


Figure 56. Location of sensors #4 and #5 (not to scale).



(i)



(ii)

Figure 57. Pulse-echo signal for (i) sensor #4.

(ii) sensor #5

in the total thickness of the composite (fig. 56). The front of the delamination was then checked by putting some dye penetrant (Spotcheck type SKL-HF, Magnaflux Corporation, Chicago, Il.). It appeared that the delamination was located under sensor #1, sensor #4 and about 10% of sensor #5 which explains its small signal at time $t = 0.6 \mu\text{s}$.

The high attenuation and the shape of the signals reflected are due to the dispersion in the composite material. Indeed a composite material is considered dispersive if the wave length (λ) of the signal transmitted is smaller than a hundred fiber diameters^{42,43}. λ can be calculated from the frequency of the pulse emitted:

$$\lambda = \frac{V}{f}$$

where V = velocity in the medium
 f = frequency of the signal (8 MHz)

V is calculated from the time taken by the pulse to travel through the thickness of the composite:

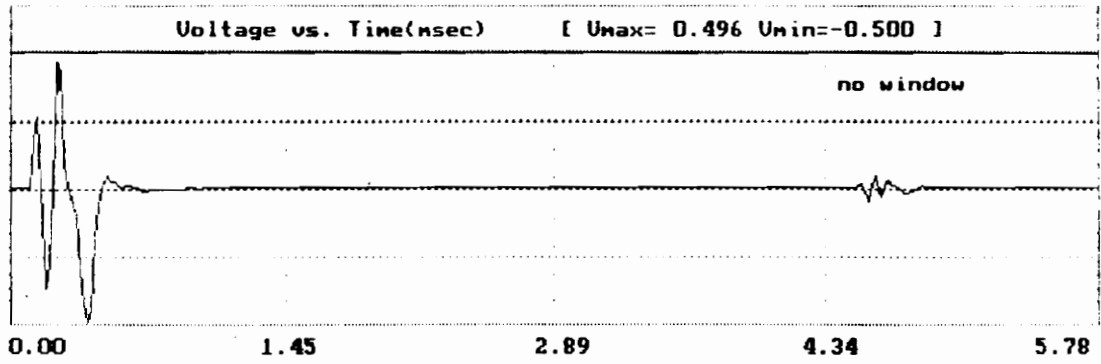
$$V = \frac{2L}{t}$$

where L = thickness of the material (0.76 mm)

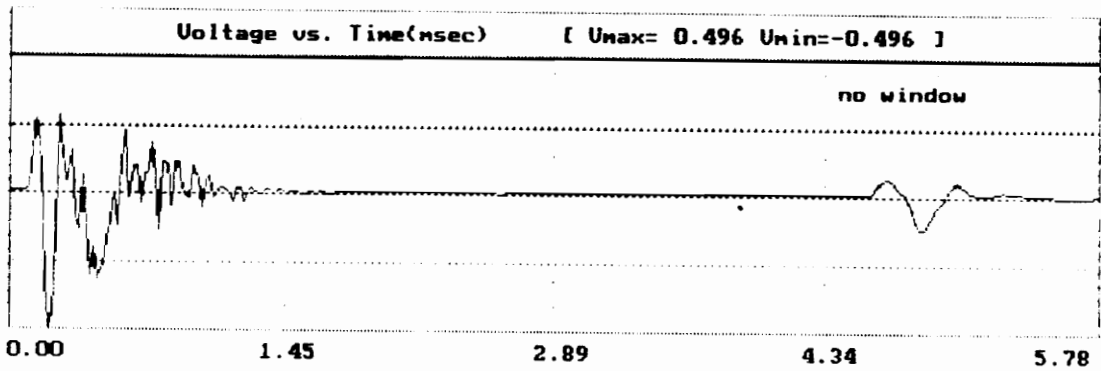
t = time between the initial pulse and its back reflection ($t = 0.60 - 0.10 = 0.50 \mu\text{s}$)

Therefore, λ was found equal to $380 \mu\text{m}$ which represents 50 times the diameter of the fibers ($7 \mu\text{m}$) used in this composite. The signals propagating in this medium are then dispersive which results in high attenuation and spreading of the wave form.

The above experiment showed that PVDF sensors could be successfully used in real structures to detect delamination. In addition to their numerous advantages already discussed throughout the previous experiments, another feature pointed out here is the heavily damped character of PVDF sensors. This property enables them to detect signals in very thin layers that ceramic transducers couldn't detect. Fig. 58 and 59 show the shape of the pulse-echo signal in plexiglas at different scale for a PVDF sensor and a ceramic transducer. In the case of the PVDF sensor, a signal can be detected $0.6 \mu\text{s}$ after the emission of the pulse whereas a ceramic transducer needs $1.6 \mu\text{s}$ to be able to detect any signal because of its ringing.

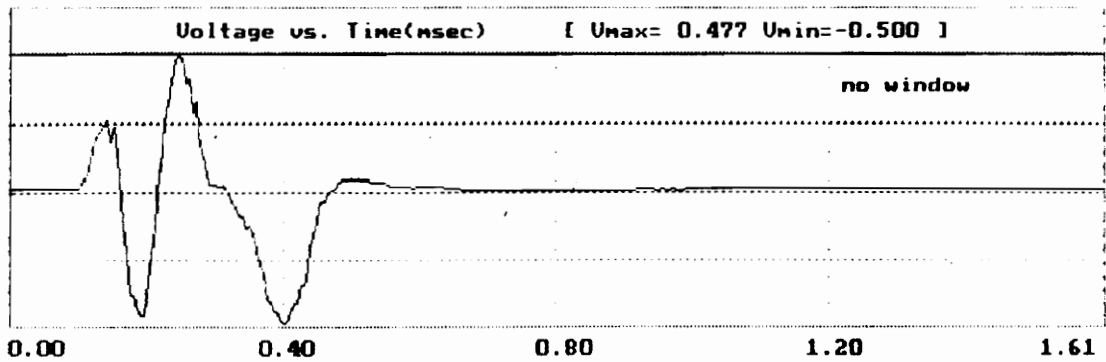


(i)

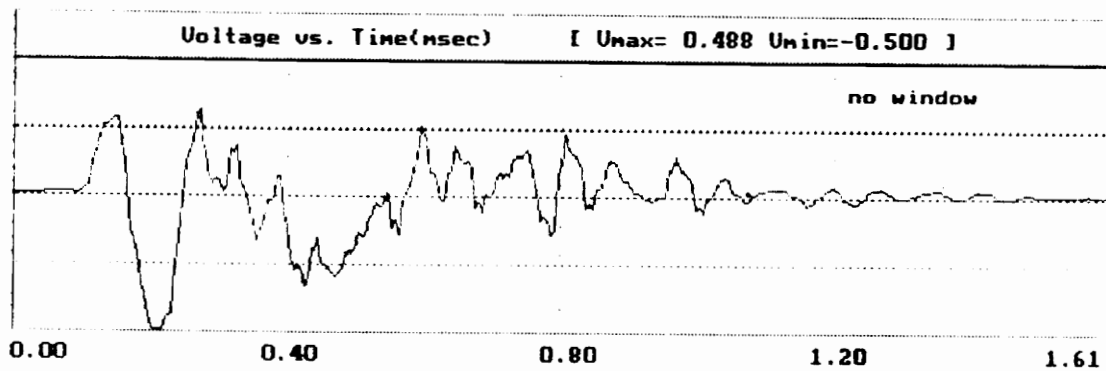


(ii)

Figure 58. Pulse-echo signal in plexiglas for (i) PVDF transducer.
(ii) ceramic transducer.



(i)



(ii)

Figure 59. Pulse-echo signal in plexiglas for (i) PVDF transducer.
(ii) ceramic transducer.

6.0 SUMMARY & CONCLUSION

PVDF sensors have been used with different types of ultrasonic techniques such as pulse-echo, through-transmission, and acousto-ultrasonic techniques to successfully detect porosity, cracks and debonds in adhesively bonded model structures (plexiglas bonded with silicone rubber). PVDF sensors have also been used in pulse-echo mode to detect delamination in a more realistic structure, namely AS4/J2 (polyamide) composite material made of twelve 0° plies. In this latter experiment, the heavily-damped character of PVDF appeared to be crucial since it enabled PVDF transducers to detect the first two reflections in the thin layer of the composites which was not possible with ceramic transducers. Another interesting use of PVDF sensors was in the monitoring of cure. If their service temperature can be increased, the advantage of this technique over the Differential Scanning Calorimetry (DSC) would be great since the adhesive would be monitored in situ with real conditions of pressure and temperature.

The potential use of PVDF sensors for NDE applications is very promising: these sensors are very cheap compared to conventional

transducers, they are light-weight, flexible and very thin (as small as 6 μm), thus it is possible to permanently attach them on a structure without disturbing the structure significantly. The fact that PVDF sensors may be permanently attached to structures gives them another advantage over ceramic transducers: they don't need any coupling agent. Indeed coupling agents can penetrate the defects and hide their presence by reducing the reflection coefficient. This problem cannot occur with the use of PVDF sensors. Moreover conventional transducers need to be held in contact with the structure. This technique is slow when large areas need to be examined, can be sensitive to contact pressure, and is not always possible where limited access areas are of concern. PVDF transducers can be installed during the manufacturing of the structure and permit monitoring of joints without needing to reach their locations; the operator would only have to connect cables to the testing instruments which would check the integrity of bonds. Because of the ease with which intricate patterns may be etched on PVDF films, multi-point arrays can easily be fabricated. By individually sending a pulse to each grid point of the array, and then processing the received signal from the same point, a discrete "C-scan" of the bond would result. These arrays could also be used with the acousto-ultrasonic technique by using different grid points as sender and receiver. PVDF films have other characteristics which give them many advantages over ceramics: they respond to a wide range of frequencies, they are heavily-damped which make them suitable for

monitoring defects in thin layers such as in composite materials or adhesive bonds, and they have a low acoustic impedance which enables them to have good acoustic matching to composites. Therefore PVDF sensors seem to be ideal sensors for monitoring damage in adhesively bonded structures.

Adhesive-bonded joints in which adhesives are used to join and reinforce materials are extensively used in aircraft components and assemblies where structural integrity is critical. When very large and costly assemblies have been bonded, the importance of good nondestructive inspection is fully appreciated to determine if adequate strength exists or if the parts need to be reworked or scrapped. PVDF sensors would have the advantage of inspecting the bonded assemblies from the very beginning (during cure cycle) of the operation until their in-service use. Provided the increasing of their service temperature, PVDF sensors could be permanently attached to structures to monitor their curing and thus detect subtle defects which are generally very difficult to detect after curing. It would moreover enable the operator to know when the adhesive is cured and then when the structure can be removed. It would also detect if the adhesive is properly set over the entire surface and not just on the edge. The same sensors would then be used to verify the quality of bonded assemblies after cure. The next important time for inspection is after the assemblies have been in use and the condition of the parts is unknown. It is necessary to determine if new delaminations have occurred or if any adherend cracks have

developed. A universally accepted single test method for evaluating bonded structures has not yet been developed. Therefore, a combination of test methods is required for complete and reliable inspection. But PVDF sensors would play an important role because the selection of the test method is based on the part configuration and material of construction, the types and size of flaws to be detected, the accessibility to the inspection area, and the availability of equipment/personnel. Indeed the method of using PVDF sensors wouldn't require any accessibility to the inspection area since the operators would only have to connect cables to a data acquisition board which would estimate the strength of the assemblies. The number of equipment and personnel involved in this operation would be few and all the material of construction and type of flaws that are usually inspected by conventional transducers should be done by PVDF transducers. Thus PVDF sensors would advantageously replace conventional transducers sparing time, personnel and money. It could also replace other methods which were used because of the non-accessibility of conventional transducers.

Nevertheless improvements need to be made in order to use PVDF sensors for long-term applications. A common need in all PVDF piezoelectric film devices is the attachment of durable electrical leads. Good mechanical and electrical attachment is desired for contact integrity. Under use conditions the lead should not detach mechanically and electrical contact should not degrade. The method used in our experiments (copper tape with conductive adhesive

pressed onto the metallized surface) doesn't suffice in the transmitting mode because high electrical fields which are imposed to yield optimum mechanical output, can cause arcing and local heating if good ohmic contact is interrupted. Configurations must be designed involving continuous metallization which serves as the electrode and covers both the film surface and the lead attachment point³¹: the lead wire can be epoxied to the PVDF surface prior to metallization; the metal electrode is then applied to the film continuously over the lead wire through a mask in a vacuum system. After metallization, an epoxy overcoating is applied which mechanically protects the contact and serves as a heat sink to dissipate electrical heat in the contact. The choice of electrode metal is dictated by several considerations. The metal should maintain its adherence to the polymer surface; it should have high electrical conductivity and a high threshold for thermal damage. The metal should also accept a low temperature solder. Silver and copper, although excellent conductors, are susceptible to corrosion. In most respects gold is acceptable and should be used in further developments. Depending on the material to be inspected, appropriate adhesives³⁶ resistant to moisture degradation and physical ageing, should also be used to permit good adhesion of PVDF sensors and thus increase the life of the smart structure. Until now, the use of PVDF sensors has been significantly limited by its service temperature since PVDF loses its piezoelectric properties above 60°C. Therefore future work on PVDF sensors must be done in

collaboration with Dr Das Gupta⁴⁰ who managed to improve their range of use by adding ceramic particles during the manufacture of PVDF films. Moreover, experimental apparatus and procedures need to be improved. Measurements of signals should be done in shielded area in order to decrease perturbations due to electromagnetic radiations. On the other hand, a more suitable pulser must be used which can generate higher voltage pulses within a large frequency range. Thus the whole possibilities of PVDF sensors as transmitter and receiver can be reached.

REFERENCES

1. C. C. H. Guyott, P. Cawley, and R. D. Adams, "The Non-destructive Testing of Adhesively Bonded Structure: A Review", *J. Adhesion*, Vol. 20, 1986, pp. 129-159.
2. R.D. Adams, P. Cawley, and C. C. H. Guyott, "Non-destructive Inspection of Adhesively Bonded Joints", *J. Adhesion*, Vol. 21, 1987, pp. 279-290.
3. ASM International, *Metals Handbook*, Vol. 17, Metal Park, Ohio, 1989, pp. 610-639.
4. M. M. Sadek, *Industrial Applications of Adhesive Bonding*, Elsevier, New-York, 1987, pp.69-87.
5. R. D. Adams, P. Cawley, "A Review of Defect Types and Nondestructive Testing Techniques for Composites and Bonded Joints", *NDT International*, Vol. 31, 1988, pp. 208-221.

6. H. G. Tattersall, "The Ultrasonic Pulse-echo Technique as applied to Adhesion Testing", *Appl. Phys.*, Vol. 6, 1973, pp. 819-832.
7. G. A. Alers, P. L. Flynn, and M. J. Buckley, "Ultrasonic Techniques for Measuring the Strength of Adhesive Bonds", *Materials Evaluation*, Vol. 35, 1977, pp. 77-84.
8. G. H. Thomas, and J. L. Rose, "An Ultrasonic Evaluation and Quality Control Tool for Adhesive Bonds", *J. Adhesion*, Vol. 10, 1980, pp. 293-316.
9. A. C. Smith, and H. Yang, "Ultrasonic Study of Adhesive Bond Quality at a Steel-to-Rubber Interface by Using Quadrature Phase Detection Techniques", *Materials Evaluation*, Vol. 47, 1989, pp. 1396-1400.
10. A. Vary, "Acousto-Ultrasonic Characterization of Fiber Reinforced Composites", *Materials Evaluation*, Vol. 40, 1982, pp. 650-662.
11. A. K. Govoda, J. C. Duke, E. G. Henneke II, and W.W. Stinchcomb, "A Study of the Stress Wave Factor Technique for the Characterization of Composite Materials", NASA Lewis Research Center, Cleveland, Ohio, NASA CR 174870, 1985.

12. H. L. M. Dos Reis, L. A. Bergman, J. H. Bucksbee, "Adhesive Bond Strength Quality Assurance using the Acousto-Ultrasonic Technique", *British Journal of Non-destructive Testing*, Vol. 28, 1986, pp. 357-358.
13. A. Fahr, S. Lee, S. Tanary and, Y. Haddad, "Estimation of Strength in Adhesively Bonded Specimens by Acousto-Ultrasonic Technique", *Materials Evaluation*, Vol. 47, 1989, pp. 233-240.
14. A. Tiwari, E. G. Henneke II, J. C. Duke, "Acousto-Ultrasonic Technique for assuring Adhesive Bond Quality", *J. Adhesion*, to be published.
15. Penwalt Corporation, *Application note number 25*, Piezo Film Sensors Division, Valley Forge, PA, 1989.
16. W. H. Chen, H. J. Shaw, D. G. Weinstein, and L. T. Zitelli, "PVF2 Transducers for NDE", *1978 Ultrasonics Symposium Proceedings IEEE*, 1978, pp. 780-783.
17. R. S. William, and P. E. Zwicke, "Assessment of Adhesive Properties using Pattern Recognition Analysis of Ultrasonic NDE Data", *Materials Evaluation*, Vol. 40, 1982, pp. 312-317.

18. R. Stiffer and E. G. Henneke II, "The Application of Poly(vinylidene Fluoride) as an Acoustic Emission Transducer for Fibrous Composite Materials", *Materials Evaluation*, Vol. 41, 1983, pp. 956-957.
19. L. F. Brown, "Piezoelectric Polymer Ultrasound Transducers for Nondestructive Technique", ASNT 1989 Fall Conference, Valley Forge Conference Center, Valley Forge, PA.
20. Pennwalt Corporation, *Kynar Piezo Film Technical Manual*, Piezo Films Sensors Division, Valley Forge, PA, 1987.
21. G. M. Sessler, "Piezoelectricity in Poly(vinylidene fluoride)", *J. Acoust. Soc. Am.*, Vol. 70, 1981, pp. 1596-1608.
22. N. Murayama, and H. Obara, "Piezoelectric Polymers and their Applications", *Japanese Journal of Applied Physics*, Vol. 22, 1983, pp. 3-6.
23. G. P. Hayward, *Introduction to Nondestructive Testing*, American Society for Quality Control, Milwaukee, 1978.
24. W. J. McGonnagle, *Nondestructive Testing*, Gordon and Breach, New York, 1966.

25. ASM International, *Metals Handbook*, Vol. 17, Metals Park, Ohio, 1989, pp. 242-277.
26. W. G. Cady, *Piezoelectricity*, McGraw-Hill, New York, 1949.
27. M. T. Kiernan, and J. C. Duke Jr, "PC Analysis of an Acousto-Ultrasonic Signal", *Materials Evaluation*, Vol. 46, 1988, pp. 1344-1352.
28. R. J. Shuford, A. F. Wilde, J. J. Ricca, and G. R. Thomas, "Characterization and Piezoelectric Activity of Stretched and Poled Poly(vinylidene fluoride)", *Polymer Engineering and Science*, Vol. 16, 1976, pp. 25-36.
29. J. V. Chatigny, L. E. Robb, "Sensors: making the most of Piezo Film", *Sensor Review*, Vol. 7, 1986, pp. 15-20.
30. Penwalt Corporation, *Application note number 11*, Piezo Film Sensors Division, Valley Forge, PA, 1989.
31. W. R. Scott, P. E. Bloomfield, "Durable Lead Attachment Techniques for PVDF Polymer Transducers with Application to high Voltage pulsed Ultrasonics", *Ferroelectrics*, Vol. 32, 1981, pp. 79-83.

32. Penwalt Corporation, *Application note number 13*, Piezo Film Sensors Division, Valley Forge, PA, 1989.
33. Penwalt Corporation, *Application note number 20*, Piezo Film Sensors Division, Valley Forge, PA, 1989.
34. G. Anderson, "Private Conversation", Virginia Polytechnic Institute and State University, Blacksburg, VA, 1990.
35. D.A. Dillard, G. L. Anderson and, D. D. Davis Jr, "A Preliminary Study of the use of Kynar Piezoelectric Film to measure Peel Stresses in Adhesive Joints", *J. Adhesion*, Vol. 29, 1989, pp. 245-255.
36. Penwalt Corporation, *Application note number 9*, Piezo Film Sensors Division, Valley Forge, PA, 1989.
37. R. A. Kline, C. P. Hsiao, M. A. Fidaali, "Nondestructive Evaluation of Adhesively Bonded Joints", *Journal of Engineering Material and Technology*, Vol. 108, 1986, pp. 214-217.
38. S. I. Rokhlim, "Evaluation of the Curing of Structural Adhesives by Ultrasonic Interface Waves. Correlation with Strength", *Journal of Composite Materials*, Vol. 17, 1983, pp. 15-25.

39. L. G. Bunton, J. H. Daly, I. D. Maxwell, R. A. Pethrick, "Investigation of Cure in Epoxy Resins: Ultrasonic and Thermally Stimulated Current Measurements", *Journal of Applied Polymer Science*, Vol. 27, 1982, pp. 4283-4294.
40. D. K. Das-Gupta, "Private Conversation", University of Wales, Wales, United Kingdom, 1990.
41. C.E. Lautzenheiser, A. R. Whiting, and R. E Wylie, "Crack Evaluation and Growth during Low-Cycle Plastic Fatigue. Nondestructive Technique for Detection", *Materials Evaluation*, 1966, pp.241-248.
42. T. R. Tauchert, A. N. Guzelsu, "An Experimental Study of Dispersion of Stress Waves in a Fiber-Reinforced Composite", *Journal of Applied Mechanics*, Vol. 39, 1972, pp. 98-102.
43. R. D. Kriz, "Private Conversation", Virginia Polytechnic Institute and State University, Blacksburg, VA, 1990.

APPENDIX A

Ingression of water

Bond integrity can be affected by environmental conditions since bonded joints are particularly susceptible to attack from aggressive chemicals and moisture. There are two different ways moisture can degrade the adhesive joint: it can diffuse into the adhesive and change its cohesive strength; it can also go in the interface between the adhesive and the adherend, and lower the adhesive strength. It was thought that both cases could be detected: the presence of water in the adhesive should indeed change its elastic properties and thus its acoustic properties. On the other hand, the presence of water at the interface should create a different acoustic impedance mismatch which could be detected also.

A specimen was fabricated on which one 25 mm X 1.6 mm PVDF sensors have been attached to the bonded joint formed by two pieces of plexiglas. The upper piece of plexiglas contained a slot allowing moisture penetration into the silicone rubber adhesive (fig. 60).

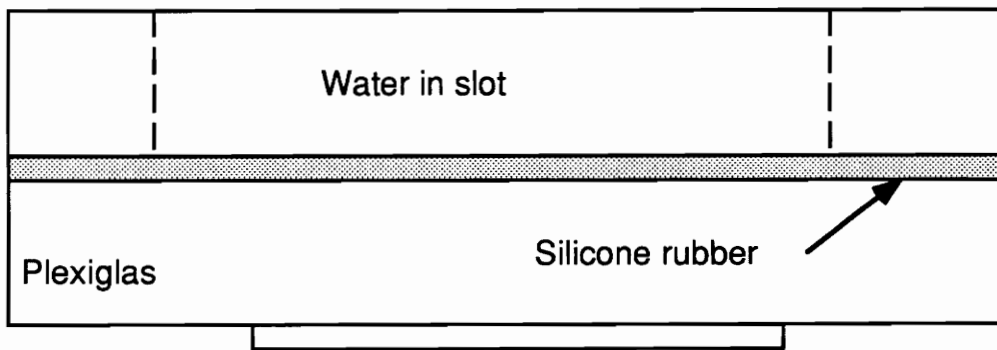
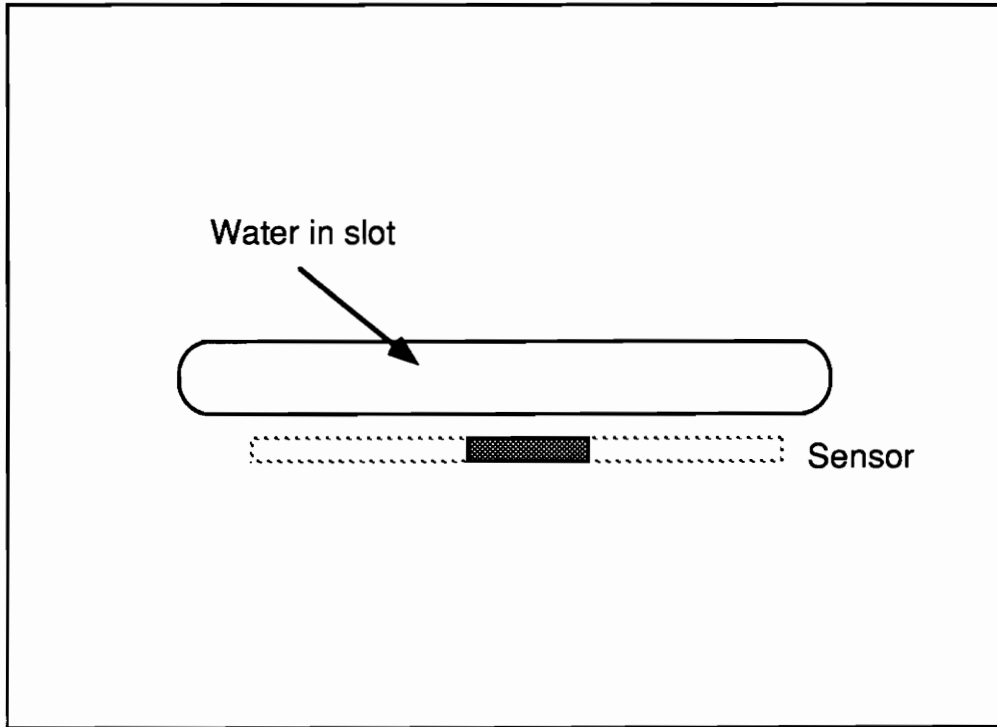
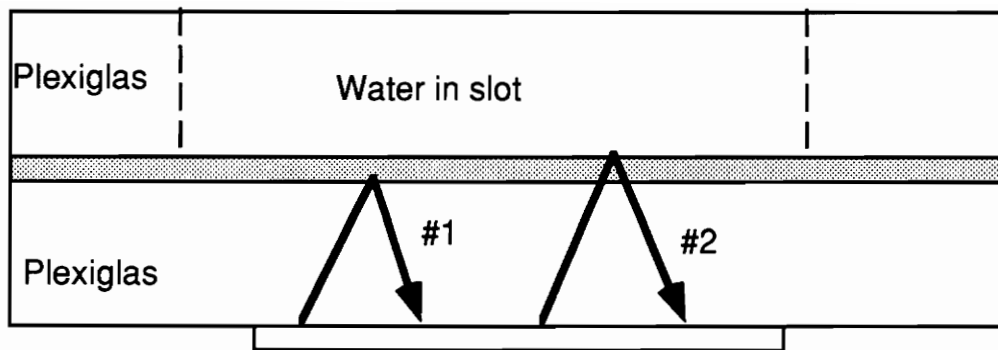


Figure 60. Specimen used to detect the ingress of water.

Ultrasonic traveling through the bond as shown in fig. 61, were sent and received by the same sensor. The signal in contact with both interfaces silicone-plexiglas was monitored and analysed (signal #2). Data were taken versus time and are shown in fig. 62. The amplitude of the signal stayed constant until time $t = 2 \text{ h. } 20 \text{ min.}$ where it decreased suddenly. At the same time, the signal shifted and was inverted as shown in fig.63.

This effect is supposed to be due to the penetration of water in the interface between the silicone rubber and the upper adherend. Indeed if water penetrated in this interface (fig. 64), it should have created a new acoustic mismatch (silicone-water) which could attenuate the signal. Moreover this thin layer of water can create a shift and an inversion of signal⁴³.

Further experiments need to be done to prove that the changes of signals observed in our experiments were really due to the presence of water at the interface. If it can be demonstrated, the technique would have be of great interest to check the integrity of adhesive bonds.



Signal #2 was the signal used to detect ingress of water inside the bond.

Figure 61. Pulse-echo signal for monitoring of water ingress.

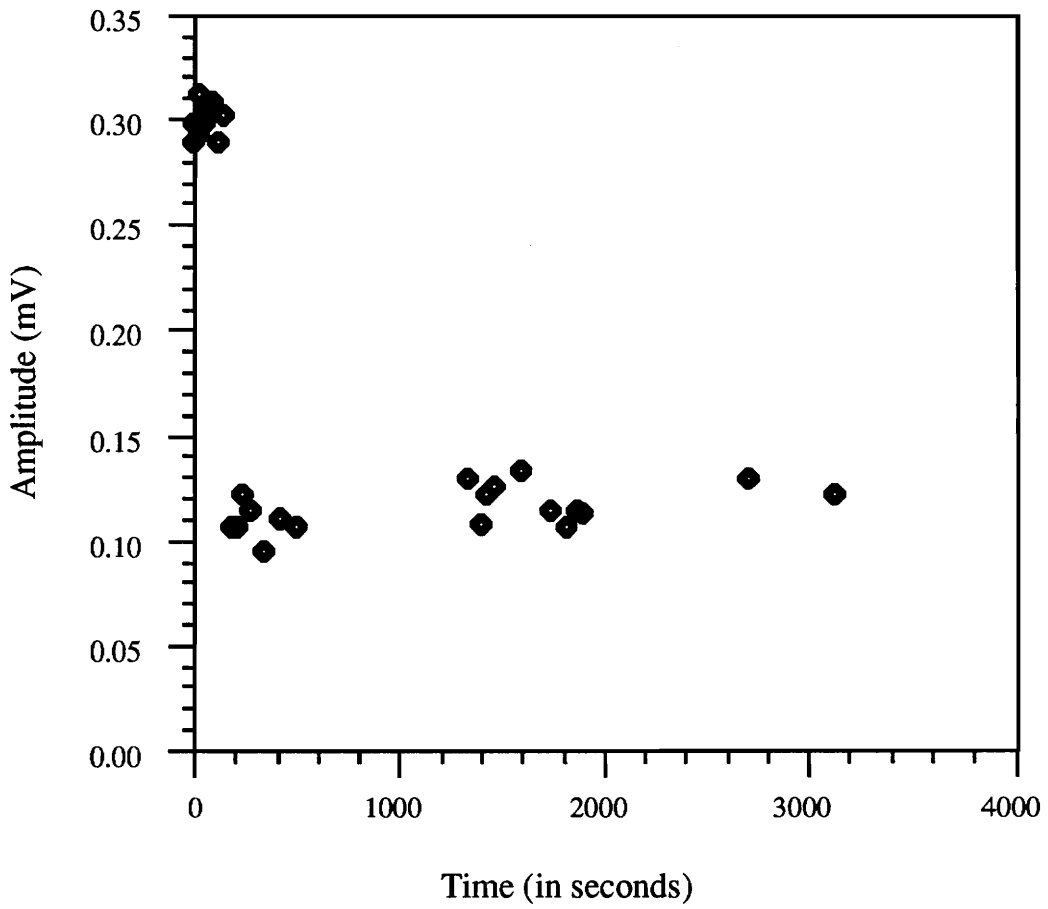


Figure 62. Amplitude of signal versus time.

(i)

(ii)

Figure 63. Comparison of the signal (i). before time $t = 2 \text{ h } 20 \text{ min.}$
(ii) after time t .

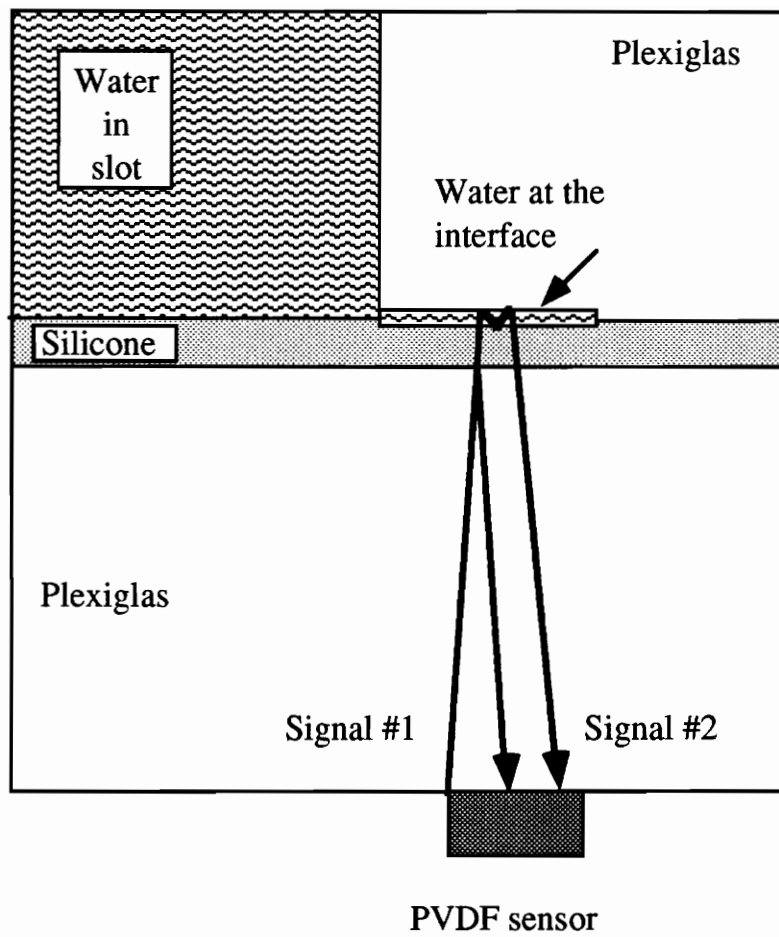


Figure 64. Schematic diagram showing the penetration of water at the interface.

APPENDIX B

Fact sheet of PVDF transducer

Feature	Selection	Comments
Thickness	6 μm to 800 μm	<ul style="list-style-type: none"> - Resonance values change with film thickness²⁰ - 52 μm thick PVDF sensors (f=22 MHz) were used in our experiments.
Electrode material	Copper, silver, nickel, aluminium, chromium, gold, copper-nickel alloy	<ul style="list-style-type: none"> - The choice of electrode metal is dictated by several considerations (high electrical conductivity, resistant to moisture, good adherence to polymer). In most respects, gold is acceptable. - Copper-nickel is sensitive to moisture
Minimum element size for our experiments	<ul style="list-style-type: none"> - 1.6 mm X 1.6 mm for pulse-echo signal in 13 mm thick plexiglas - 3 mm X 3mm for pulse-echo signal in 0.8 mm thick graphite epoxy 	The minimum size element depends on the length of the path and the attenuation of the medium studied
Shielding	<ul style="list-style-type: none"> - shielded area - overlapping of PVDF sheet to create shield 	<ul style="list-style-type: none"> - shielding is necessary to avoid electromagnetic radiations. - the overlapping method doesn't work with copper-nickel electrode layer.
Attachment	Adhesive recommended by Pennwalt ³⁶	Mbond 200 was used in our experiments.

APPENDIX C

Analytical method to calculate the acoustic impedance of an adhesive during curing

If ultrasound is incident normally on an interface between two isotropic elastic media, part will be reflected, and part will be transmitted. On the assumption that:

- (i) the media are ideally elastic
- (ii) displacements and stress are continuous across the boundaries

it is possible to calculate the amplitude of the pulse-echo signal shown in fig. 65 by using the following equations:

$$V_1 = R V = \frac{Z_1 - Z_2}{Z_1 + Z_2} V \quad (1)$$

$$V_1' = R T^2 V = \frac{4Z_2^2(Z_1 - Z_2)}{(Z_1 + Z_2)^3} V \quad (2)$$

$$V_1'' = R^3 T^2 V = \frac{4Z_1^2(Z_1 - Z_2)^3}{(Z_1 + Z_2)^5} V \quad (3)$$

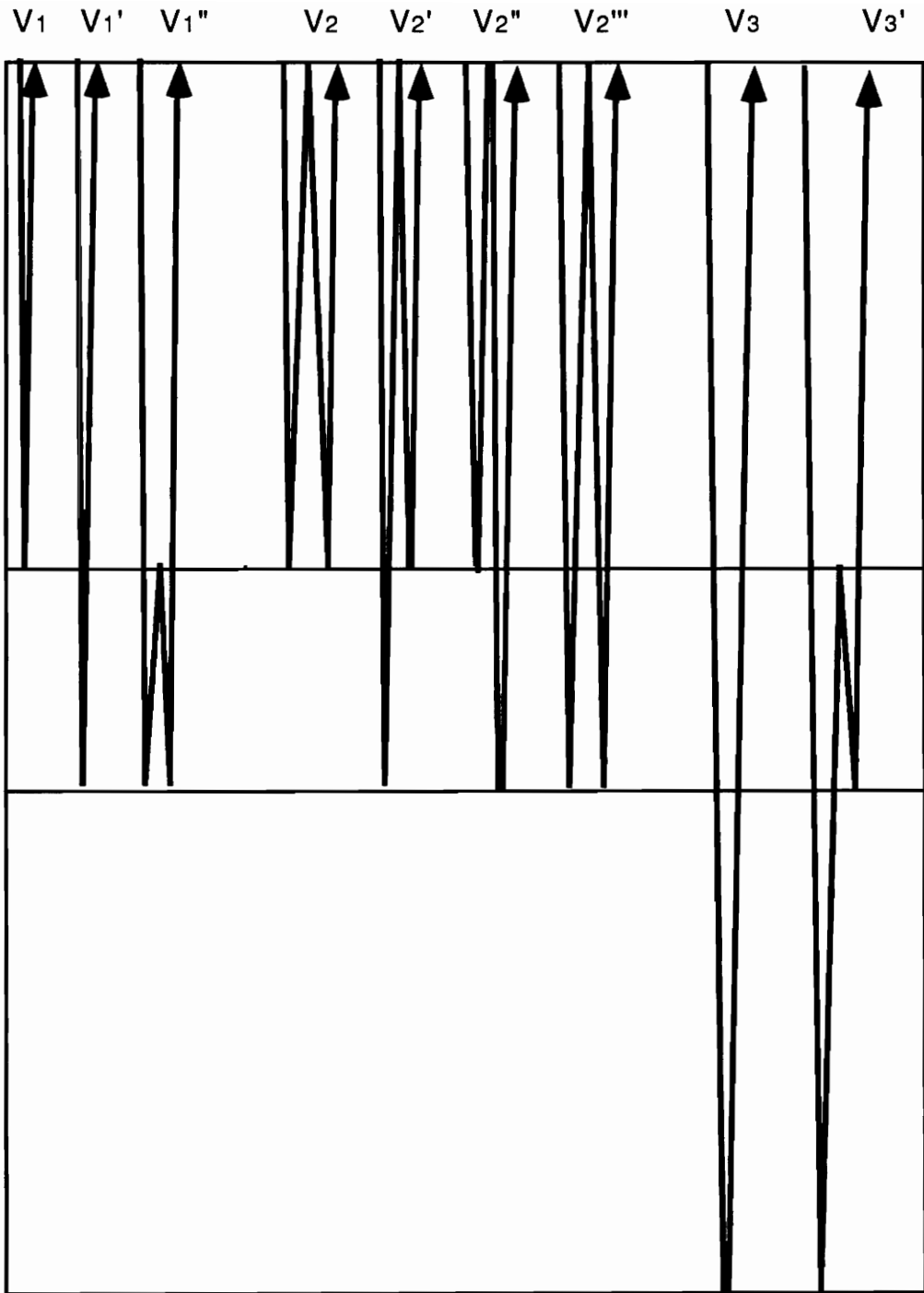


Figure 65. Pulse-echo signals used for the calculations.

$$V_2 = R^2 V = \frac{(Z_1-Z_2)^2}{(Z_1+Z_2)^2} V \quad (4)$$

$$V_2' = V_2'' = T^2 R^2 V = \frac{4Z_2^2(Z_1-Z_2)^2}{(Z_1+Z_2)^4} V \quad (5)$$

$$V_2''' = R^2 T^4 V = \frac{16Z_2^4(Z_1-Z_2)^2}{(Z_1+Z_2)^6} V \quad (6)$$

$$V_3 = T^4 V = \frac{16Z_2^4}{(Z_1+Z_2)^4} V \quad (7)$$

$$V_3' = R^2 T^4 V = \frac{16Z_2^4(Z_1-Z_2)^2}{(Z_1+Z_2)^6} V \quad (8)$$

- Where
- V: amplitude of the signal sent by the transducer
 - V_i : amplitude of the signal received by the transducer
 - R: reflection coefficient between the adhesive and the adherend
 - T: transmission coefficient between the adhesive and the adherend
 - Z_1 : acoustic impedance of the adherend
 - Z_2 : acoustic impedance of the adhesive

In the case of the curing of the epoxy, Z_1 is the acoustic impedance of plexiglas (3.2 MRayls) and Z_2 is the acoustic impedance of the epoxy (Z_2 varies during curing).

$$Z_2(t) = \rho_2(t) \sqrt{\frac{E_2(t)(1-\nu_2(t))}{\rho_2(t)(1+\nu_2(t))(1-2\nu_2(t))}} \quad (9)$$

where $\rho_2(t)$: density of the epoxy

$\nu_2(t)$: Poisson's ratio of the epoxy

$E_2(t)$: Young's Modulus of the epoxy

If we assume that V_1'' is negligible compared to V_1 and V_1' , and that the thickness of the adhesive is very thin (V_1 and V_1' are superposed) (see fig. 66), then it is possible to calculate $Z_2(t)$ by using eq. (1) and eq. (2).

$$V_1(t)+V_1'(t) = \frac{(Z_1-Z_2(t))((Z_1+Z_2(t))^2+4Z_2^2(t))}{(Z_1+Z_2(t))^3} V \quad (10)$$

If we call $A(t) = \frac{V_1(t)+V_1'(t)}{V}$ (11)

After development of eq. 10, we obtain the following cubic equation:

$$(A(t)+5)Z_2^3 + 3Z_1(A(t)-1) Z_2^2 + Z_1^2(3A(t)-1) Z_2 + Z_1^3(A(t)-1) = 0 \quad (12)$$

Using the data from fig. 26, and assuming that the epoxy is cured at time $t = 1000$ s., it is then possible to estimate V with eq. 10

$$V_1(1000)+V_1'(1000) = 0.05 \text{ mV}$$

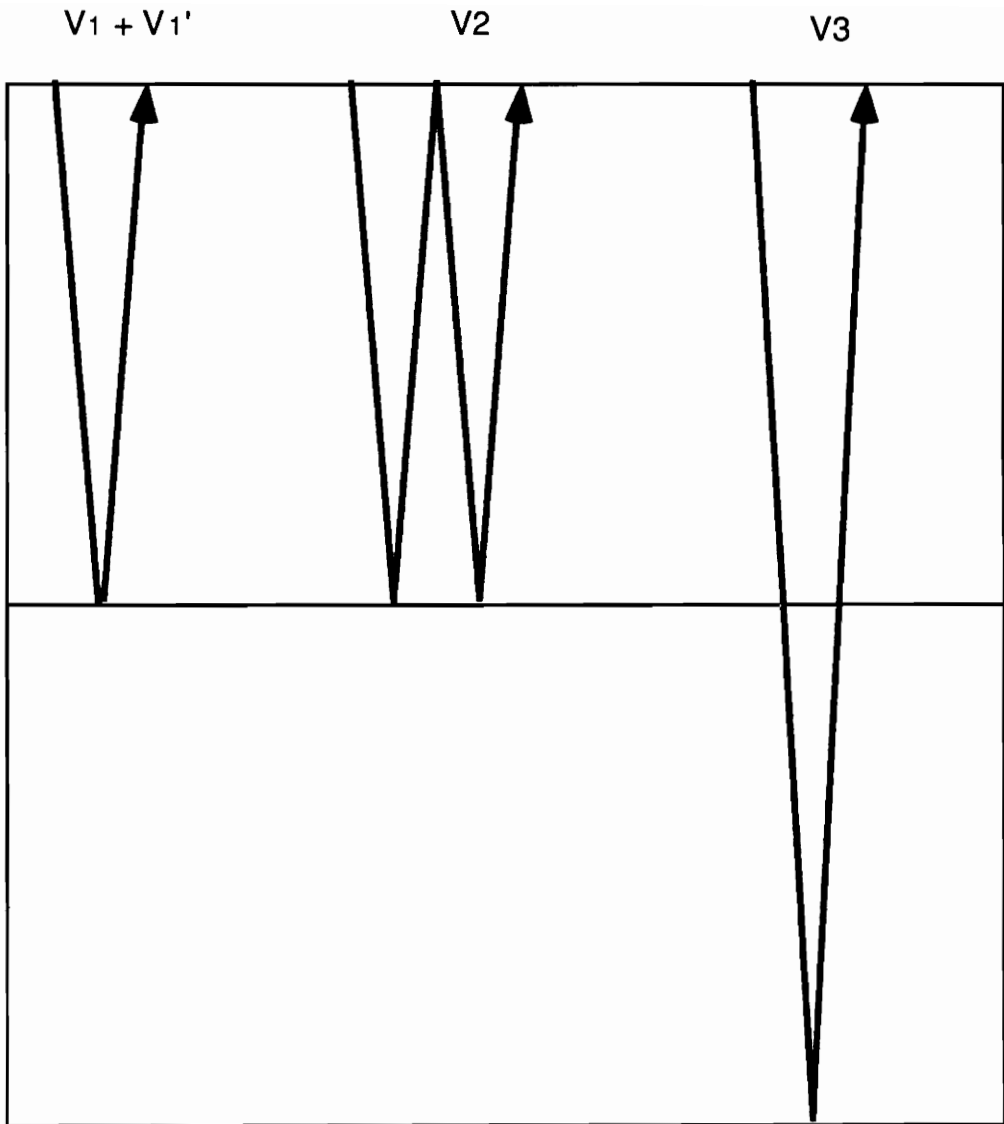


Figure 66. Pulse-echo signals when the adhesive is thin.

$$Z_1 = 3.2 \text{ MRayls}$$

$$Z_2(1000) = 3 \text{ MRayls}$$

Thus $V = 8.8 \text{ mV}$

It is now possible to calculate $Z_2(t)$ for any t by solving eq. 12 using the data from fig.26 (see fig. 67)

As the thickness of the adhesive is assumed to be thin (fig. 66), we can approximate:

$$V_2 \approx V_2 + V_2' + V_2'' + V_2''' \quad (13)$$

$$V_3 \approx V_3 + V_3' \quad (14)$$

As both adherends have the same thickness, V_2 and V_3 are superposed. If we call:

$$V_4 = V_2 + V_3 \quad (15)$$

Then it is possible to calculate the value of V_4 versus time (fig. 68) by using the value of $Z_2(t)$. Fig. 68 has the same shape as fig. 27 with a time shift. This time shift is explained by the fact that fig. 27 was obtained by a different experiment than fig. 26. Thus the initial time $t = 0 \text{ s}$. for which the epoxy began to cure, was not the same for both experiments.

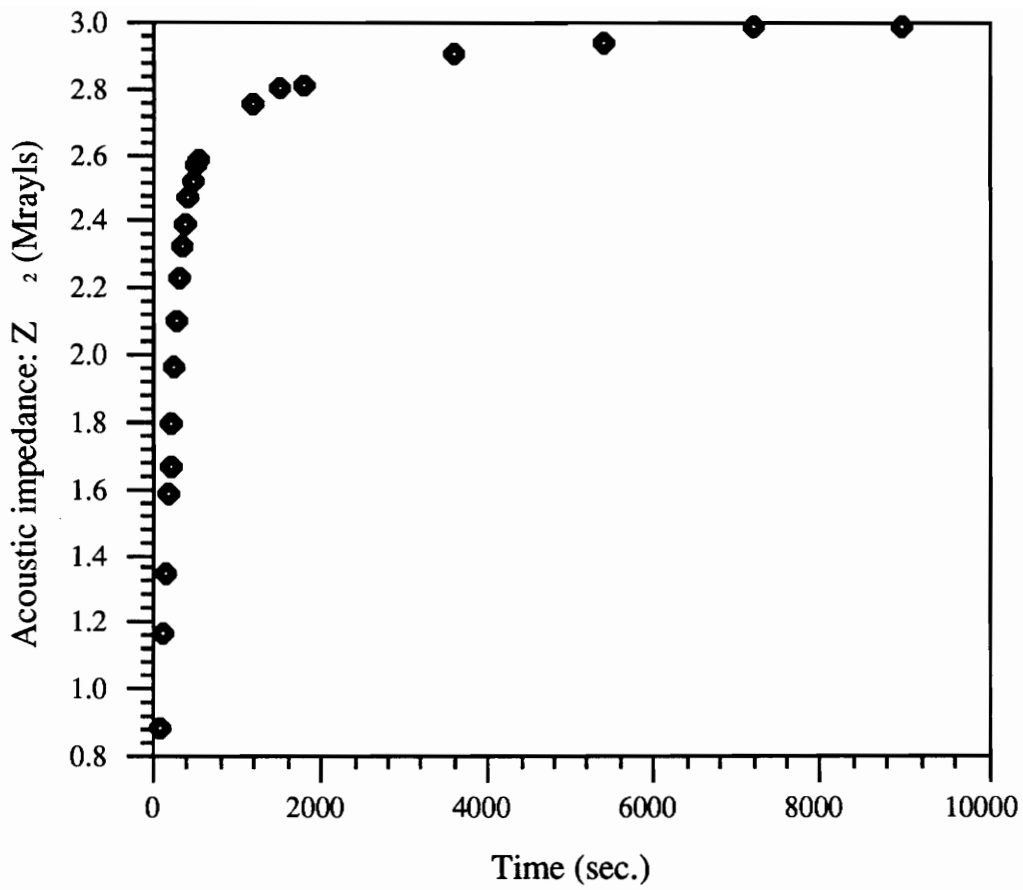


Figure 67. Acoustic impedance of the epoxy during curing.

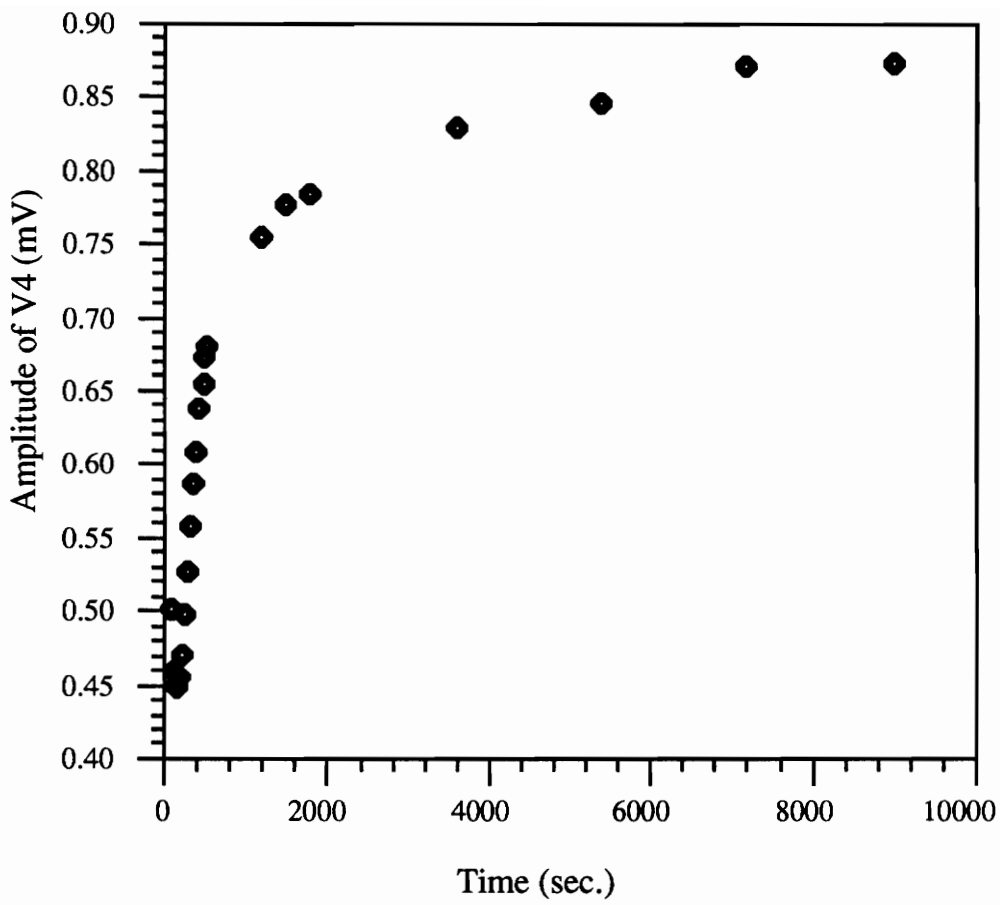


Figure 68. Amplitude of the second pulse-echo (V4) versus time.

The wave length (λ) of the signal sent through the specimen was found equal to 340 μm which represents only 4 times the thickness of the epoxy (75 μm). Therefore, there may be some interference problems which have been neglected in our calculations.

VITA

Joseph Mommaerts was born on May 7, 1966, in Tours, France. After he completed his High School studies at the "Lycée Descartes" in Tours, he spent two years at the "Lycée G. Touchard" in Le Mans to prepare for the "Grandes Ecoles" entrance examination. In July 1986, he entered the "Ecole Nationale Supérieure d'Arts et Métiers" in which he followed a three-year program regarding a broad formation in engineering and management science. He obtained his diploma in general mechanics engineering from the "Arts et Métiers" in July 1989. Joseph enrolled at Virginia Polytechnic Institute and State University in August 1989 and joined the Master of Science program in the Engineering Science and Mechanics Department.